Final report Work Package 3: The potential of satellite imagery to assess forest degradation in Congo and Gabon

REDDiness

Support C-Africa in EO driven forest monitoring for REDD

Authors: **A Vrieling, M Rahm, B Mertens, C Delloye, L Mané, B Cherubins, B Nkoumakali, N Stephenne**

Executive summary

REDD+ aims at decreasing carbon losses from the forest sector through five activities: reducing deforestation, reducing forest degradation, forest enhancement, sustainable management of forests, and forest conservations. Obtaining compensations due to REDD+ presupposes the development of a robust, reliable and transparent forest monitoring system and requires an accurate measuring, reporting and verification (MRV) system at the national level. REDDiness offers support in the definition and set up of this system in Republic of Congo and Gabon.

The REDDiness consortium decided to focus on forest degradation following three main considerations: (i) avoidance of overlap with other REDD+ related projects in both study countries, (ii) the results of a quantitative survey carried out through a questionnaire in both countries (26 answers received) and (iii) the advices of the participants (partners and scientific advisor) to the project meeting held in Kinshasa in October 2011. Because REDDiness is a research project, European Commission encourages the testing of new options and techniques regarding the REDD+ MRV system. The agreed research and development objective for REDDiness is to evaluate the effectiveness of different types of satellite imagery in detecting and monitoring forest degradation. This study focus on the direct approach requiring frequent mapping and targeting the degradation features of interest (small clearings, canopy gaps…).

To evaluate the potential of satellite remote sensing to directly detect forest degradation processes, a single site of 20x10km which experiences a persistent cloud cover was selected in each country. Among seven criteria of selection, four were determinants to localize both study sites: the presence of (i) human settlements, (ii) a national road, (iii) a forest concession and (iv) the archive availability of good-quality very high resolution satellite imagery. The areas of Youbi (Congo) and Koulamoutou (Gabon) were selected. Both sites suffered from deforestation and degradation; the main causes of deforestation in Koulamoutou are (i) the logging for timber and construction and (ii) the development of agricultural activities. In Youbi, these activities play also a role but the main cause of deforestation is the population growth.

The project intends to evaluate a variety of satellite image types, including optical and radar data, whose resolution can address the issue of degradation (high (30m) to very high (<1m) resolution). In addition, field visits were organized to provide evidence of ongoing forest cover change. Given the short duration of the project, existing archive data are an essential element of the analysis, but a number of new acquisitions were also ordered. Three remote sensing approaches were tested, namely 1) spectral unmixing from high resolution optical data (Landsat), 2) image semi-automatic classification from very high resolution (VHR) optical data (QuickBird, WorldView) and 3) a visual evaluation of information contained in radar imagery from a number of platforms.

The potential of Normalized Difference Fraction Index (NDFI), successfully applied in the Brazilian Amazon to identify and distinguish forest degradation, was tested by OSFAC.

Following a literature review, VHR optical images were classified following the best suited methods: (i) semi-automatic classification, (ii) object-based and (iii) multi-date segmentation. The maps (Forest/non-forest; Forest loss and regeneration; Degradation) were produced in a logical order from the deforestation scale to the degradation one, allowing the detection of small degradation features (<0.5ha) and the identification of degradation intensity levels. A map of forest types was also

produced to identify through a spatial analysis in which types of forests canopy cover loss had occurred. Although we have shown the effectiveness of optical very high resolution imagery for detecting small degradation features, some limitations were raised, namely (i) the difficulty to acquire good-quality cloud-free imagery, (ii) (pre-)processing procedure often requires advanced processing tools, (ii) costs of very high resolution data could be prohibitive for national coverage.

To deal with the problem of the persistent cloud cover, a visual analysis of several radar image types was performed in comparison with optical images and field data. The analysis was performed in three steps. Firstly, the mono-temporal detection of degradation signs (focuses on logging roads and canopy gaps). Secondly, a multi-temporal change detection focused on the smallest visible changes and thirdly, a large-scale differentiation of forest types. The study showed that radar images can provide a good separation between forest and non-forest, at least at large spatial scales. Detection of small-scale features or changes is possible but depends highly on (i) the size, (ii) the spatial resolution of the sensor, (iii) the viewing geometry versus the orientation of the feature and (iv) the slope of the terrain. Interpretation of radar imagery can be challenging and requires knowledge about radar imaging characteristics and about viewing geometry, especially when focussing on small-scale feature detection.

As last part of the report, we provide a summary of the capabilities of each image type studied in REDDiness to evaluate forest degradation, as well as, an overview of the alternative satellite sensors and the future satellite systems which present a potential to detect forest degradation. Very high resolution optical imagery is effective for detecting forest degradation, nevertheless, the persistent cloud cover reduces its utility in the Congo basin and VHR SAR images, as TerraSAR-X, should be considered as an alternative option. Considering the fast regeneration of vegetation and the cloud cover in the Congo Basin, a high temporal resolution is required; thereby, satellites as Sentinel-1 and 2, despite their lower resolution (10m), are foreseen to be efficient to detect forest changes (>1ha).

The conclusion on the potential of remote sensing data to assess the degradation is rather positive. We specifically evaluated the possible detection and change analysis of narrow (<5m wide) logging roads and small forest canopy gaps (<0.5ha). The REDDiness project was a short focussed project with limited resources, and as such cannot be expected to provide a definite answer as to how systems for monitoring forest degradation should be set up. Nonetheless, based on our analyses we drawn a number of general conclusions allowing orientating the technical choice to assess forest degradation with remote sensing data.

Résumé exécutif

REDD+ vise à réduire les émissions de carbone du secteur forestier à travers cinq activités: la réduction de la déforestation, la réduction de la dégradation des forêts, l'expansion des forêts, la gestion durable des forêts, et la conservation des forêts. L'obtention de compensations dues à la REDD+ suppose le développement d'un système robuste, fiable et transparent de surveillance des forêts et nécessite un système précis de mesure, notification et vérification (MNV) au niveau national. REDDiness offre un soutien à la définition et à la mise en place de ce système en République du Congo et au Gabon.

Le consortium de REDDiness a décidé de se concentrer sur les aspects liés à la dégradation des forêts. Ce choix est basé sur trois considérations principales: (i) éviter le chevauchement des activités avec d'autres projets REDD+ en cours dans la région, (ii) les résultats d'une enquête quantitative sur les besoins des utilisateurs réalisée par le biais d'un questionnaire dans les deux pays (26 réponses reçues) et (iii) les conseils des participants (partenaires et conseillers scientifiques) à la réunion du projet qui s'est tenue à Kinshasa en Octobre 2011. REDDiness étant un projet de recherche, la Commission européenne encourage l'expérimentation de nouvelles solutions techniques relatives au système MNV de la REDD+. Suite à un accord trouvé au sein du consortium, les axes de recherches pour le projet REDDiness se focalisent sur l'évaluation de l'efficacité de différents types d'imageries satellitaires à détecter et surveiller la dégradation des forêts. La méthode directe, nécessitant une cartographie fréquente et ciblant la mesure sur les petites zones de coupes, est considérée dans cette étude.

Pour évaluer le potentiel de la télédétection par satellite pour détecter directement les processus de dégradation des forêts, un site de 20x10km situé dans une zone à couverture nuageuse persistante a été sélectionné dans chaque pays. Parmi les sept critères de sélection, quatre étaient déterminants pour localiser les deux sites: la présence de: (i) établissements humains, (ii) une route nationale, (iii) une concession forestière et (iv) la disponibilité d'archive de données à très haute résolution. Les domaines de Youbi (Congo) et Koulamoutou (Gabon) ont été sélectionnés. Des phénomènes de déforestation et de dégradation sont présents dans les deux sites, les principales causes de la déforestation dans Koulamoutou sont (i) l'exploitation forestière pour le bois de construction (ii) le développement des activités agricoles. A Youbi, ces activités jouent également un rôle, mais la cause principale de la déforestation est l'augmentation de la population.

Le projet vise à évaluer une variété de types d'images satellites, y compris des données optiques et radar, dont la résolution peut aborder la question de la dégradation (résolution haute (30 m) à très élevée (<1m). En outre, des visites de terrain ont été organisées pour fournir des preuves de changement du couvert forestier continu. Compte tenu de la courte durée du projet, l'archivage des données existantes sont un élément essentiel de l'analyse, mais un certain nombre de nouvelles acquisitions ont également été commandées. Trois approches de détection ont été testées, à savoir 1) l'analyse spectrale mixte (spectral mixture analysis – SMA) à partir de données optiques à haute résolution (Landsat), 2) classification semi-automatique à partir de données optiques à très haute résolution (THR) (QuickBird, WorldView) et 3) une évaluation visuelle de l'information contenue dans l'imagerie radar à partir d'un certain nombre de capteurs.

Le potentiel de l'indice Normalized Difference Fraction (NDFI), appliqué avec succès dans l'Amazonie brésilienne pour identifier et distinguer la dégradation des forêts, a été testé par OSFAC.

Après une revue de la littérature, les images THR optiques ont été traitées suivant les meilleures méthodes rapportées: (i) la classification semi-automatique, (ii) à base d'objets et (iii) la segmentation multi-date. Les cartes (forêt / non-forêt, perte de couverture forestière et régénération; dégradation des forêts) ont été produites dans un ordre logique en partant de l'échelle spatiale de la déforestation à celle de la dégradation. Ceci a permis d'identifier au sein de la forêt, la détection des caractéristiques de dégradation de petite taille (<0,5 ha) et d'identifier des niveaux d'intensité de dégradation. Une carte des types de forêts a également été produite afin d'identifier par analyse spatiale dans quel type de forêt la perte de couvert a eu lieu. Même si nous avons prouvé l'efficacité de l'imagerie optique à très haute résolution pour la détection de la dégradation, certaines limites à l'utilisation de ces données ont été soulevées, à savoir (i) la difficulté d'acquérir des images de bonne qualité sans nuage, (ii) les étapes de (pré-) traitement nécessitent souvent des outils de traitement avancés, (ii) les coûts liés aux données à très haute résolution peuvent être prohibitif pour effectuer une couverture nationale.

Pour faire face aux problèmes de couverture nuageuse persistante, une analyse visuelle de plusieurs types d'images radar a été réalisée en comparaison avec les images optiques et des données de terrain. L'analyse a été réalisée en trois étapes. Tout d'abord, la détection mono-temporelle des signes de dégradation qui se concentre sur la détection des chemins forestiers et des trouées dans la canopée. Deuxièmement, la détection multi-temporelle des changements centrée sur les plus petits changements visibles et troisièmement, une différenciation à grande échelle des types de forêts. L'étude a montré que les images radar peuvent fournir une bonne séparation entre forêt et non forêt, du moins à de grandes échelles spatiales. La détection de la dégradation à petite échelle et/ou des changements est possible mais dépend fortement de (i) la taille, (ii) la résolution spatiale du capteur, (iii) la géométrie de visée par rapport à l'orientation de la zone de dégradation et (iv) la topographie du terrain. L'interprétation de l'imagerie radar peut être difficile et nécessite des connaissances sur les caractéristiques de ces images et sur la géométrie de visée, en particulier lorsque l'accent est mis sur la détection de la dégradation à petite échelle.

En dernière partie du rapport, nous présentons un résumé des capacités de chaque type d'image étudiée dans REDDiness pour évaluer la dégradation des forêts, ainsi qu'une vue d'ensemble des futurs capteurs satellitaires qui présentent un potentiel pour la détection de la dégradation des forêts. L'imagerie à très haute résolution optique est efficace pour détecter la dégradation des forêts, néanmoins, la couverture nuageuse persistante réduit son utilité dans le bassin du Congo et les images radar à THR, comme TerraSAR-X, doivent être considérée comme une option alternative. Compte tenu de la rapidité de régénération de la végétation et de la couverture nuageuse persistante dans le bassin du Congo, une haute résolution temporelle est nécessaire; ainsi, les satellites Sentinel-1 et 2, en dépit de leur plus faible résolution (10 m), pourraient être efficace pour détecter les changements forestiers (> 1 ha).

La conclusion sur le potentiel des données de télédétection pour évaluer la dégradation est plutôt positive. Nous avons évalué spécifiquement le potentiel de détection des étroites routes forestières (<5 m de large) et des trouées dans la canopée (<0,5 ha). Le projet REDDiness est un projet ciblé de courte durée avec des ressources limitées, qui ne permet donc pas de fournir une réponse définitive quant à la façon dont les systèmes de surveillance de la dégradation des forêts devraient être mis en place. Néanmoins, d'après nos analyses, nous avons tiré un certain nombre de conclusions générales permettant d'orienter les choix techniques quant au suivi et à la détection de la dégradation des forêts par télédétection.

Table of contents

1 Introduction

Deforestation and forest degradation cause an increase of greenhouse-gas emissions. Together they constitute the second largest anthropogenic source of carbon in the atmosphere[1]. To mitigate climate change, the United Nations Framework Convention on Climate Change (UNFCCC) has adopted the REDD+ programme. REDD+ aims at decreasing carbon losses from the forest sector through five activities: reducing deforestation, reducing forest degradation, forest enhancement, sustainable management of forests, and forest conservations. Implementation of the REDD+ programme should lead to payments to developing countries if they can proof that activities in the forest sector significantly reduce their carbon emissions as compared to reference levels. This requires an accurate measuring, reporting and verification (MRV) at the national level.

To measure, report, and verify carbon emissions, countries need to design and operationalize national forest monitoring systems. Besides field inventory approaches, remote sensing is an important input to such monitoring systems[2]. Repetitive acquisitions of satellite imagery provide synoptic overviews that can identify changes in forest cover for larger areas, as compared to ground-based surveys. While deforestation can be estimated accurately through remote sensing, the other four activities under REDD+ are more difficult to assess[3]. In those cases, forest is not replaced by a different land use, but change occurs in forest land remaining forest land[2]. However, including processes like forest degradation in MRV systems seems important to avoid leakage: if a country only regulates and monitors deforestation, forest loggers could avoid detection of their practices by adapting them towards degradation[4].

For REDD+ purposes, forest degradation means a reduction of carbon stock in forest land that remains forest land. Herold et al. (2011) define degradation as a human-induced negative impact on carbon stocks, with measured forest variables (i.e. canopy cover) remaining above the threshold for the definition of a forest[3]. Other definitions also stress that changes should be persistent over a longer time span[5]. To define suitable methodologies for MRV, it is essential to understand the drivers causing forest degradation within national and regional contexts[3]. Drivers can include the extraction of forest products (fuelwood, fruit, fodder, timber) for subsistence and local use, commercial timber extraction, or uncontrolled human-induced wildfires.

Two main approaches exist for mapping and monitoring forest degradation. The first is the direct approach, i.e. the use of remote sensing to identify forest canopy gaps caused by selective logging. The second is the indirect approach, which uses the concept of intact versus non-intact forests[2,4,6]: the presence of anthropogenic disturbance factors (roads, logging trails, settlements, fire

[1] van der Werf, G.R., et al., 2009. CO2 emissions from forest loss. Nature Geoscience 2, 737-738.
[2] GOFC-GOLD, 2011. A sourcebook of methods and procedures for monitoring and reporting anthropogenic greenhouse gas emissions and removals caused by deforestation, gains and losses of carbon stocks in forests remaining forests, and forestation: GOFC-GOLD Report version COP17-1. GOFC-GOLD Project Office, Natural Resources Canada, Alberta, Canada
[3] Herold, M., et al., 2011. Options for monitoring and estimating historical carbon emissions from forest degradation in the context of REDD+. Carbon Balance and Management 6, 13.
[4] Bucki, M., et al., 2012. Assessing REDD+ performance of countries with low monitoring capacities: the matrix approach. Environmental Research Letters 7, 014031.
[5] Penman, J., et al., 2003. Definitions and methodological options to inventory emissions from direct human-induced degradation of forests and devegetation of other vegetation types IPCC.
[6] Potapov, P., et al., 2008. Mapping the World's Intact Forest Landscapes by Remote Sensing. Ecology and Society 13.

occurrence) is used as a proxy for newly degraded areas. The indirect approach is less effective for repeated forest degradation[7].

The work package 3 (WP3) of REDDiness provides an assessment of the potential of satellite imagery to detect and monitor forest degradation in the Congo Basin, more specifically within study sites in Gabon and the Republic of Congo. We follow the direct approach, i.e. the observation of changes in forest cover, including the detection of small (<1ha) forest gaps and narrow (unpaved) logging roads. Moreover we evaluate whether at the aggregate level (using classification or indices) we can obtain information about degraded forests. Our overall aim is to contribute to the definition of national REDD+ monitoring strategies for the two countries and provide recommendation as to whether and how forest degradation assessment from remote sensing could be included. Our topical focus follows from the extensive user requirements study (work package 2), an inventory of other REDD+ related projects in both countries and avoidance of overlap with these, and a project meeting in Kinshasa in October 2011 that involved scientific expert advice. We focus on two small (20x10 km) study sites which experience a persistent cloud cover. In the project a variety of remote sensing approaches were tested, including 1) spectral unmixing from high resolution optical (Landsat) data, 2) image classification from very high resolution optical data (QuickBird, WorldView), and 3) a visual evaluation of information contained in radar imagery from a number of platforms. Field visits were organized to provide evidence of ongoing forest cover change.

This report is structured as follows:

- Chapter 2 discusses in detail how REDDiness arrived at the topical focus of forest degradation assessment by describing major outcomes of work package 2 that impacted our work.
- Chapter 3 further discusses forest degradation and evaluates the importance of forest degradation for the Republic of Congo, and Gabon.
- Chapter 4 explains how we selected the two 20x10 study sites.
- Chapter 5 provides a description of key characteristics of the two study sites.
- Chapter 6 lists the satellite archive imagery and new acquisitions that were made.
- Chapter 7 described the fieldwork activities that were carried out at both sites.
- Chapter 8 explains the normalized difference fraction index (NDFI) methodology and its application to Landsat data of both study sites.
- Chapter 9 provides an overview of the image analyses carried out with the very high resolution optical data.
- Chapter 10 illustrates and discusses the potential value of radar imagery to assess forest degradation.
- Chapter 11 provides a summary of our perspective on the usefulness of different satellite data sources to detect forest degradation, drawing on conclusions from the remote sensing analyses in chapters 8, 9, and 10. We also discuss costs and upcoming satellite missions.
- Chapter 12 gives final conclusions on work package 3 of REDDiness.

[7] Herold, M., et al., 2011.

2 Thematic focus: forest degradation

During work package 2 of REDDiness a user requirements analysis was performed. This consisted of two parts: (i) a literature and contextual review of REDD+ MRV methods, projects and initiatives in Central Africa, and (ii) a quantitative survey carried out through a questionnaire. These two approaches are separately described in sections 2.1 and 2.2. In addition, section 2.3 presents the results of the REDDiness progress meeting, which took place in Kinshasa in October 2011. At this meeting, participants (partners and scientific advisors) reviewed items (i) and (ii) to decide on the topical focus and scope for the REDDiness Work Package 3. The WP3 focus is described in section 2.3.

2.1 Overview of REDD+ related initiatives and projects in the Congo Basin (WP2)

An analysis of international and regional agreements, actors and ongoing projects in relation to REDD+ was performed to identify potentially relevant interactions for REDDiness. This analysis refers specifically to the current status of negotiations, actors and pilot projects in the two countries covered by REDDiness (Congo and Gabon). The existing methods, data and projects which can be related to REDDiness are described in WP2 reports that are publicly available on the REDDiness website (www.reddiness.eu).

Table 2.1 summarizes the projects or programs that relate directly or indirectly to the national REDD+ programmes in Congo and Gabon. It focuses on design and implementation projects that monitor land use changes as requested by MRV systems. The definition of REDD+ strategies is the responsibility of countries but they receive technical assistance through the Forest Carbon Partnership Facility (FCPF: Table 2.1c).

REDDiness aimed from its conception to operate in synergy with existing or planned initiatives, i.e. to reduce any overlap between REDDiness and other projects, but aim for collaboration where relevant. Our contextual analysis indicated that two pilot projects existed in Congo before the start of REDDiness, which are led by the Congolese National REDD Coordination in collaboration with the German GAF and with the World Resources Institute (WRI)[8]. These projects develop earth observation tools for (i) forest change estimation (rate of deforestation and degradation) and (ii) biomass estimation. The two projects have higher budgets as compared to REDDiness but similar objectives. The collaboration with the WRI project is guaranteed by the presence of its coordinator in the REDDiness advisory board. The link with the GAF project is supported by the participation of IRD in both consortiums. Moreover, the Congolese National REDD Coordination who is responsible for coordinating all REDD+ initiatives in the Republic of Congo is the local partner of REDDiness (CNIAF). REDDiness aims to reinforce the ongoing REDD+ activities in the countries by avoiding duplication.

[8] Coordination National REDD, 2011. Proposition pour la Préparation à la REDD+ (RPP) République du Congo

Table 2.1: National and regional initiatives in forest monitoring and Carbon emissions

(a) Regional Initiatives

Project	Leader	Partners	Funder	Duration	Synergy	Coverage
CEOFAC (ex-FORAF)	CIRAD	CIFOR, FRM, JRC, UCL	EU	Phase 2 2011-2013	Capacity building, Data access, experience sharing	Countries of COMIFAC
CoForChange	CIRAD	CNRS, FRM, IRD, JRC, ABDN, FSUAGx, Oxford University, IRET, MNRST, Université de Bangui, Université Yaounde 1, Universié Marien Ngouabi and private companies	ANR, NERS	2009-2012	Research on forest dynamics & capacity building	Congo, Cameroun, Gabon, CAR
FACET	UMD	UMD, NASA, OSFAC	CARPE (USAID)		Forest monitoring and capacity building	DRC, Congo
FRA 2010 / TREES 3	FAO/JRC	UCL	FAO/JRC		Forest monitoring and capacity building	Tropics
UN-REDD	FAO, UNDP, UNEP					RDC, Congo
Projet regional de renforcement de capacités REDD	BM		GEF	2011-2013	Capacity building, research network	COMIFAC

(b) National initiatives

Project	Leader	Partners	Funder	Duration	Synergy	Coverage
GSE-FM Cameroon	GAF	MINFOF, MINEP, KfW, ESA, GTZ-COMIFAC	ESA	2007-2010	forest monitoring and capacity building	Cameroun
GSE-FM Congo and gabon	GAF	SIRS, Cemagref, IRD, JR, AGEOS-Tech, Gabon, MDDEFE-RoC	ESA	2009-2012	forest monitoring and capacity building	Congo, Gabon
REDD Alert	MLURI	UCL, VU, UGOE, ICRAF, CIFOR, IITA, CIAT, IRAD			forest monitoring	Cameroun
Quantifying carbon stock in Congo	WRI	SDSU, Winrock, IMAZON, OSFAC, CNIAF	CBFF	2010-2013	forest monitoring and capacity building	Congo
CANOPY	IRD/AMAP	FRM			forest dynamics supported with VHR data	Cameroun
REDDiness	Eurosense	ITC, IRD, MEF (Gabon), CNIAF (Congo)	EU	2011-2013	forest monitoring and capacity building	Congo, Gabon
REDDAF	GAF	University of Bangui, GTG-Cameroon, Joanneum Research, Cesbio, Mesa-Consult, SIRS	EU	2010-2012	forest monitoring and capacity building	Cameroun, RCA
SEAS Gabon	AGEOS	IRD, INPE	Gabon	2010-2012	Data access and sharing, forest monitoring and capacity building	Gabon, with regional dimension

(c) CBFF projects

Project	Leader	Partners	Funder	Duration	Synergy	Coverage
Development of National MRV Systems with a Regional approach for the Congo Basin countries	FAO	INPE Points focaux Climat et administration en charge des forêts/environnement	CBFF	3 years	MRV system and capacity building	COMIFAC
Inventaire forestier multi ressources en vue de l'élaboration du plan d'affectation des terres	CNIAF		CBFF	30 months	Mapping, data collection and geo- processing	Congo
Elaboration du plan d'affectation des terres et inventaire multi ressources des aires protégées prioritaires en vue de produire les plans d'aménagement	MEF		CBFF	3 years		Gabon

2.2 User requirements survey

During WP2, a quantitative survey was conducted with two main objectives: (i) to assess the level of knowledge regarding REDD+ and earth observation techniques of relevant stakeholders, (ii) to understand what local users perceive as their main needs in terms of MRV (monitoring, reporting, and verification). This survey confirmed that the internal coordination for REDD+ and REDD-awareness are still at an initial stage in Congo and Gabon. Both countries have limited technical and human resources to develop a forest monitoring system meeting UNFCCC requirements. The setup of the survey and the main results are described in the following four sections: (i) questionnaire structure and survey implementation, (ii) presentation of participants, (iii) methodology used for analysis and (iv) results.

2.2.1 Questionnaire structure

A quantitative survey was performed in order to analyze and compare stakeholder's responses in an objective way. In addition, the survey contained several open questions to gather general information about the survey participants and their involvement in REDD initiatives or projects. The questionnaire's body includes multiple choice questions about geomatics (data used, expertise, hard and software resources) and the participants' knowledge regarding the REDD+ mechanism (political and scientific knowledge, interesting products and definitions or parameters which are useful in setting up a MRV). A total of 26 surveys were received corresponding to a 59% response rate.

2.2.2 Participant institutions

The majority of the responding institutions have a national status (54%) and to a lesser extent an international one (27%) (Figure 2.1). They mainly represent research and administration (58%) in the fields of natural resource management, forestry or environment (Figure 2.1b). Only 32% of the institutes are involved in REDD+ projects and a mere 13% reports having a good knowledge of the REDD+ process.

For the REDD+ MRV context, the survey questions particularly focused on the types of spatial data and tools used by REDD+ stakeholders. Nearly all institutions (91%) produce and use thematic maps. A majority of participants make direct use of optical satellite imagery (70%) and aerial photographs (61%) while radar imagery (including satellite radar) is used only by 39%. LIDAR data acquired by satellite or airplane is relatively unknown (4 and 9%). The survey also provided information on existing software and technical expertise. ArcGIS / ArcView and MapInfo, the most well-known GIS/mapping software programs, are available in most institutions (87% and 65% respectively). Remote sensing software (e.g. ENVI and ERDAS Imagine) is available in only 26% of the institutions. Concerning technical expertise, most institutions are able to create geo-referenced databases (70%) but less than 50% are able to perform basic image processing, such as unsupervised classifications (48%). Hence, although a large part of the organizations report a direct use of satellite imagery, in many cases software (and knowledge) for advanced analysis of these data seem unavailable.

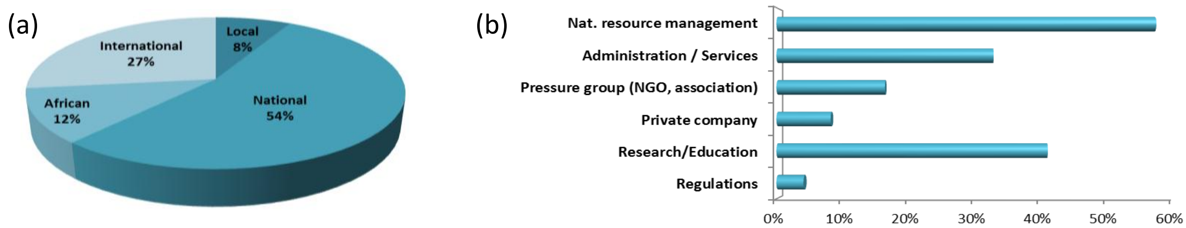

Figure 2.1: (a) Management level of the 26 institutions surveyed in REDDiness. (b) Domain of application.

Not all respondents understood the questions equally well. Unanswered or incomplete answers demonstrate a limited level of knowledge about REDD+ and MRV implementation. This confirms the need for capacity building on REDD+ and forest monitoring in the countries involved[9]. REDD+ projects have a role in strengthening the dissemination of information on the objectives and implementation of REDD+, in Africa in general, and in the Congo Basin in particular.

2.2.3 Methodology

The number of questionnaires received (26) did not allow for a reliable statistical analysis. For the quantitative analysis, we selected the surveys containing the most comprehensive responses. These included the potentially relevant partners for REDDiness in the implementation of these MRV systems in Congo and Gabon. Three selection criteria were used (Figure 2.2) i.e. (i) knowledge of REDD, (ii) completeness of responses, (iii) consistency of responses evaluated by two sub-criteria, compliance with instructions and logical link between two specific responses. A threshold of 79% in the sum of these criteria identifies eight institutions, four per country, for which the quantitative responses on REDDiness products and data were analyzed in detail (Figure 2.2).

For Congo, we selected four REDD+ actors, which include government body - CNIAF, Non-Governmental Organization - OCDH, research centre - CERGEC and private actor - CIB. For Gabon, this quantitative analysis includes two governmental services: DG-Aqua and DG-Wood and two research centres: IRSH –CNDIO and IRET. In addition to these institutions, our local partner in Gabon (MEF) identified a number of other potential stakeholders, such as LAGRAC (Laboratoire de Graphique et Cartographie of geographic department of the University Omar Bongo) and DG Forests. For those, filled questionnaires were received but did not meet our selection criteria for the quantitative analysis.

	REDD knowledge		Completeness *23 questions)*	Consistency		Total (%)	REDD project
	Pol. *(/5)*	Scient. *(/5)*		Compliance *(/2)*	Link *(/1)*		
Congo							
CNIAF Centre National d'Inventaire et Aménagement des Ressources Forestières - Fauniques	3	3	23	2	1	87%	OUI
OCDH Observatoire Congolais des Droits de l'Homme	5	4	22	1.5	0.5	79%	OUI
CERGEC Centre de Recherche Géographique et de Production Cartographique	3	4	23	1	1	85%	NON
CIB Congolaise Industrielle des Bois	2	3	23	2	1	87%	NON
CNIAF							
DG-Wood General Directorate of industries, timber trade and exploitation of forest products from the Ministry of Forestry (mapping service)	2	3	22	2	1	85%	OUI
DG-Aqua General Directorate of aquatic ecosystems of the Ministry of Forestry (mapping service)	3	3	23	2	1	87%	NON
IRET Institut de Recherche en Ecologie Tropicale	3	3	23	2	1	87%	NON
IRSH-CNDIO Institut de Recherche en Science humaine - Centre National de Données et d'Information Océanographique	4	5	23	2	0.5	92%	NON

Figure 2.2: Selection criteria and selected institutions.

[9] Herold, M. (2009). An assessment of national forest monitoring capabilities in tropical non-Annex I countries, Recommendations for capacity building, GOFC-GOLD Land Cover Project Office, Friedrich Schiller University Jena

2.2.4 Survey results

This survey assisted in defining needs of earth observation data and monitoring schemes to be developed in both countries. Regarding the perceived need in the framework of REDD+ monitoring, no clear consensus exists between the participants on earth observation data types to be used. However, most of them point out high-resolution satellite imagery (Landsat) as their first choice (5 out of 8). More consensus existed on the relevance of potential earth observation directions to be developed (Figure 2.3): forest change estimation (rate of deforestation and degradation) and biomass estimation. Spatially-explicit forest degradation monitoring is seen as the third important element to be addressed by the national REDD+ strategy. The contextual analysis indicated that other projects such as the two first pilot projects led by the Congolese National REDD Coordination in collaboration with GAF and WRI (CN-REDD, 2011[10]) develop the first two activities. To avoid overlap and increase significance of the project, REDDiness proposes to focus on earth observation techniques for the third topic, i.e. spatially-explicit forest degradation monitoring.

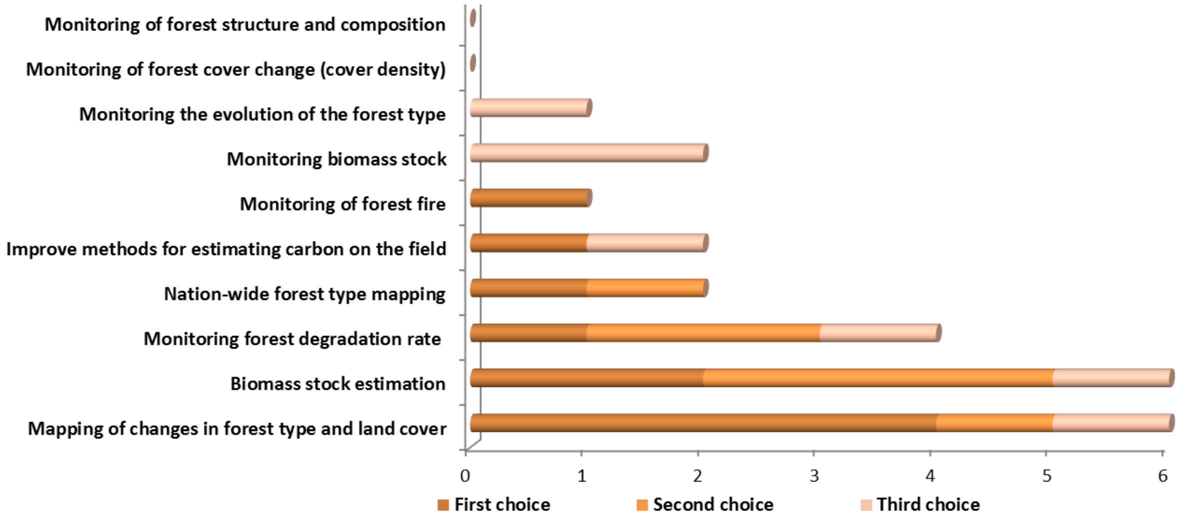

Figure 2.3: Order of importance in the three most useful products for REDD strategy and forest monitoring

2.3 Advise scientific experts and proposed scope of WP3

Earth observation techniques need to be tailored to local conditions before effective implementation of monitoring, reporting, and verification (MRV) systems in both countries. The user survey and the knowledge acquired on other projects in the region directed to a topical focus for REDDiness, i.e. forest degradation assessment and monitoring. This priority was reinforced during the project progress meeting that took place in Kinshasa in October 2011. At this occasion, project partners and scientific advisors discussed the results of the user requirements study and set directions for the way forward for REDDiness. A consensus was achieved between the participants on the main objective of work package 3 (earth observation development) of REDDiness. To support the meeting decisions, several technical and methodological choices faced by REDD projects (or participating countries) were identified, i.e. principal theme (deforestation/degradation/carbon), study zone and sampling, and the spatial and temporal resolution to be used. Figure 2.4 shows the different options that were discussed for REDDiness during the meeting. Several options in this figure are related: for example it was agreed that assessing forest degradation is impossible with low spatial resolution or infrequent observations, especially for the Congo Basin.

[10] Coordination National REDD, 2011. Proposition pour la Préparation à la REDD+ (RPP) République du Congo

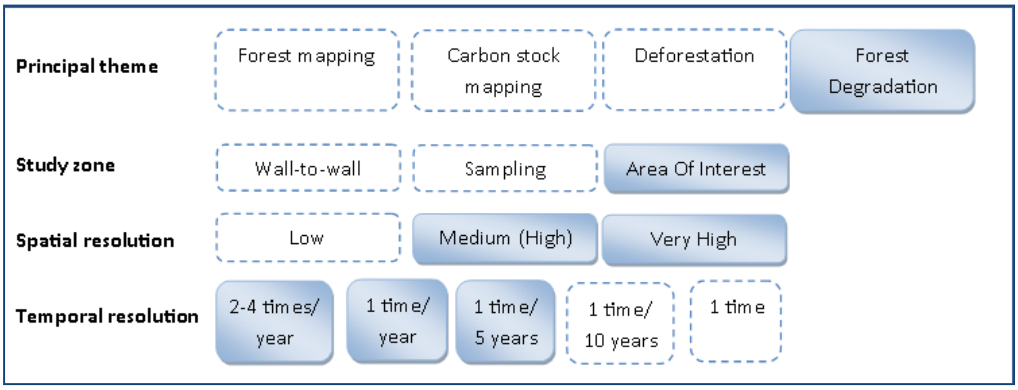

Figure 2.4: Selection of REDDiness focuses by surveying 4 main questions within the consortium.

The agreed research and development objective for REDDiness is to evaluate the effectiveness of different types of satellite imagery in detecting and monitoring forest degradation. Such an evaluation is urgently needed given 1) the importance of forest degradation in REDD+ which is currently not addressed in detail especially in Central Africa, 2) the difficulty to assess forest degradation due to spatial size and pattern of the process - in the Congo Basin forest degradation is often characterized by small scale changes in forest cover-, 3) the limited time frame in which to detect degradation given the potential quick regeneration of vegetation, and 4) the frequent cloud cover in both countries limiting optical image acquisition. The defined priority objective is supported by the European Commission (EC). The EC requested to avoid overlap with other existing projects to optimally use EC resources. Because REDDiness is a research project, EC encourages the testing of new options and techniques regarding REDD+. The project intends to evaluate a variety of satellite image types, including optical and radar data of high (30m) to very high (<1m) resolution. Given the short duration of the project, existing archive data will be an essential element of the analysis, but a number of new acquisitions are essential and foreseen. The focus will be on two study areas of limited extent, one in Congo and one in Gabon. In addition based on current commercial costs and planned satellite missions, we intend to provide a future outlook of how forest degradation may be included in an MRV system for countries in the Congo Basin.

3 Forest degradation in Congo and Gabon

3.1 Forest degradation

Forest degradation is a serious environmental, social and economic problem, particularly in developing countries, and is one of the major sources of GHG emissions, but its significance has not been yet quantified on a global scale[11]. Perceptions and processes of forest degradation are many and varied and so are its drivers: degradation is therefore technically and scientifically difficult to define and measure.

With respect to mitigation of climate change, in the framework of the REDD+ international negotiations under UNFCCC, forest degradation refers to a loss of carbon stock within forests that remains forest. Forest degradation is defined by the Intergovernmental Panel on Climate Change as "a direct human-induced long-term loss (persisting for X years or more) of at least Y per cent of forest carbon stocks (and forest values) since time (T) and not qualifying as deforestation »[12]. The thresholds for carbon loss and minimum area affected as well as long term need to be specified to make this definition operational[13], since the values depend on the different degradation activities, forest composition and the required methodology[14].

The definition of forest degradation can have policy implications, which further complicates reaching a consensus and developing common approaches applicable at both international and national scale[15]. For countries and regions with low deforestation and high forest cover such as Gabon and Congo, forests are relatively undisturbed, but deforestation and degradation may occur increasingly in the future: these countries are likely to have the most interest in accounting for degradation because they are less likely to benefit from 'avoiding deforestation'.

Forest disturbances that lead to degradation such as over-harvesting, forest fires, pests and climatic events including drought, wind, snow, ice, and floods have been estimated to affect roughly 100 million of hectares globally per year, which represents almost 10 times the area that is affected by deforestation globally (i.e. 13 million $hayr^{-1}$ for 2000-2005)[16]. In particular, tropical regions are well known for large scale disturbances that lead to forest degradation[17]. In Africa, the annual rate of degradation is almost 50 per cent of the deforestation rate[18]. Tables 3.1 and 3.2 illustrate the recent trends of deforestation and degradation in the Congo basin[19].

[11] Simula, M. and Mansur, E. (2011). A global challenge needing local response. Unasylva, 62, 238, 3-8.
[12] IPCC (2003). Definitions and methodological options to inventory emissions from direct human-induced degradation of forests and devegetation of other vegetation types. Intergovernmental Panel on Climate Change.
[13] GOFC-GOLD (2011).
[14] DeFries R et al. (2007) Earth Observations for Estimating Greenhouse Gas Emissions from Deforestation in Developing Countries. Environmental Science and Policy 10: 385 394.
[15] Simula and Masnur, 2012
[16] Romijn, E et al.(2012). Assessing capacities of non-Annex I countries for national forest monitoring in the context of REDD+. Environmental Science and Policy, 19-20, 33-48.
[17] Asner, G. (2009). Tropical forest carbon assessment: integrating satellite and airborne mapping approaches. Environmental Research Letters, 4, 3.
[18] Lambin et al. (2003), cited by Murdiyarso et al., 2008. Lambin, E., Geist, H., Lepers, E. (2003). Dynamics of land use and land cover change in tropical regions. Annual Review of Environement and Resources, 28:205-241.
[19] De Wasseige et al. (2012). Les forêts du bassin du Congo – Etat des forets 2010. Office des publications de l'Union Européenne, 276p.

Table 3.1: Deforestation and reforestation trends (% per year)

Country	1990-2000				2000-2005			
	N	Gross deforestation	Gross reforestation	Net deforestation	N	Gross deforestation	Gross reforestation	Net deforestation
Congo	70	0.08	0.04	0.03	40	0.16	0.08	0.07
Gabon	58	0.08	0.03	0.05	12	0.07	0.07	0.00
Congo Basin	547	0.13	0.04	0.09	337	0.26	0.09	0.17

Source: de Wasseige et al., 2012. Statistics based on a sampling sheme (N = number of observations)

Table 3.2: Forest degradation and regeneration trends (% per year)

Country	1990-2000				2000-2005			
	N	Gross degradation	Gross regeneration	Net degradation	N	Gross degradation	Gross regeneration	Net degradation
Congo	70	0.04	0.01	0.03	40	0.08	0.05	0.03
Gabon	58	0.05	0.01	0.04	12	0.04	0.04	0.00
Congo basin	547	0.07	0.01	0.05	337	0.14	0.04	0.09

Source: de Wasseige et al., 2012. Statistics based on a sampling sheme (N = number of observations)

Many activities cause degradation of carbon stocks in forests. To develop a monitoring system for degradation, it is essential to first identify the drivers and activities causing forest degradation and their likely impacts[20]. Such information is needed not only for formulating appropriate REDD+ strategies and policies, but also for the definition of suitable methods for measuring and monitoring. Various types of degradation will have different effects on the forest and will result in different types of indicators, which can be used for monitoring degradation from in situ and remote methods[21].

- *Selective logging*. Timber harvesting (both legal and illegal) leads to degradation through the direct removal of trees, through collateral damage to live trees by logging equipment and skid trails, and by increasing the effects of drought, windthrow, and fire in forest fragments. Forests affected by selective logging with the presence of gaps in canopy, roads and log decks observable in remote sensing imagery. A combination of legal logging followed by agricultural practises and illegal activities in the same concession is likely to cause more degradation and more change in canopy characteristics. The forests in the Congo Basin are increasingly affected by artisanal or informal wood harvesting activities, for both the national and international markets: recent estimates show that the informal sector actually provides much more volume than the formal and industrial sector;
- *Fires*. Human-induced fire, often associated with agricultural clearing, can affect surrounding forests, resulting in reduction of forest carbon stocks. Ecologically appropriate prescribed burning would not be considered degradation since it often leads to no net loss of carbon stocks or even to an increase of carbon stocks in the long-term (Herold et al., 2012). Degradation of carbon stocks by forest fire could be more difficult to monitor with existing satellite imagery, depending on the frequency, severity and extent of forest fires. Practically, all fires in tropical forests have anthropogenic causes;
- *Fuel wood collection and charcoal production*. Significant reductions in forest carbon stocks can result from fuelwood harvesting either by individuals, where population pressure is

[20] GOFC-GOLD, 2011
[21] Romijn et al. 2012

strong, sustainable practices are not used, and alternative fuels are not available, or due to commercial felling of large trees for direct sale to urban areas or for the production of charcoal. Degradation by over exploitation for fuel wood, which is likely not to be detectable from satellite image, unless the rate of degradation was intense causing larger changes in the canopy. Fuel wood collection, mainly in densely populated areas and around cities is greatly affecting forest environment and resources;

- *Forest products for local markets*. Extraction of forest products for subsistence and local markets: privately or communally managed forests are often subject to extraction of forest products for immediate use or sale by local households, such as collection of fuelwood for cooking, collection of fruits, roots and other edible or medicinal tree parts, collection of fodder for livestock, and harvesting of timber and thatch for construction. In addition, most developing countries have seen rapid urbanization in recent decades, which has created a market for forest-based products (i.e. charcoal) that, in some cases, has resulted in forest degradation[22].

Besides drivers and activities mentioned above, it is essential to consider the potential role of shifting cultivation in the forest degradation process: indeed, following the adopted national definition of forest (canopy cover above 30%), large areas under shifting cultivation or fallow can actually be classified under the "forest" or "forest land remaining forest land" categories, and therefore not considered as deforestation. In terms of carbon budget, these forest-agriculture mosaics do present a much lower rate of C/ha as compared to undisturbed forests.

Forest degradation processes may or may not affect large areas, but usually they are not equally distributed over the country's territory. This should be considered in national measurement and monitoring efforts. Not all countries are at the same point on the forest transition curve, reflecting the dynamics of agriculture and forest rents over time[23]. As a result, degradation is a more critical issue in some countries than others. Thus the location of a country on the forest transition curve will influence its motivation for investing in degradation accounting and the suitability of the measurement and monitoring option[24].

3.2 Forest sector and condition in Congo and Gabon[25]

3.2.1 Republic of Congo

The Republic of Congo covers 342,815 km^2 and has an estimated population of 3.6 million, corresponding to a relatively low population density of 10.5 inhabitants per km^2. This population is mostly urban, with more than half of all Congolese living in the six largest cities. Population growth remains high, although its rate is decreasing at about 2.9% per year. There are strong regional disparities: the forest area in the north is very sparsely populated with less than 1.5 persons/km^2 in the departments of Sangha and Likouala. This population is distributed along the main transportation axes, leaving vast areas uninhabited. The forests in the south are more populated and these face

[22] Romijn et al. (2012)
[23] Angelsen, A. Ed. (2008). Moving ahead with REDD: issues, options and implications. CIFOR, Indonesia
[24] Murdiyarso, D et al. (2008). How do we measure and monitor forest degradation? In: Angelsen, A. Ed. Moving ahead with REDD: issues, options and implications. CIFOR, Indonesia.
[25] The Forests of the Congo Basin - State of the Forest 2008, Editors : de Wasseige C., Devers D., de Marcken P., Eba'a Atyi R., Nasi R. and Mayaux Ph., 2009, Luxembourg: Publications Office of the European Union.

more serious threats from activities such as subsistence farming, hunting, and intensive logging for many years without any management planning to date.

The forestry sector contributes significantly to the national economy, although in relative terms less than during the period up to the early 1970s. In 1974, timber generated 85% of export earnings and accounted for 10% of GDP. The rise of oil has diminished the importance of the forestry sector. Production of timber and processed products represents the major part of the formal sector's contribution to the economy. In 2006 forestry products made up only 5.6% of the GDP. This figure masks the fundamental role played by the forest sector in terms of job creation and regional development in the most disadvantaged rural areas.

Forests occupy fast areas in the Republic of Congo, with area estimates ranging from 22.4 million hectares[26] to 25.9 million hectares[27]. The most recent remote sensing based forest cover estimate is 18.5 million hectares[28]. The Congolese forest covers two thirds of the Congolese territory.

The estimated annual rate of deforestation is very low, with a net rate of 0.02%. Gross deforestation is a little higher, at 0.07% per year, but this is off-set by reforestation of 0.05%[29]. The deforestation rate is almost zero in the north of the country. These figures do not well-represent the situation in the south because of the lack of available optical satellite images (due to cloud cover), which can lead to an underestimation of national deforestation rates. Shifting cultivation is the main cause of deforestation. This can be observed on satellite images around the main cities (Brazzaville, Pointe-Noire, Nkayi, Dolisie, Ouesso) and along roads. Human activities such as logging, firewood harvesting and bush fires can cause forest degradation (a reduction in biomass) and potentially affect biodiversity, without having a major effect on the evolution of forest cover and without compromising forest sustainability. At present, mining and agro-industry have no marked impact on Congo's forests. But many mineral operations are currently underway (approximately 60,000 km^2 in 2005, while 17.5% of the forest estate is designated for mining permits). These could result in future extraction of the identified deposits. Also a revival of agro-industrial activities is possible given the current global food crises, which could generate increased pressure on the forests.

3.2.2 Republic of Gabon

Gabon covers 262,090 km^2. In 2005 Gabon was reported to have 1.3 million inhabitants giving an average population density of 5 inhabitants per km^2. For the period 2005 to 2010, the average rate of demographic growth was estimated at 1.48%. There is strong disparity between the rural environment, which is sparsely populated and the urban zones, where most of the population is based (85 % of the total). Urban population is currently growing at a rate of 2.2%.

In the rural zones traditional agriculture and agro-industry are under-developed. The population ratio per hectare of arable and cultivated land is 0.9. This figure is the lowest in Central Africa (with an average of 2.02 for the Congo Basin countries). Cropped areas represent about 5% of national surface area.

---

[26] CNIAF, (2008)

[27] Mayaux P. et al. (2003). A Land Cover Map of Africa, Joint Research Centre, EUR 20665 EN (European Commission, Luxembourg).

[28] The Forests of the Congo Basin - State of the Forest 2008

[29] Duveiller G et al. (2008). Deforestation in Central Africa: Estimates at regional, national and landscape levels by advanced processing of systematically-distributed Landsat extracts. Remote Sensing of Environment, 112 (5), pp. 1969-1981.

Gabon has dense forests that covering about 21 million ha, i.e. more than 80% of the national territory. This coupled with low population density results in Gabon having the highest rate of forest surface per capita in Africa. Between 1990 and 2005, the recorded loss of national forest cover loss was very low, 0.15 million hectare (less than 1%). Natural resource exploitation is the cornerstone of the Gabonese economy: oil, forests and mining make up half of the GDP. The oil sector alone accounts for 42.4% of GDP. The forest sector is in second place (6.0%) followed by mining (1.9%).

Three main types of dense rain forest can be distinguished in Gabon, i.e. coastal forests (at 0-300 m altitude): 32.6%, intermediary forests (300-1000 m): 66.7%, and flooded forest and mangrove: 0.7%. The rest of the country is made up of forest-savannah mosaic, swampy zones and mangrove. Recent analysis of satellite data[30] estimated the change in forest cover over all countries in the Congo Basin region. In terms of deforestation rate, Gabon, the Republic of Congo and the Central African Republic, are among those countries where the deforestation dynamic is still relatively low with an annual rate of 0.09% for a regional average of 0.21% per year (± 0.05%). In the framework of the GSE Forest monitoring initiative, measured statistics on deforestation rate indicate even lower figures: the annual rate of deforestation for Gabon was estimated to 0.02% for the period 1990-2000, and 0.004% for the period 2000-2010[31]. As for the net rate of degradation of forest cover, Gabon has a rate of 0.08% for a regional average of 0.15% per year (± 0.03%). However, in our view, these results should be interpreted with care, given the low volume of optical remote sensing data available and used for this country.

[30] Coordination National REDD, 2011. Proposition pour la Préparation à la REDD+ (RPP) République du Congo

[31] Sannier, C., Massard, E., Fichet, L.-V., Mertens, B., Huynh, F. 2011. Monitoring of forest cover change in the Republic of Gabon between 1990, 2000 and 2010 following IPCC guidelines, International Symposium on Remote Sensing of the Environement.

4 Study site selection

4.1 Study site selection criteria

To evaluate the potential of satellite remote sensing to directly detect forest degradation processes, we decided to select a single site in each country: i.e. one in Congo and one in Gabon. Given limited resources and timeframe of the project, and the small scale of the forest degradation process, this was agreed as the optimal solution by all partners. The initial design was to have per site a broad area of 40x40 km with inside two focal areas of 10x10 km. These smaller focal areas could then be studied with very high resolution data. Eventually (as shown later in this report) we concentrated on a single 20x10 km site in each country for all our analyses. Here also the fieldwork took place. The study sites were selected based on several criteria:

- The areas should not have been extensively studied by other projects;
- They should experience persistent cloud cover thus imposing a constraint on remote sensing solutions (south of Congo, Gabon, see Figure 4.1);
- Forest degradation should likely have occurred in the past 5 years, or is likely to occur within six months according to information from local experts (local partners or references);
- The area should be accessible because this:
  - determines an external pressure (demand for fuel wood from villages, towns, or near road) which can cause uncontrolled use of forest resources (and consequent degradation)
  - is needed for the validation fieldwork;
- A forest concession is present in part of the area (possible data availability on wood extraction);
- Otherwise data are available which relate to forest degradation (concessions, statistics from the ministry, studies performed);
- The areas have limited relief to facilitate radar analysis;
- The sites should have at least a basic availability of optical very high resolution data (satellite or aerial photography).

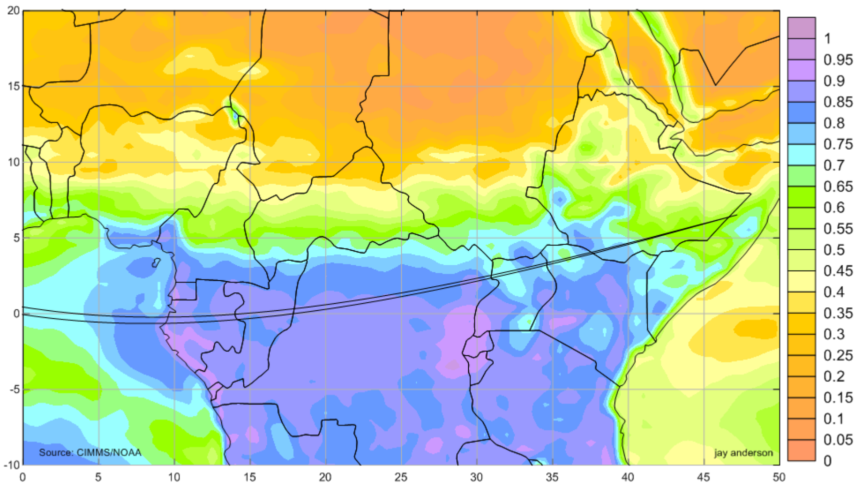

Figure 4.1: Average cloud cover in tenths across Africa, based on 24 years of satellite measurements. Data CIMMS/NOAA

4.2 Options and applying criteria

This section describes the process for the final selection of study sites in Congo and Gabon. The process took place in three stages:

1. Local partners proposed regions of interest where forest degradation is likely to occur.
2. Based on the criteria, we selected the best area in which we set the study site of 40x40 km.
3. Within the 40x40 km, two focal areas of 10x10 km were chosen according to the availability of archive VHR images. This availability was evaluated through an extensive search in the archives from 2007 to present for a large number of sensors (EROS B, WorldView-1 and -2, QuickBird-2, IKONOS, GeoEye-1, ALOS-Prism and SPOT-5). We queried the archives for both study sites of 40x40 km using a maximum cloud cover percentage of 20 per cent.

4.2.1 Study site in Congo

Local partners identified three areas of interest: Youbi, Ngoua, and the Saras (Figure 4.2). These are located in two departments, i.e. Kouilou and Niari. During the evaluation of these areas, two additional areas were proposed (Mila Mila forest and Mapati forest). However, this proposal came late when the selection procedure had already been largely performed. Moreover, the Youbi area met all selection criteria described in section 4.1 (Table 4.1) and resulted as a good candidate study site in Congo. Therefore we did not extend our analysis to the additional proposed areas.

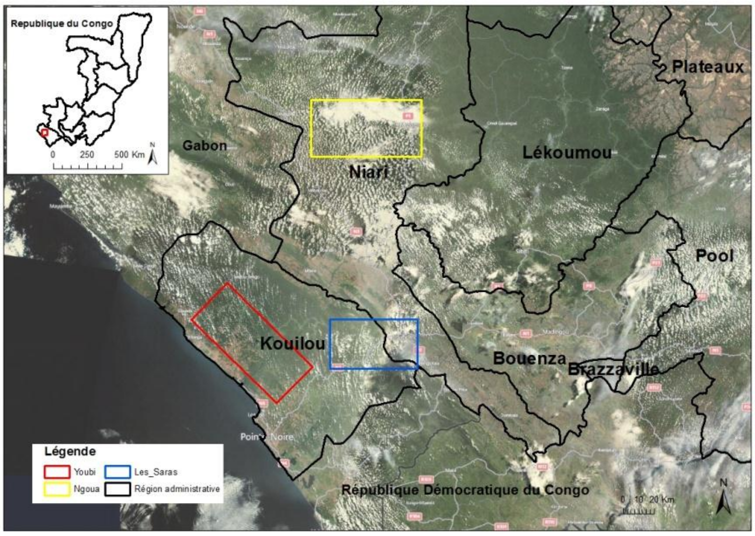

Figure 4.2: Location of three areas of forest degradation identified by local partners in Congo

The location of the 20x10 km focal area was determined by:

- the location of good-quality VHR satellite imagery (see discussion below);
- the location of the village of Youbi;
- presence of a national road;
- overlap with the forest concession and the protected area.

The results of the very high resolution (VHR) optical archive data search for the 40x40km study site are shown in table 4.2. The location of the VHR scene outlines was mapped and we discussed with all partners to agree on the most relevant study site based on this availability.

Table 4.1: Applying the selection criteria to the Youbi area

#	Selection criteria (see 4.1)	Youbi	References
1	Frequent cloud cover	OK	Figure 5, Fabing et al., 2001[32].
2	Forest degradation	OK	Confirmed by local partner and several studies (Fabing et al., 2001[10]; Missamba-Lola, 2005[33]; Yembé Yembé, 2007[34]).
3	Accessibility	OK	Area near Youbi village and crossed by a national road (N6).
4	Forest concession	OK	Forest concession of Nanga (see Figure 7).
5	Degradation data	OK	Several studies on degradation were conducted in the region (see #2). Missamba-Lola gathered perceptions of local people on forest conditions in the villages Youbi and Koutou[11]. According to local partners, as the site belongs to the UFA Sud 2-Kayes (Unité forestière d'aménagement), statistical data should be available at the Ministry.
6	Limited relief	OK	
7	VHR data	OK	Aerial images of Winrock (2007) and Quickbird, Worldview.

Table 4.2: List of available VHR archive data within the 40x40km test site in Congo

Archive VHR					
Sensor	**Resolution (m)**	**Number of images**	**Cloud cover**	**Acquisition date**	**Comment**
Eros B	0.7	0			
Worldview-1	0.5	0			
Worldview-2	0.5	1	3%	29/08/2011	Cloud cover is around 20% within the study site
QuickBird-2	0.6	1	26%	30/12/20009	
IKONOS	1	1	9%	30/12/20009.	Image does not fully cover study site (figure 4.3)
GeoEye-1	0.5	0			
SPOT-5	2.5	0			
Kompsat-2	4	6	Between 10% and 20%	2008, 2009 and 2010	
ALOS-Prism	2.5	2	Very high (>30% in AOI)	04/12/2007	

The location of the VHR images is not ideal for the 40x40km study site and the quality of several images is low (significant cloud cover). The WorldView-2 image of 29 Augustus 2011 (Figure 4.3) is of reasonable quality and fully covers the 20x10 km focal area indicated below. Although the cloud cover percentage of the entire image is low (3%), the cloud cover in the focal areas is higher (around 20 %). Nonetheless together with local partners (and based on overlap with village, road, and concession) we decided to use this 20x10 km area for our detailed analyses (Figure 4.4). A multi-temporal analysis could be carried out in combination with a Kompsat-2 image of 8 March 2009. The Kompsat-2 image seems of good quality but we could not obtain this image through the GMES Space

[32] Fabing A., 2001 – Bilan spatial et structurel de l'antagonisme « Préssion Anthropique/Dynamique forestière naturelle» en zone de forte croissance urbaine. Le cas de Pointe Noire et de sa Région R. du Congo. Thèse d'université, Biogéographie. Faculté de Géographie, 46 Université de Strasbourg I. France, 321 p.

[33] Missamba-Lola, A.-P. 2004. Typologie et méthodes de réhabilitation des forêts secondaires et dégradées de Youbi (Région du Kouilou-Congo). Mémoire de maîtrise. Université Marien Ngouabi. Laboratoire de géographie physique. Biogéographie et restauration forestière. 68p.

[34] Yembé-Yembé, R. 2007. Étude de l'organisation de la filière bois-énergie en zones forestières au Congo : étude du cas des villages de la périphérie du parc national Conkouati Douli. Université Marien Ngouabi. IDR. 52p. in http://www.fao.org/docrep/013/i1973f/i1973f00.pdf

Component Data Access Portfolio. Kompsat-2 also offers significantly lower spatial resolution than WorldView-2 (4m versus 0.6m), which reduces its usefulness in for example the detection of individual trees. To complete and facilitate the multi-temporal analysis, we have requested new acquisitions at the same resolution of the WorldView-2 (see Chapter 6 on remote sensing data). In addition to the available VHR satellite images for the focal areas of 10x10km, aerial photography of 2007 received from Winrock partially covers these areas (Figure 4.3).

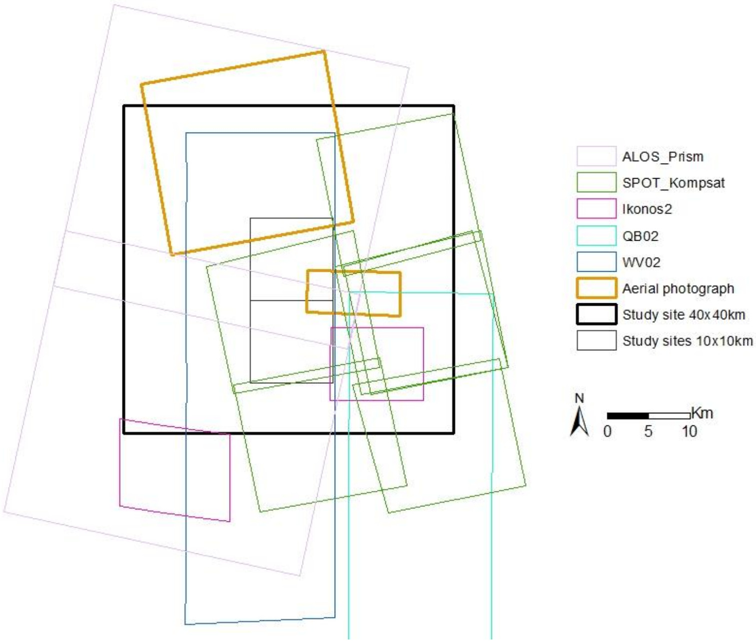

Figure 4.3: Availability of archive VHR optical images in the 40x40km Youbi test site (Congo)

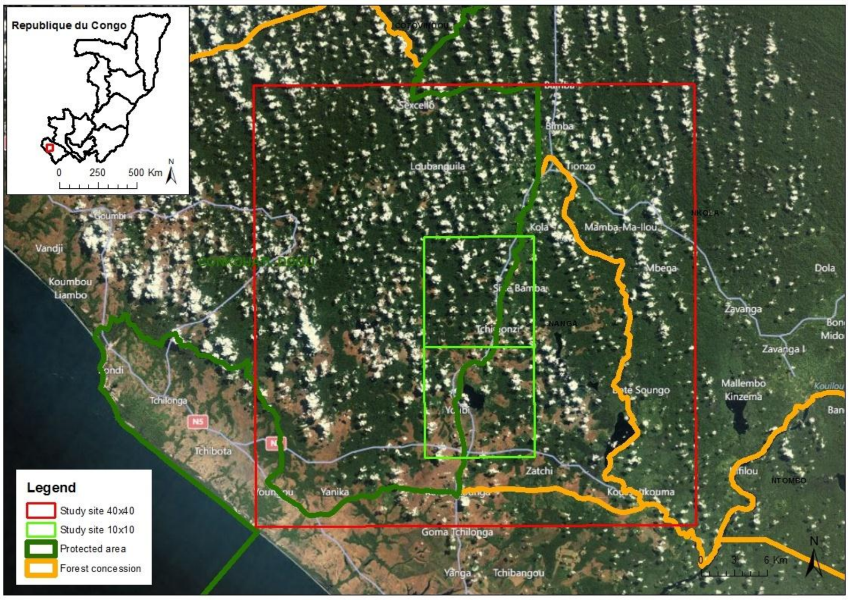

Figure 4.4: Location of the selected 20x10 km focal area (in green) for REDDiness in the area of Youbi.

4.2.2 Study site in Gabon

For Gabon, the partners MEF and IRD proposed three areas of interest: Oyem (Wloleu Ntem), the areas around the forest concessions of 'Compagnie des Bois du Gabon' (CBG in Ogooué Maritime province), and the concession of 'Société des bois de Lastourville' (SBL) near Koulamoutou (Ogooué Lolo province: Figure 4.5). The Koulamoutou area best met the selection criteria (table 4.3).

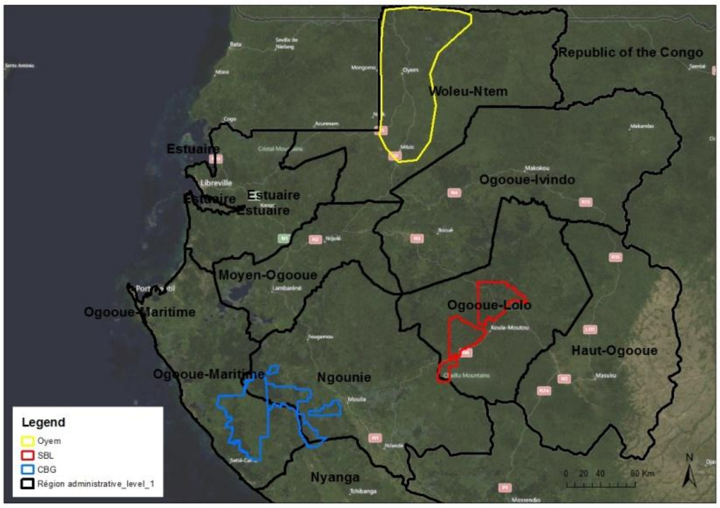

Figure 4.5: Location of the areas identified by MEF and IRD

Table 4.3: Comparison of the characteristics of the Koulamoutou area with the selection criteria

#	Selection criteria (see 4.1)	SBL	References
1	Frequent cloud cover	OK	Figure 5
2	Forest degradation	OK	Presence of forest exploitation (2008-2012) and small scale agricultural expansion
3	Accessibility	OK	Area near the town of Koulamoutou and Lastourville and crossed by a major national road (N3 and N6).
4	Forest concession	OK	SBL Forest concession
5	Degradation data	OK	Collaboration with ongoing PhD research carried out in partnership with forest companies (SBL, CBG) and Ministry of Forest. Access to statistical data on forest exploitation and management.
6	Limited relief	OK	
7	VHR data	OK	Satellite images: Quickbird

Within the Koulamoutou area, two potential study sites were proposed by IRD and local partners (figure 4.6). **Area 1** (figure 4.6: blue square) should contain logging areas, with distinct annual cutting areas from 2008 to 2012. However, from Landsat data between 2000 and 2011 this is not very visible (only a few logging roads). The site is also characterized by the presence of agricultural areas and the national road linking Lastoursville (where timber industry is present) to Koulamoutou.

Area 2 (figure 4.6: yellow square) overlaps two concessions owned by SBL. Regarding the observation of Landsat images available between 2000 and 2011, this area looks intensively exploited (opening of many forest tracks). It seems that SBL has focused its business operations in this area.

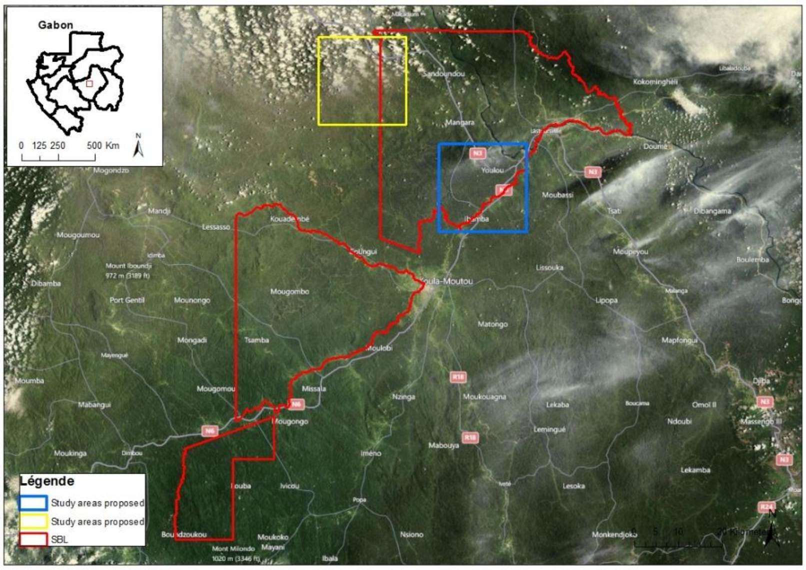

Figure 4.6: Study areas considered by local partners within the concession of SBL

To maximize our chances of observing forest degradation processes we placed our 40x40 km study site on both areas (figure 4.8). The location of the 20x10km focal area was determined by the availability of archive VHR data in the 40x40 km site.

The results of the VHR archive data search for the 40x40km study site of Gabon are illustrated in table 4.4. Figure 4.7 illustrates that archive imagery is not available in the area located in the north-west part of the 40x40 km. Therefore we selected two contiguous 10x10km sites as focal area in the southwest area (figure 4.8). A QuikBird-2 image of 25 December 2010 covers these two 10x10km test sites. The image has a reasonable quality. To complete and facilitate the multi-temporal analysis, we have requested a new acquisition of QuickBird (see Chapter 6 on remote sensing data).

Table 4.4: List of available VHR archive data within the 40x40km test site in Gabon

Archive VHR					
Sensor	**Resolution (m)**	**Number of images**	**Cloud cover**	**Acquisition date**	**Comment**
Eros B	0.7	0			
WorldView-1	0.5	1	24%	17/12/2011	40x40 area not well covered (Figure 4.7)
WorldView-2	0.5	0			
QuickBird-2	0.6	1	20%	25/12/2010	
IKONOS	1	0			
GeoEye-1	0.5	0			
SPOT-5	2.5	0		04/12/2007, 07/01/2010, 09/04/2010	
Kompsat-2	4	2	30% and 40%	12/06/2011	
ALOS-Prism	2.5	3	Between 10%and20%	40x40 area not well covered (Figure 12)	40x40 area not well covered (Figure 4.7)

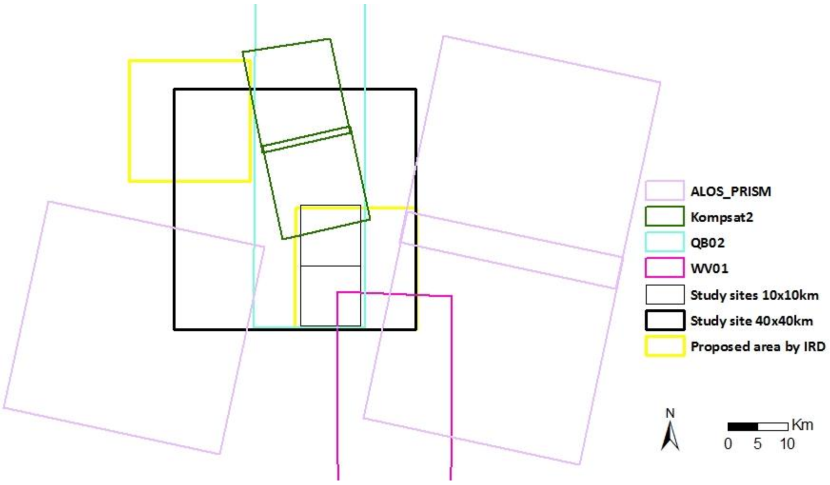

Figure 4.7: Availability of archive optical images in the 40x40km study area of Gabon

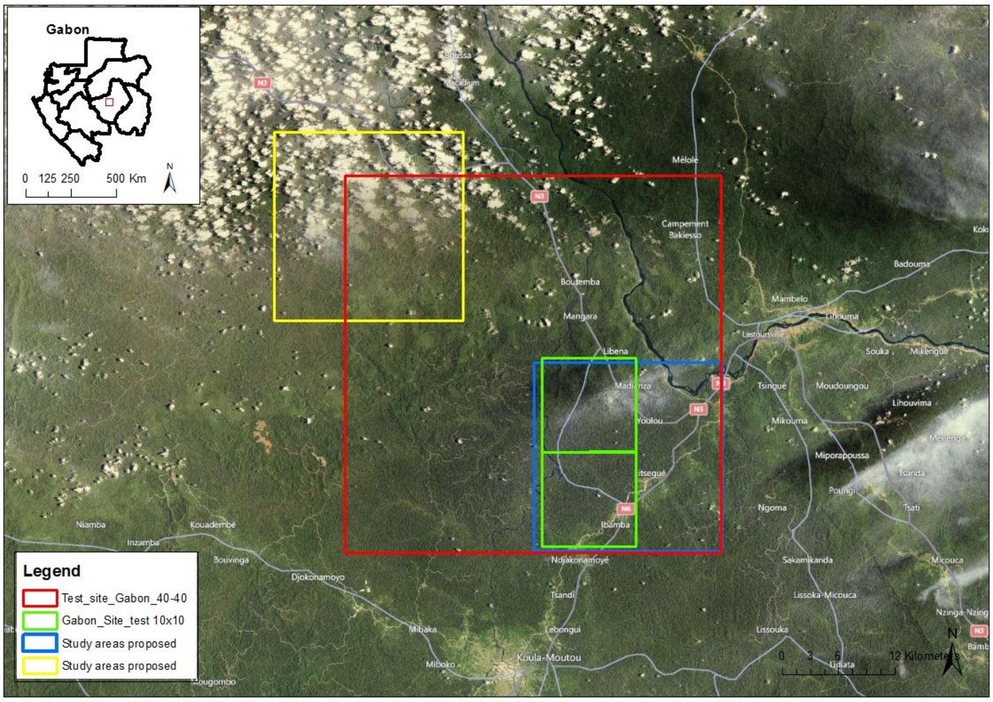

Figure 4.8: Location of the study site of REDDiness in the forest concession of SBL

5 Description of study sites

5.1 Youbi (Congo)

Youbi is a village located 90km north-west of Pointe-Noire and part of the district of Kayes Madingo. This district is one of the least populated of the Department of Kouilou with a density of 1.4 persons/km^2. According to census figures (1996), Youbi has about 500 inhabitants. The density of the area around Youbi is much higher (10.7 persons/km^2) than the entire district of Madingo-Kayes. This is related to a concentration of population along the lines of communication, allowing the flow of food, wood and charcoal.

The forest of Youbi is part of the Forest Management Unit Sud-2[35]. This Unit includes the Conkouati Reserve and the Nanga forest concession, attributed for production in 2004 to CITB. This area suffered from deforestation and degradation during its history caused mainly by forest logging and shifting cultivation agriculture[36]. In southern Congo, as in southern Gabon, there is a natural trend towards reforestation observed in forest-savannah transition areas[37].
The consequence of the demographic explosion and the rural exodus is an urban concentration, which comes with environmental effects. These include an increase of human pressure on areas up to 100 km around the urban centres (here Pointe-Noire). In these areas forests are frequently replaced by degraded formations, which have no time to develop into a secondary forest stage. This depends on many factors: shifting cultivation (reduced fallow time), fuel wood extraction (firewood and charcoal exploitation to supply the Pointe-Noire agglomeration). Even along the road network, the human settlements and the associated agricultural extension impose constraints on the forest resource (degradation in a belt of 5 to 10 km around the villages).

On the other hand, areas that are far away from the agglomeration became human deserts in which forest expands with only bush fires potentially stopping this expansion. In these areas, logging does not lead to forest degradation in the case where logging is not followed by agriculture.[38]

The main factors and activities leading to forest degradation in and around the study area are:

- *Population growth* is probably the main factor of deforestation and forest degradation. Population density in Kouilou (7 inhab/km2) is among the highest –densities in the country. Population is concentrated on the coastal areas, near the infrastructure. The economic conditions of the region are considerably degraded since 15 years, which has led to a comeback of urban inhabitants to the rural areas[39]. Natural resource exploitation is often the only way for rural and also urban people to ensure their subsistence, since other economic activities do not exist. A distinction of urban and rural people is necessary in order to describe the deforestation process. An increase of rural population leads to a reduction of the fallow duration and, in the midterm, to land degradation. It often takes place in the

[35] The Congolese permanent forest domain is divided into Forest Management Units (FMU). FMU have specific management objectives, which can be production (forest concession) or conservation (national park and other types of natural resources protection areas). Some FMUs, such as the FMU Sud 2, can be further subdivided into smaller units with specific management objectives.
[36] Missamba-Lola, A.-P. (2004).
[37] Bigot, 1996. Stabilité de la variation pluviométrique de l'Afrique tropicale entre 1951 et 1988, Dynamique à long terme des écosystèmes intertropicaux, CNRSI Orstom : 13-16.
[38] Fabing A. (2001).
[39] Fabing A. (2001).

secondary forest but when the population pressure becomes stronger, primary forest can be attacked. An urban population growth (natural growth and migrations) increases the food demand and creates an economic market which initially is a subsistence system: in this way the impact on deforestation depends on the accessibility, and therefore on the road network quality.

- Degradation is mainly associated with the *supply in fuel wood for the city*: it becomes an easy way to earn money, and is the principal activity of the migrants out of the civil war (refugees village where the main activity is the charcoal production). The study area is located in the provision area of large cities, such as Pointe Noire.
- The *logging concessions* do not represent a major risk of degradation; usually they exploit a few valuable species (Niove, Okoumé etc.) without drastically reducing the canopy cover. On the other hand, logging operations open new forest tracks for exploitation: cultivators use these new openings to penetrate into deep forest.
- *Burned areas* are often found in secondary forests, since regular fires are important components of the shifting cultivation system, these fires are spatially limited by the forest-savannah boundary but can be amplified by the wind.

5.2 Koulamoutou (Gabon)

Koulamoutou is located 350km south-west of the capital city Libreville, and is the capital (chef lieu de province) of the Ogooué Lolo province in central Gabon. The estimated population of the city is 15,000 inhabitants, corresponding to one of the smallest provincial capitals of the country, mainly because of its isolation from the main transportation network and low accessibility. Koulamoutou lies at the confluence of the rivers Lolo and Bouenguidi, and the N6 road. The area is located at 50km of the town of Lastourville (6,000 inhabitants), which is linked with Libreville by railway. The Ogooué Lolo province is one of the lowest populated areas in Gabon (1.7 persons/km^2).

The study site covers a part of the SBL (Société des Bois de Lastourville) forest concession (Concession forestière sous aménagement durable, CFAD). Rural population around the SBL forest concession is estimated to 9,000 inhabitants, mainly located along the road axes[40]. The forest company is installed in Lastourville since 1986, mainly exploiting the forest concessions attributed alongside the creation of the railway (ZACF: zone d'attractivité du chemin de fer). Since the end of the 1990s, SBL has implemented a transformation unit in Lastourville. A management plan for the forest concession is approved since 2003.

Visible anthropogenic drivers of deforestation and degradation are not well documented in Gabon. Despite the difficulty to evaluate their significance, the main, direct causes of deforestation and degradation in and around the study area include:

- *Development of agricultural* activities and settlement of populations near urban areas and along the main infrastructure: even if demographic pressure is not a decisive factor of deforestation and degradation given the low level of population in the area, movement of rural populations towards urban centers clearly put pressure on forest areas located near cities and roads;
- *Logging* for timber and construction is the main cause of degradation. The province is covered for about 90% by logging concessions. The opening of the railway in 1986 las led to

[40] SBL (2004). Plan d'aménagement de la CFAD SBL/TRB.

the attribution of large areas of forest for production in the so-called ZACF. The study area almost fully included in the SBL forest concession.

6 Remote sensing data

6.1 Optical images

REDDiness concentrates on forest degradation which implies that expected changes mostly occur at finer scales. Therefore, the availability of optical images was evaluated through an extensive search in the archives of very high and high resolution data (see also Chapter 4 on site selection for very high resolution data). Coarse resolution data (>50m) such as MERIS, MODIS and SPOT VEGETATION is considered irrelevant for our project. The availability of optical high and very high resolution data from 2007 to present has been analysed. In order to perform change detection analysis and monitor forest degradation on both sites, new VHR imagery acquisitions were ordered on February 1, 2012. The following data parameters were requested in the Service Project off-line Data Request Form (SPDRF, see annex 1 and 2): Orthorectified bundle (Multispectral + Panchromatic) imagery of 0,6m sensor resolution with a maximum cloud cover of 20%. In additional comment, we specified a preference for an acquisition from the same sensor than the archive imagery to facilitate image comparison.

6.1.1 Congo optical imagery

Table 6.1 summarizes the optical very high and high resolution images that were used in the REDDiness project for the Congo site. As very high resolution, we acquired two images. (1) One Worldview-2 imagery (8 multispectral bands; 2m pixel size and 1 panchromatic band; 0,5m pixel size) acquired on 11th Augustus 2011 from the archive. (2) One QuickBird image acquired on 12th July 2012, it is a new acquisition that was requested through the GMES Space Component Data Access Portfolio. Although the acquisition request was made in February 2012 for both sensors – QuickBird and WorldView-, it took more than five months before the first acceptable acquisition was made and we didn't get a WorldView. This long interval is due to the persistent cloud cover in the area. Figure 6.1 shows an overview of the very high resolution imagery for the Congo study site. For high resolution data, 45 DMC images were found on archive but none of these had a reasonably low cloud cover. The Landsat archive provides only a limited number of images of good quality (low cloud cover) which suffer from the SLC-off (Scan Line Corrector Failure) since May 2003. Only one SPOT image was found in the archives below the cloud cover threshold of 40% (for 4 February 2011 with 8% cloud cover). Nonetheless, it was too hazy to be used in a degradation purpose.

Table 6.1: Summary of optical scenes used for the Congo study site.

Satellite	Sensor	Resolution MS (Pan)	Number of bands (MS)	Cloud cover % in 20x10km site	Dates
WorldView-2	WorldView-2	2.0m (0.5m)	8	15 (archive)	2011-08-29
QuickBird	BGIS	2.4m (0.6m)	4	15 (new)	2012-07-12
Landsat-7	ETM+	30m (15m)	7	9	2011-04-08
				25	2009-12-30

In addition to the optical satellite images, through Winrock we obtained a set of aerial photographs that were acquired between 28th and 31st October 2007. The aerial photos consist of three bands acquired from a reflex numerical camera (Canon Marc III) linked to a GPS and an IMU (inertial measurement unit) station put in an airplane. 185 aerial photographs covering an area of 22 km^2 in the north east part of the study site (Figure 6.1) were acquired by the Winrock team on 28th, 29th, 30th and 31st October 2007.

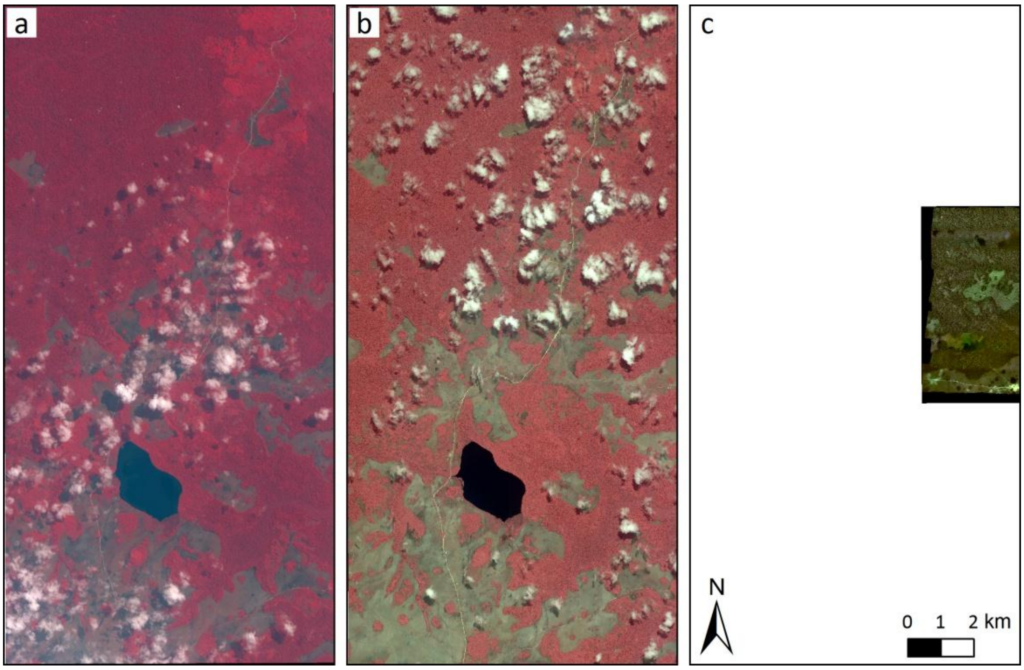

Figure 6.1: Overview of the very high resolution images available for the 20x10 km Congo study site: a) QuickBird image of July 2012, b) WorldView-2 image of August 2011, c) aerial photographs from Winrock (October 2007).

6.1.2 Gabon optical image availability

Figure 6.2 shows the optical very high and high resolution images that were used in the REDDiness project for the Gabon site. We acquired two QuickBird images: (1) one from the archives of 29th December 2010 (4 multispectral bands; 2,4m pixel size and 1 panchromatic band; 0,6m pixel size); (2) one new acquisition, requested together with the images for the Congo test site. The acquisition interval for the Gabon test site was shorter, a little more than one month. For high resolution, as for Congo, a good number (44) of DMC images was in the archives, but none of them had a reasonably low cloud cover. The Landsat archive has better availability of imagery with limited cloud cover, although it has the SLC-off (Scan Line Corrector Failure) problem since May 2003 (Table 6.2).

Table 6.2: Summary of optical scenes used for the Gabon study site.

Satellite	Sensor	Resolution MS (Pan)	Number of bands (MS)	Cloud cover estimate (%) in 20x10km site	Dates
QuickBird	BGIS	2.4m (0.6m)	4	7	2012-03-12
				10	2010-12-25
Landsat-7	ETM+	30m (15m)	7	5	2011-03-04
				2	2009-05-20

The analysis of the SPOT archive (10 and 20m resolution) with a maximum of 40% cloud cover showed that 3 images could be partly used but their cloud cover percentage is relatively high (>30%). As for the Congo, these images aren't useful in the purpose of mapping the degradation.

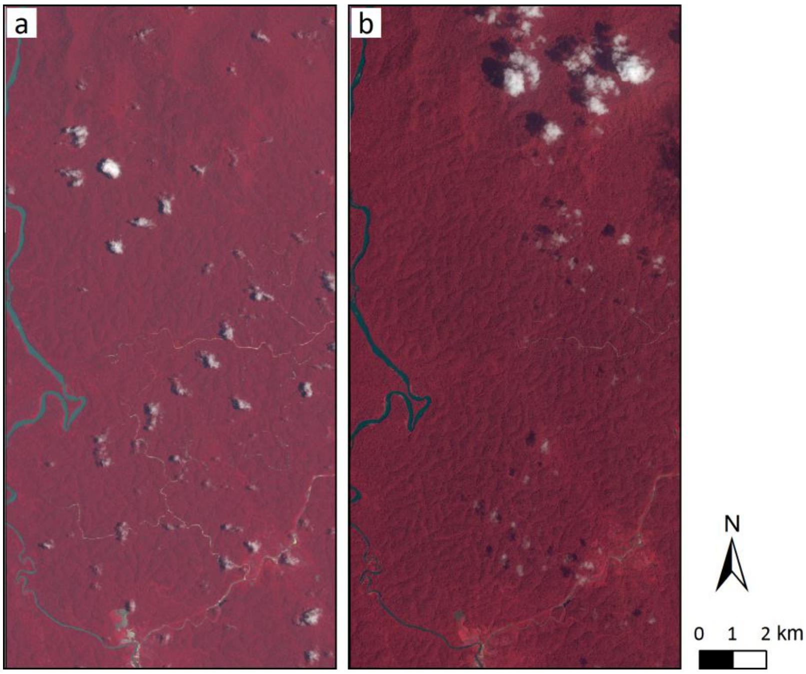

Figure 6.2: Overview of the QuickBird images for the 20x10 km Gabon study site: a) July 2012, b) December 2010.

6.2 SAR images

A detailed analysis of archive SAR data was performed to establish SAR satellite data availability (high and very high resolution) for both study areas during the past 10 years. Several of the current SAR systems can acquire data at multiple resolutions through imaging in different modes. For example COSMO-SkyMed offers very-high resolution SAR (up to 1m), but for both sites (and generally also over large parts of the country) the archives only contain data in wide mode (i.e. 30 m resolution). Below we separately summarize the acquired SAR data for Congo and Gabon. All archive and new acquisitions were freely obtained through the GMES Space Component Data Access Portfolio. All 2012 imagery resulted from image acquisition requests.

6.2.1 Congo SAR data

The Congo study site had limited availability of very high resolution SAR data in existing archives. The most interesting acquisition available was a single TerraSAR StripMap scene (3m resolution) acquired on 8 June 2010. We complemented this archive scene with a new acquisition using the same imaging characteristics. In addition we acquired one new very high resolution (1m) TerraSAR acquisition for the 20x10km study area to evaluate the added value of increased resolution in SAR data. The archive image availability was larger for recent high resolution data. A priori, we judged ENVISAT ASAR and ALOS PALSAR to be the most useful for their multi-temporal coverage with the same imaging characteristics. While we planned on a large number of new SAR acquisitions with ENVISAT (including multi-temporal dual-polarized data), unfortunately ESA lost contact with the satellite during April 2012. In addition we found interesting RADARSAT-2 acquisitions that could be complemented with two new acquisitions using the same mode and incidence angle. Table 6.3 summarizes the SAR data that was acquired for the Congo site. All images fully cover the 20x10 km study site, with the only exception of the TerraSAR High Resolution SpotLight images that miss out on the western and eastern edges (at maximum 1 km).

Table 6.3: Acquired SAR scenes for the Congo study site.

Satellite	Sensor	Resolution	Band	Polarization	Dates	Details
TerraSAR-X	Idem	1m	X	HH	5 dates between 2012-02-25 and 2012-04-20	High Resolution SpotLight HS-300 39° incidence angle
TerraSAR-X	Idem	3m	X	HH	2010-06-08 2012-05-01	StripMap 37.8° incidence angle
ENVISAT	ASAR	30m	C	VV	2006-04-21 2011-03-24 2012-03-18	Image mode 23° incidence angle
ENVISAT	ASAR	30m	C	VV	2010-04-27	Alternating Polarization 33°
ALOS	PALSAR	20m	L	HH+HV	2007-08-22 2008-08-24 2008-10-09 2009-07-12 2009-10-12 2010-05-30 2010-08-30 2010-11-30	Fine Beam Dual 38.8° incidence angle ascending
ALOS	PALSAR	10m	L	HH	2007-02-19 2007-10-07 2008-04-08 2009-02-24 2010-04-14 2011-03-02	Fine Beam Single 38.8° incidence angle ascending
ALOS	PALSAR	+- 30m	L	HH+HV+VH+VV	2009-03-20 2010-11-08 2011-03-26	Fine Beam Polarimetric 24° incidence angle
RADARSAT-2	SAR	8m	C	HH	2009-12-09 2010-03-15 2012-03-04	Multi-Look Fine 34.8° incidence angle ascending
RADARSAT-2	SAR	8m	C	HH	2009-12-13 2010-03-19 2011-04-01	Multi-Look Fine 48.1° incidence angle descending

6.2.2 Gabon SAR data

After careful examination of TerraSAR, RADARSAT-2, and COSMO-SkyMed, we found that at the start of 2012 no very high resolution SAR data was available for the study site. Therefore within the REDDiness project it was not possible to perform multi-temporal comparison of high resolution SAR data at the Koulamoutou site. Nonetheless we acquired a number of new TerraSAR acquisitions, including a 3m resolution StripMap scene, and a 1m resolution High Resolution SpotLight coverage of the 20x10 km area (consisting of five scenes) for mono-temporal comparison with optical data, and evaluating whether forest degradation signs can be detected. High resolution SAR data was available in the archives from ENVISAT ASAR and ALOS PALSAR including multi-temporal coverage. As for Congo, we planned to acquire a large number of new SAR acquisitions with ENVISAT (including multi-temporal dual-polarized data), but this was impossible after ESA lost contact with the satellite in April 2012. Table 6.4 summarizes the SAR data that was acquired for the Gabon site. As for Congo, the TerraSAR High Resolution SpotLight images miss out on the western and eastern edges (at maximum 1 km) of the 20x10 km site.

Table 6.4: Acquired SAR scenes for the Gabon study site.

Satellite	Sensor	Resolution	Band	Polarization	Dates	Details
TerraSAR-X	Idem	1m	X	HH	5 dates between 2012-02-20 and 2012-04-04	High Resolution SpotLight HS-300 33° incidence angle
TerraSAR-X	Idem	3m	X	HH	2012-04-15	StripMap 33° incidence angle
ENVISAT	ASAR	30m	C	VV	2005-08-19 2006-12-22 2011-03-24 2012-03-18	Image mode 23° incidence angle
ENVISAT	ASAR	30m	C	VV	2010-04-27	Alternating Polarization 33°
ALOS	PALSAR	20m	L	HH+HV	2007-08-17 2008-08-19 2008-10-04 2009-07-07 2009-10-07 2010-08-25 2010-10-10	Fine Beam Dual 38.8° incidence angle ascending
ALOS	PALSAR	10m	L	HH	2007-02-14 2008-02-17 2009-02-19 2010-02-22 2011-01-10 2011-02-25	Fine Beam Single 38.8° incidence angle ascending
ALOS	PALSAR	+- 30m	L	HH+HV+VH+VV	2010-11-03	Fine Beam Polarimetric 24° incidence angle

7 Fieldwork missions and reference data collection on forest degradation patterns and processes

7.1 Introduction

The main objective of the fieldwork missions was to collect ground observations in terms of forest degradation patterns and processes, by means of field interviews, GPS receivers (georeferenced data), informed by a fieldwork observations form and illustrative pictures. As additional objective, the missions aim to strengthen the capacities of local staff and partners. The participants were trained on the use of GPS and the collection of georeferenced data, the integration of data in ArcGIS and on the comparison of degradation evidences seen on the satellite images and on the field. The training is described in more details in the report of the WP4.

These data observed and collected on the ground were selected to be representative of the various land use and land cover change in the study areas of the project. The observations collected at the level of the selected transects or priority zones will have to allow to verify and/or to support the interpretation of the satellite images available on the study areas (optical and radar). The proposed protocol for data collection does not aim to supply a statistical validation of the results.

7.2 Methodological approach

7.2.1 EO data processing

The EO data acquired in the framework of this project were processed according to the methods described in the next paragraph. To support the field protocol for reference data collection, preliminary classifications of the VHR optical images and visual analyses were done. The data acquisition has been oriented mainly on changes areas and on areas where the land cover was not obvious. As additional reference data for the Gabon, a Landsat based map – Forest cover and forest cover change[41] - has been used to guide the mission (Figure 7.1). The main preliminary results considered for both study areas are listed in Table 7.1.

Table 7.1: EO data used for field mission support

Datasets	Gabon Koulamoutou study area	Congo Youbi study area
Landsat ***Chapter 8***	Preliminary NDFI analyses	Preliminary NDFI analyses
VHR ***Chapter 9***	Land cover and land cover change maps based on Quickbird 2010 and 2012	Land cover and land cover change maps based on Worldview 2011
Radar ***Chapter 10***	-	Areas of interest based on Radarsat-2 2010 and 2012

[41] Mbeme, F. (2012). Télédétection et SIG : Applications à l'étude de l'évolution des modes d'occupation du sol et des changements du couvert forestier du Sud Est Gabon, région de Koulamoutou – Lastrouville entre 2000 et 2011. Stage de Master 2 GEEFT, AgroParisTech.

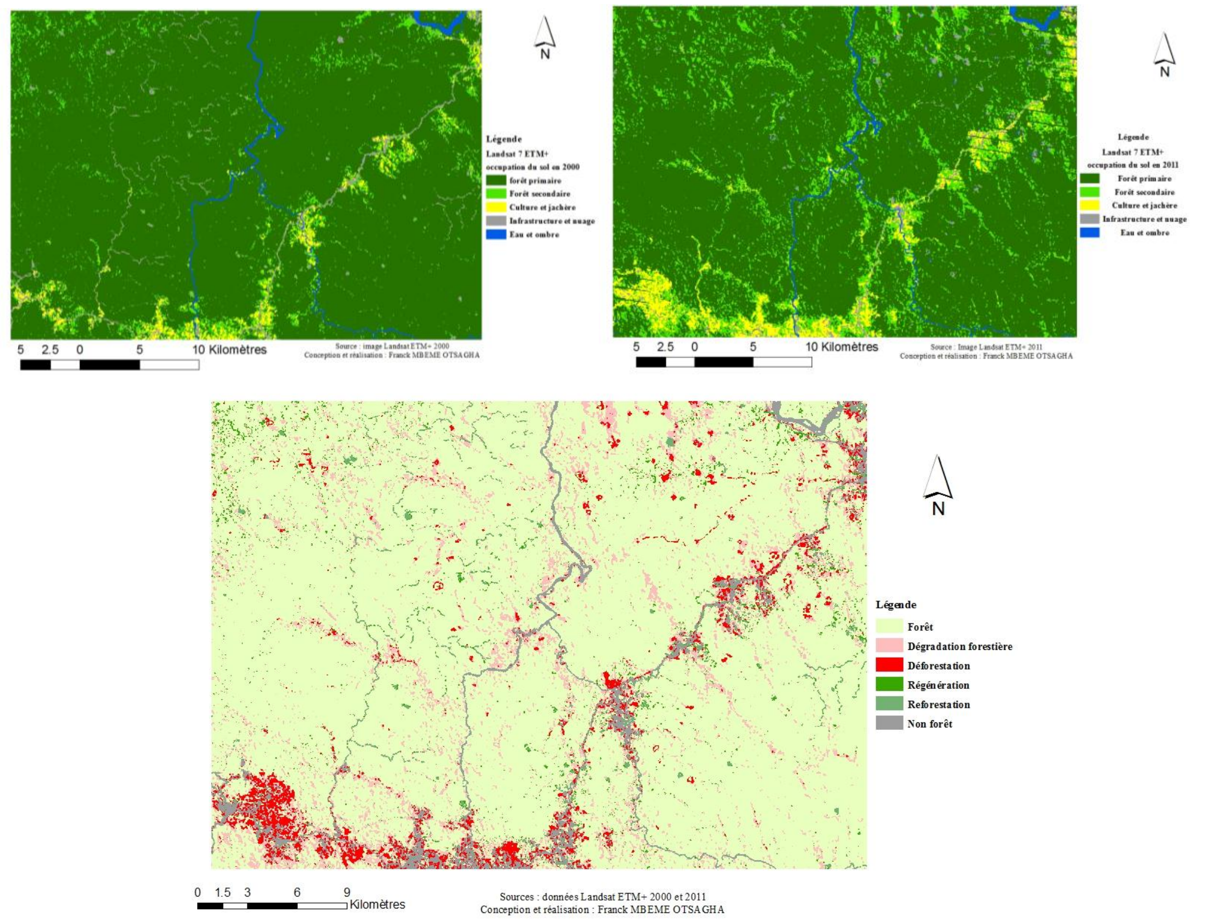

Figure 7.1: Forest cover and forest cover change maps based on Landsat 2000 and 2001 Koulamoutou area, Gabon. The images represent: (a) Land cover map 2000; (b) Land cover map 2011 and (c) Forest cover change map 2000-2011.

7.2.2 Field data collection protocol and activities

The proposed protocol for data collection did not aim to supply a statistical validation of the results: the data collected on the ground were selected in order to be representative of the various land use and land cover change in the study areas of the project. Figure 7.2 shows the priority area and the distribution the ground control points (GCPs) taken by GPS for both study sites. The number of points is limited by the budget which constrained the acquisitions along roads and waterways mainly. For a set of ground control points, a field form was completed and illustrative pictures were taken to further support the EO data processing. The field form elaborated for these missions is presented in annex (Annex 13.1). Field missions planning, duration and teams are presented in Table 7.2.

The main expected outcomes from these field missions were:

- field observation form completed for selected GCPs;
- georeferenced field observation pictures;
- GPS points and transects;
- field observation on land cover and land cover change maps preliminary results;
- field report.

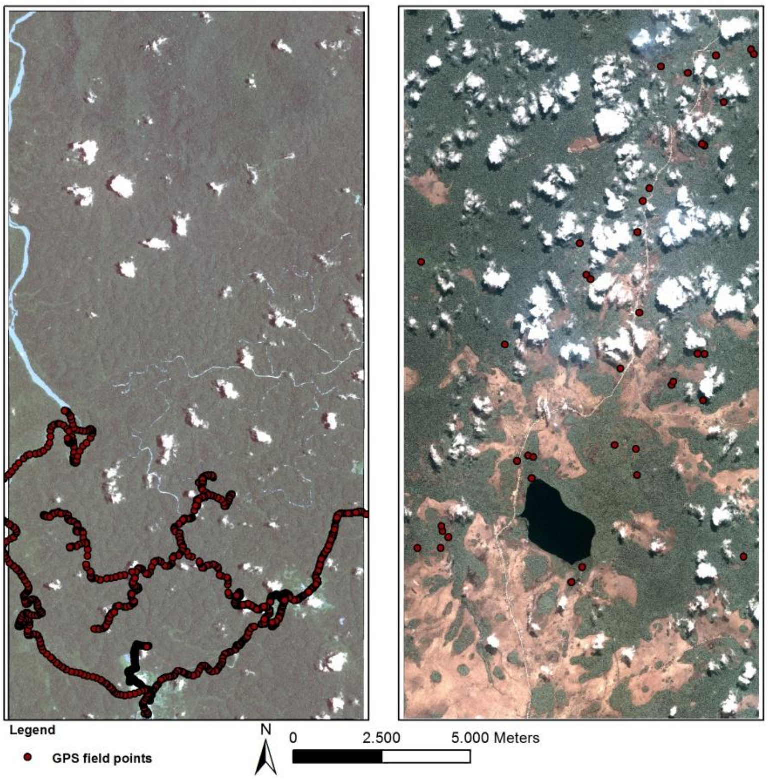

Figure 7.2: Location of the GCPs taken on the field for both study sites: (a) Koulamoutou area, Gabon – image QuickBird 2012 and (b) Youbi area, Congo – image WorldView 2011.

Table 7.2: Field missions planning, duration and teams for Gabon and Congo

	Gabon Koulamoutou study area	Congo Youbi study area
Date	June 4-16, 2012	August 20 – September 4, 2012
Activities	Field planning and training session (June 4-8) Field mission (June 9-16)	Field planning (August 20-22) Field mission (August 26 – September 4)
Team	Bruno NKOUMAKALI Sylvestre MAKAK Franck Landry MPAGA Jean Olivier BIVIGOU Franck LEMPEMANGOYE Médard OBIANG EBANEGA Jean Aurélien MOUKANA LIBONGUI Benoit MERTENS Paulin Franck MBENE Louis Fichet Caltrant Evrard MAYOMBA Willia LITCHANGOU NKOLO AGANGA Aston Saturnin NDOTITMANGHIENGA	Fidèle NGOUISSANI (Chauffeur) Yvon NGONGOYOU Chérubins Brice OUISSIKA Dabney MATOKO KOUEDIATOUKA Bertrand ONKA TSIBA

7.3 Field observations and reference data

Preliminary versions of the field missions for both study areas are available, and produced in the Framework of the WP4:

- Nkoumakali, B., Mertens, B. (2012). Rapport intermédiaire des actions de renforcement de capacités au Gabon: sessions de formation en télédétection et mission de terrain. REDDiness WP4. Del. 4.1.a
- Ouissika, C.B. (2012). Rapport intermédiaire de mission à Youbi, Congo. REDDiness WP4. Del. 4.1.b

These reports provide details on field activities, methods and results, including the ground observations and pictures for the selected priority areas or points of interest identified. Figure 7.3 provides an example of ground observations linked with EO data processing.

Figure 7.3: A Ground observation transects, and geo referenced field pictures – Gabon. (Google earth view for illustration)

8 NDFI analysis from high resolution optical data

8.1 NDFI: an introduction

The Normalized Difference Fraction Index (NDFI) is a method successfully applied in the Brazilian Amazon to identify and distinguish forest degradation caused by selective logging and associated forest fires from other natural disturbances[42]. The NDFI combines the information of several component fraction images defined by Spectral Mixture Analysis (SMA). The interpretation of NDFI images are facilitated by a contextual classification algorithm (CCA). The CCA uses the location of log landings as contextual information and the NDFI as the spectral information sensitive to canopy damages. Tested in the Southern Brazilian Amazon, this method is currently being tested in the Congolese context within the WRI project. OSFAC has been trained to apply NDFI methods to map forest degradation in Congo. Within REDDiness, OSFAC will test the NDFI approach in our two study areas.

According to Souza et al.[43], the Spectral Mixture Analysis (SMA) overcomes some of the problems of visual interpretation and conventional image processing techniques. The soil fraction derived from SMA enhances the detection of the log landings and logging roads, which have been recognized as the spatial signature of mechanized logging in tropical forests. Green vegetation (GV) fraction is used to estimate forest canopy damage associated with selective logging. The non-photo-synthetic vegetation (NPV) fraction quantifies levels of forest degradation caused by burning. NDFI combines the GV, NPV, soil and shade fractions that were extracted through SMA (using Landsat imagery). NDFI showed a higher percent change between intact forest and forest degradation classes, when compared to the changes detected by any of the individual fraction images. However, the authors mentioned that detection of non-mechanized logging seems not possible with this technique. Given the general small-scale changes in the central African context (i.e. different degradation processes), the potential of NDFI for Congo and Gabon needs to be examined.

8.2 Methods

The NDFI is calculated using "ImgTools" developed by Imazon for quantitative analysis of forest degradation and deforestation[44]. Figure 8.1 shows the equation with which NDFI is calculated. The NDFI has generally been applied on multispectral Landsat data, although it could potentially work on other multispectral data. We applied the NDFI to available Landsat imagery for both study sites. Some steps of the image processing were done with ENVI software (creating a multi-bands image, calculation of reflectance). To calculate NDFI for each image, we followed four main steps:

[42] Souza, C.M., Roberts, D.A., Cochrane, M.A., 2005. Combining spectral and spatial information to map canopy damage from selective logging and forest fires. Remote Sensing of Environment 98, 329-343.
[43] Souza and al, 2005.
[44] Souza and al, 2005.

$$NDFI = \frac{GV_{Shade} - (NPV + Soil)}{GV_{Shade} + NPV + Soil}$$

$$GV_{Shade} = \frac{GV}{100 - Shade} \qquad -1 \leq NDFI \leq 1$$

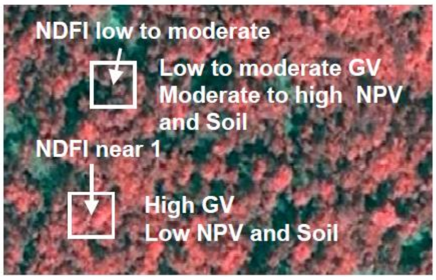

Figure 8.1: Calculation of the Normalized Difference Vegetation Index (Souza et al., 2005)

8.2.1 Data preparation

For each Landsat scene we selected the 6 spectral bands at 30m resolution in the visible and near infrared and created a data stack.

8.2.2 Pre-processing

Generally, the radiance that is recorded in optical satellite images is normally affected by atmospheric effects due to the presence of for example aerosols and clouds. Effective analysis of the optical remote sensing imagery requires a correction for such effects.

The image preprocessing is to eliminate fog, perform radiometric calibration and atmospheric corrections. The parameters used for atmospheric corrections are: type of sensor, images acquisition date, time when satellite pass, sensor altitude, topography, pixel size, aerosol, ground visibility, etc. (Figure 8.2). Elimination of fog and radiometric calibration are realized in “ImgTools”, while atmospheric corrections in ENVI.

8.2.3 Processing

The processing consists in Spectral Mixture Analysis (SMA) to calculate the reflectance images, remove clouds, water bodies and finally calculation of NDFI.

The NDFI is scaled between -1 and 1. However, the ImgTools software scales these values between 0 and 200 (8-bit output). This output is normally displayed with a specific colour scheme to improve the readability of the image and facilitate its interpretation. This can be done following this procedure:

- ENVI →File →Open Image file→ Select the created NDFI image (ex. 184_61_20090520_ndfi)
- On the window where the NDFI image is displayed, click →**Tools**→ Color maping→ENVI Colors tables→NDFI[45].
- Then in the same window, do : **Enhance**→Interactive stretching→Stretch : 1st value = 0 and 2nd value is 200.

[45] A specific ENVI colour scheme (*.tbl) for NDFI needs to be copied in: **C:\Program Files\ITT\IDL708\resource\colors**

8.2.4 Classification and Post Classification

Results of the NDFI calculation can show changes in a holistic manner without differencing between classes of deforestation and those of forest degradation; classification and post classification must be done (accuracy test) to better discriminate types of changes.

8.3 Results

The NDFI is calculated for both 20x10 km sites using Landsat images of the years 2009, 2011 for Gabon and 2009 and 2011 for Republic of Congo (RoC). For Gabon, changes are not visible in the area of interest except for the south, along the roads and around human settlements. For the Republic of Congo, the NDFI calculation was made on 2009 and 2011 images. Because of the poor quality of the 2009 image (presence of many clouds), it was not possible to compare multi-temporal images that would allow to identify changes. Figures 8.2 shows the results of the NDFI calculation for both countries (Gabon and Congo).

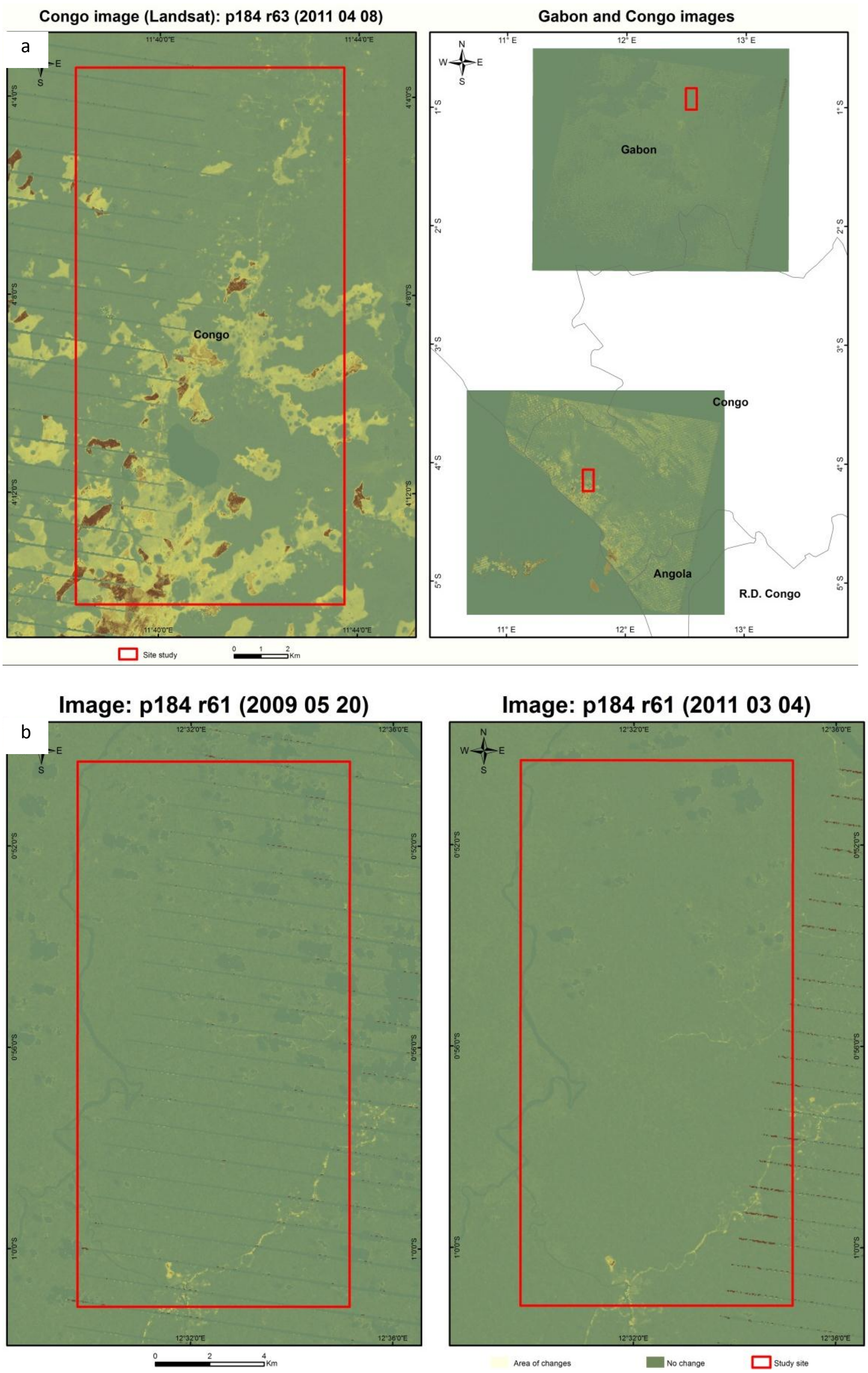

Figure 8.2: NDFI results for Congo (a) and Gabon (b)

8.4 Conclusions

The objective of this study is to examine the possibility of using NDFI to detect forest degradation in Central Africa.

Application of NDFI method shows some changes (deforestation and forest degradation) in the southern part of Gabon site, along roads and around human habitat. Thematic classification using field data/field observations may allow discriminating areas of deforestation and those of degradation.

In Republic of Congo, it was not possible to compare images to highlight the changes due to the quality of the second (2009) images used (presence of clouds).

Ultimately, we can note that:

- In some areas of Central Africa, permanent clouds make very difficult the use of optical images as Landsat for forest monitoring. To ensure correct application of NDFI method, it would be necessary to increase the frequency of image acquisition to have chance to find some data cloudless or little contaminated.
- Forest degradation in Central Africa often involves little extensive areas while pixel resolution of Landsat imagery used is 30 m. May need to check the possibility of using high spatial resolution images such as SPOT, ASTER, etc. for NDFI analysis.

9 Optical very high resolution

9.1 Introduction

In the Congo Basin, forest degradation is often characterized by small scale changes in forest cover. However, as stated by the GOFC-Gold sourcebook, gaps in the canopy caused by certain non-mechanized selective logging activities (both illegal and legal) cannot be detected using high resolution data such as Landsat because these activities create small forest gaps and little canopy damage. Very high resolution imagery, such as Quickbird or Worldview, is required to directly map forest canopy damage of these types. Therefore, within REDDiness, we tested whether very high resolution optical data is able to detect forest canopy gaps and small clearings. At this resolution, two approaches are generally used to map forest canopy damage, namely (i) visual image interpretation and (ii) automated segmentation. Visual delineation of canopy gaps and small clearing is more accurate but time-consuming, whereas automated segmentation is faster but provide false positive errors that usually requires some visual interpretation and manual editing after classification which lead to a semi-automatic classification.

We choose to apply the semi-automatic classification methodology to detect canopy gaps and small clearings. This methodology combines advantages of manual and automatic techniques. Besides classification from mono-temporal images, multi-temporal analysis is carried out to (i) enhance areas where changes occurred and (ii) estimate different levels of degradation by creating a classification highlighting differences between both dates. The classification results are subsequently compared to field survey data obtained from both study sites (see Chapter 7).

As described in the section 6.1, the persistent cloud cover in the Congo Basin limits the availability of optical imagery and induces a large delay in the acquisition of our new images, especially for Congo. This delay had a negative impact on the project schedule by limiting drastically the time period needed to perform change detection analysis. Moreover, the presence of a relatively high percentage of cloud cover (~20%) over the acquired images decreases areas where change detection can be performed. These acquisition limitations underline the difficulty of obtaining optical satellite imagery in the Congo Basin and confirm that the REDDiness consortium took the right strategic decision when we decided to evaluate in parallel the potential of radar data.

This chapter reports on the methods used for pre-processing and change detection analysis (section 9.2). Then, it provides separately results for the study sites in Congo and Gabon (section 9.3). Finally, we draw overall conclusions on the usefulness of VHR optical data to detect forest degradation (section 9.4).

9.2 Methods

Deforestation or forest degradation maps can be derived in two ways from optical VHR data: visually by a human interpreter or quantitatively by a computer-based automated procedure. The former method has the advantage of using human pattern recognition, which is still far superior to any machine-based vision technique in terms of accuracy. Unfortunately, it is also tediously slow when compared to the processing speed of automated procedures. Most of the time, semi-automated image classification methods are proposed to combine the advantages of both techniques. The most common techniques to quantitatively derive thematic maps from remotely sensed imagery are either pixel-based or object-based. Van de Voorde et al. (2004)[46] compared both techniques while dealing with VHR imagery and concluded that object-oriented methods are potentially best suited to manage the increase in resolution and the complex content of these images. As stated by Duveiller et al. (2008)[47], no automated change detection method was found to be as efficient as visual interpretation. Therefore, a semi-automatic classification was chosen in the image processing method carried out in this study. The automatic classification, used to produce all optical maps, is an object-based image analysis approach applied in the eCognition software, which enables to partition an image into precise object shapes (segments) and assign them a class[48].

Monitoring forest degradation using remote sensing techniques implies to monitor area changes within forest land which leads to changes in carbon stocks[49]. According to Herold et al. (2011)[50], the features of interest to be enhanced and extracted from the satellite imagery to directly detect forest degradation consist of forest canopy gaps and small clearings. As the study sites of REDDiness are located in a forest concession, logging activities are assumed. Therefore, damage is supposed to be associated with areas of tree fall gaps and clearings associated with logging roads, log landings (i.e., areas cleared to store harvested timber temporally) and skid trails[51].

Forest change detection requires a preliminary forest delineation to exclude irrelevant other classes and focus the analysis only on forest changes[52]. The method tested here for forest degradation mapping includes 4 steps: (1) the image pre-processing, (2) the forest/non-forest classification, (3) the multi-date segmentation and (4) the forest change detection. Based on the pre-processed satellite images, a forest/non forest classification is performed for each image (t_0 and t_1). Both classifications are then superposed to identify areas of forest at t_0 remaining forest at t_1. All changes superior to 0.5ha are considered as deforestation and are not used in the following developments. On the contrary, all changes below 0.5ha are kept to analyse the degradation processes (see Figure 9.1 and section 9.2.2 for more details). The subsequent change detection analysis is performed within these areas to stratified forest degradation into different disturbance levels. The processing steps are illustrated in the chart below (Figure 9.1).

---

[46] Van de Voorde, T., De Genst W., Canters F., Stephenne N., Wolff E., Binard M., 2004, Extraction of Land Use / Land Cover - Related Information from Very High Resolution Data in Urban and Suburban Areas, 23rd EARSeL Annual Symposium 2003, Gent, Belgium; 2-5 June 2003.

[47] Duveiller G, Defourny P, Desclée B, Mayaux P. 2008, Deforestation in Central Africa: estimates at regional, national and landscape levels by advanced processing of systematically-distributed Landsat extracts. Remote Sensing of Environment 112: 1969–1981

[48] Baatz, M. & Schäpe, A. 1999. Object-oriented and multi-scale image analysis in semantic networks. Proc. of the 2nd International Symposium on Operationalization of Remote Sensing, August 16th-20th 1999. Enschede. ITC

[49] GOFC-GOLD, 2010, A sourcebook of methods and procedures for monitoring and reporting anthropogenic greenhouse gas emissions and removals caused by deforestation, gains and losses of carbon stocks in forests remaining forests, and forestation. GOFC-GOLD Report version COP16-1, (GOFC-GOLD Project Office, Natural Resources Canada, Alberta, Canada)

[50] Herold et al.(2011). Options for monitoring and estimating historical carbon emissions from forest degradation in the context of REDD+. Carbon Balance and Management 6:13.

[51] GOFC-GOLD, (2011)

[52] Coppin, P. R., Bauer, M. E., 1996. Digital change detection in forest ecosystems with remote sensing imagery. Remote Sensing Reviews, 13, pp. 207-234. In Desclée, B., de Wasseige, C., Bogaert, P., Defourny, P. 2006. Tropical forest monitoring by object-based change detection: towards an automated method in an operational perspective. Proceedings of the 1st International on Object Based Image Analysis,(OBIA2006) Salzburg University, July 4-5, 2006.

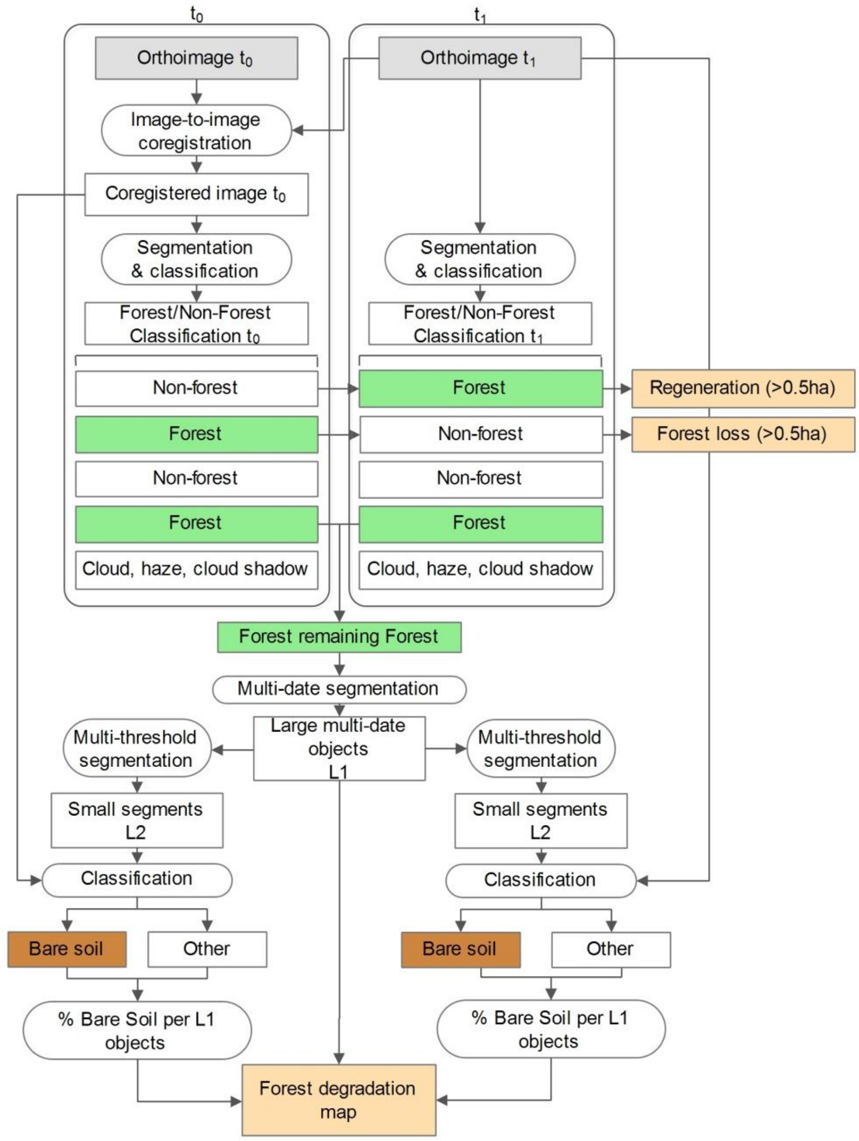

Figure 9.1: Deforestation and degradation mapping methodology steps

In the context of REDD+, the MRV system requires the monitoring of two components to estimate the emissions associated with forest degradation: 1) Activity data, i.e. changes in forest areas that remain forest and 2) Emission factors, i.e. changes in forest carbon stocks due to the degradation processes per unit area and forest types. The methodology illustrated in figure 9.1 focuses on measuring activity data by estimating the extent of forest which undergoes degradation. However, emissions associated with this activity data will be influenced by the type of forest in which the changes occurred. Although the calculation of emissions is outside the scope of the project, we wanted to go a little further in the methodology by distinguishing three different types of forest. This analysis is quickly described in section 9.2.5.

9.2.1 *Image pre-processing*

Dealing with multi-date image datasets requires that images obtained by various sensors at different times are comparable. The pre-processing includes four steps, namely radiometric calibration, geometric correction, pan-sharpening and bands ratios calculation.

Standard VHR products are delivered with a "Standard Geometrically Corrected" calibration including already minimum radiometric and sensor distortion corrections. "Radiometric corrections include relative radiometric response between detectors, non-responsive detector fill, and conversion for absolute radiometry. Sensor corrections include corrections for internal detector geometry, optical distortion, scan distortion, line-rate variations and mis-registration of the multispectral bands where applicable"[53].

All VHR images acquired in this study were delivered as orthorectified products by the image provider. However, geometric corrections were still needed to reduce the remaining shift of approximately 10m between each pair of images (one pair for Congo and one pair for Gabon). Each pair of images was coregistred using the older imagery (WV-2011 for Congo and QB_2010 for Gabon) as reference data. GCP's were derived automatically and manually from the interpretation of the images. The most recent image of each pair was geometrically corrected using 30 GCP's and the 3rd degree polynomial geometric model type (Root Mean Square Errors (RMSE) =0.5 pixel). The shift between each pair of images was reduced to approximately one pixel (~3m) which can have an influence on the classification (see section 9.2.2).

The pan-sharpening technique is based on pixel-level fusion method, in which high-resolution panchromatic and lower resolution multispectral imagery are merged to create a single high-resolution colour image. Pan sharpening methods can result in spectral distortions because of the low spectral quality of the panchromatic image[54]. Therefore, the pan-sharpened images were not used for the semi-automatic classification but only for visual interpretation and validation.

Before starting with the classification process, three band combinations were calculated in eCognition to enhance the discrimination between classes, the Normalized Difference Vegetation Index (NDVI), the green NDVI and the brightness index. NDVI is the ratio near-infrared radiation minus the red radiation divided by near-infrared radiation plus visible radiation, and provides information regarding the presence of photosynthetically-active green vegetation. The green NDVI uses the green band instead of the red band in the NDVI equation. The brightness index is the sum of the visual band plus the infra-red band divided by the total number of bands of the equation, namely four. This index was used, especially, to distinguish and isolate clouds and shadows in the classification.

9.2.2 *Forest/Non-forest classification*

For both study sites, a semi-automated object-based classification was developed to separate forest from non-forest areas on each image pair of the study site, hereafter named image t_0 for the archive image (QB_2010 for Gabon and WV_2011 for Congo) and image t_1 for the new acquired image (2012 for Gabon and Congo). Three classes were discriminated: no data, forest and non-forest. No data gathers clouds, haze and cloud shadows. Forest corresponds to forested areas with a closed canopy.

[53] http://www.digitalglobe.com/downloads/DigitalGlobe_Core_Imagery_Products_Guide.pdf

[54] Liu, Lining; Wang, Yunhong; Wang, Yiding. 2011. Adaptive steepest descent method for pan-sharpening of multispectral images. Optical Engineering, ISSN : 0091-3286, Volume : 50, Numéro : 9

Non-forest includes large clearings and logging roads, roads, built-up areas, agricultural fields, savannah, fallow land and water bodies.

The presence of haze and cloud shadows in the vicinity of clouds modifies the spectral values of the image which limits automatic classifications. Therefore, these three classes (cloud, haze and shadow-cloud) were classified as “no data” because no land cover information were extracted from them. A “no data” mask was realized for each image (one for image t_0 and one for image t_1). Clouds were classified automatically by using a threshold on the blue band for the Quickbird imagery and on the coastal band for the WorldView imagery. Haze was masked using a semi-automatic technique based on a threshold applied on the spectral mean value per object and on the object geometry. Cloud shadows were automatically discriminated by using a threshold on the NDVI index. Quality assessment was performed visually and the automatic cloud, haze and shadow masks were manually enhanced when necessary.

The forest/non-forest classification discriminates forest from non-forest with the multi-threshold segmentation algorithm which partitions the image in objects based on spectral value and scale parameters and, assigns them a class. Thresholds were set on the green spectral band and the NDVI index, and 0.5ha was set as minimum mapping unit. The same classification rule set was applied on image t_0 and t_1 to obtain two mono-temporal forest/non forest classifications. Realizing such a mask of forest optimizes the processing time needed for forest degradation mapping because it avoids producing the time consuming classification of the many different classes included in non-forest.

A first multi-temporal analysis was then performed between both mono-temporal forest/non forest classifications to identify changes and focus the subsequent analysis only on areas of forest that remain forest, i.e. on forest degradation. As a result of this union, four classes were extracted, namely forest, non forest, forest loss and regeneration. A minimum threshold of 0.5ha was defined to classify an area as forest loss or regeneration. This threshold refers to the forest definition of the FAO[55]. The method of classification is described in detail below:

- Objects classified as forest at t_0 and remained forest at t_1 were classified as **forest**, hereafter named forest t_0/t_1.
- Objects classified as non-forest at t_{+0} and remained non-forest at t_1 were classified as **non-forest**, hereafter named non-forest t_0/t_1.
- Objects that changed from forest (t_0) to non-forest (t_1) were classified as **forest loss**, if the object size was larger than 0.5ha. If the object size was smaller than 0.5ha, the object was classified as forest t_0/t_1.
- Objects that changed from non-forest (t_0) to forest (t_1) were classified as **regeneration** if the object size was larger than 0.5ha. If the object size was smaller than 0.5ha, the object was classified as forest t_0/t_1.
- Very small objects (~one pixel size) located along roads, water bodies or human settlements which changed from class (forest to non-forest or non-forest to forest) between t_0 and t_1, because of the shift between both images, were removed from the classification and classified as non-forest t_0/t_1.

[55] Land spanning more than 0.5 hectares with trees higher than 5 metres and a canopy cover of more than 10% or trees able to reach these thresholds in situ. (FAO, FRA 2010)

The resulting classification obtained from the union between forest/non-forest classifications at t_0 and t_1 lead to an intermediate product, namely a forest loss and regeneration map (see 9.3.2.2).

The subsequent steps of the methodology focus on the detection of small (<0.5ha) degradation features (logging roads and clearings) within the class forest t_0/t_1.

9.2.3 Multi-date segmentation

The second multi-temporal analysis aims to create a forest degradation map between both dates that estimates the level of forest degradation within the class forest t_0/t_1. The approach is based on multi-date segmentation. This technique uses satellite images of the same area at different dates to create multi-date objects which group pixels that are spatially, spectrally and temporally similar[56]. In the eCognition software, the multi-date image is segmented into multi-date objects based on three user defined parameters: scale, colour and shape. The scale parameter determines the size of image objects. If the scale value is high, the variability allowed within each object is high and image objects are relatively large. Conversely, small scale values restrain the variability within each segment, creating relatively smaller objects. The colour parameter trades the percentage contribution of the spectral values versus the object shape. The value for colour or shape criteria affects the resulting image object by determining the spectral or spatial homogeneity. Within the shape criterion, the user can also alter the compactness of the object and the smoothness of the objects boundaries[57,58].

In this study, two levels of segmentation were performed based on two different techniques. **The first level (level 1)** is based on a multi-date segmentation approach to delineate **"large multi-date objects"** using image t_0 and t_1 as input data. The scale parameter was set to 100 and the colour parameter was set to 0.9 in order to obtain very spectrally homogeneous objects. Smoothness and compactness were equally balanced and both set to 0.5. This first multi-date object level will be used for the change detection analysis. **The second segmentation level (Level 2)** creates small objects within the large level 1 objects. This segmentation was applied separately on each image (image t_0 and t_1) using a multi-threshold segmentation technique and the output of level 1 objects to constrain the detection of **small patches of bare soil** (canopy gaps and small clearings). The spectral information of the blue visible band was used to detect bare soil and the scale parameter was set to 1 in order to detect the smallest area (1 pixel size - ~5m^2). Figure 9.2 shows an image subset of segmentation levels 1 and 2 on both images in Gabon (t_0 and t_1).

---

[56] Desclée, B., de Wasseige, C., Bogaert, P., Defourny, P. 2006. Tropical forest monitoring by object-based change detection: towards an automated method in an operational perspective. Proceedings of the 1st International on Object Based Image Analysis,(OBIA2006) Salzburg University, July 4-5, 2006.

[57] Jacob C. Brenner, 2009. Structure, Agency, and the Transformation of the Sonoran Desert by Buffelgrass (Pennisetum Ciliare): An Application of Land Change Science

[58] Desclée, B., de Wasseige, C., Bogaert, P., Defourny, P. 2006. Tropical forest monitoring by object-based change detection: towards an automated method in an operational perspective. Proceedings of the 1st International on Object Based Image Analysis,(OBIA2006) Salzburg University, July 4-5, 2006.

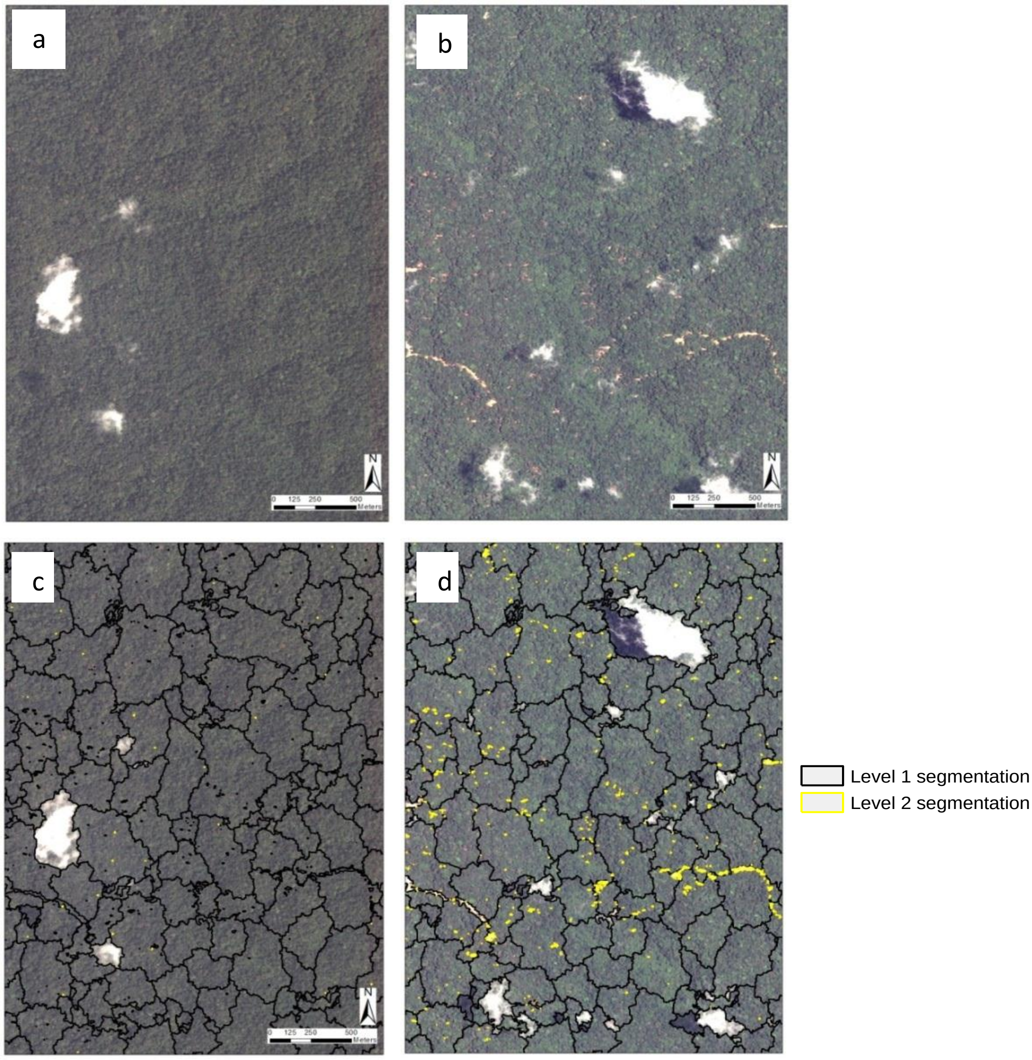

Figure 9.2: Illustration of the two levels of image segmentation where a) is a subset of the Quickbird image of 2010 (t0), b) is a subset of the Quickbird image of 2012 (t1), c) shows the delineation of the two levels of image segmentation for image t0, d) shows the delineation of the two levels of image segmentation for image t1.

9.2.4 Forest change detection

This change detection analysis was performed to create a classification highlighting differences in forest degradation levels between image t_1 and t_0. Firstly, for each image, the percentage of small patches of bare soil (level 2 objects) was calculated per level 1 object. Secondly, a new multi-date image classification was created according to the percentage difference of small patches of bare soil per level 1 object between t_1 and t_0 (= t_1-t_0). Five levels of forest degradation were defined based on this percentage difference:

- Degrad 1: 0.5% < difference of canopy gaps between t_1 and t_0 < 10%
- Degrad 2: 10% < difference of canopy gaps between t_1 and t_0 < 30%
- Degrad 3: 30% < difference of canopy gaps between t_1 and t_0 < 50%
- Degrad 4: 50% < difference of canopy gaps between t_1 and t_0 < 70%
- Degrad 5: 70% < difference of canopy gaps between t_1 and t_0

Two additional classes were added in case of no degradation:

- No Degrad: -0.5% < difference of canopy gaps between t_1 and t_0 < 0.5%
- Regeneration: difference of canopy gaps between t_1 and t_0 < -0.5%

An error margin of 0.5% was applied in the definition of the class "No Degrad" to avoid false positive or negative errors due to misclassified objects and the spatial shift between both images.

9.2.5 Forest types

In the context of REDD+, the MRV requires monitoring of two components to estimate the emissions associated with forest degradation: 1) Activity data, i.e. changes by forest type in forest areas that remain forest and 2) Emission factors, i.e. changes in forest carbon stocks due to the degradation processes per unit area and forest types[59].

The methodology described above focuses on measuring activity data by estimating how much forest, and where, is undergoing degradation. However, emissions associated with this activity data are influenced by the type of forest in which the changes occurred. Therefore, we decided to take the analysis a step further by distinguishing three types of forest, namely primary forest, secondary forest and woodland. These classes are defined below:

- Primary forest is a mature forest with a canopy cover of more than 60%
- Secondary forest is a non-mature forest with a canopy cover of more than 60%
- Woodland is defined by a density between 30% and 60%

A map distinguishing these forest types was produced to then identify through a spatial analysis in which types of forests canopy cover loss had occurred.

9.2.6 Accuracy assessment

Depending on the availability, different kind of data can be used to verify the thematic accuracy of the produced maps. Recent data as for e.g. field work, aerial imagery, pictures, maps are preferred. If this is not available other accessible data like Google earth, pictures etc. can be used. In our case, no enough independent reference data are accessible. Therefore, the images used for the classification are also used for the accuracy assessment. Considering the delay in the delivery of the VHR images, we decided to validate only a part of our products (four maps).

The thematic accuracy of the forest maps is assessed via a stratified random sampling strategy. For the two basic maps of Gabon – ***Forest/Non-forest*** – (9.3.2.1) a fixed number of random distributed points are created (in total 200). For the maps ***forest loss and regeneration map*** of Gabon (9.3.2.2) and ***Forest types* in Congo**, a fixed number of points – between 5 and 20 – is attributed to each class depending on his area.

For each land cover classification, the overall accuracy, the omission and commission error per class are calculated. The Overall Accuracy is the number of correct classified validation points divided by the total number of validation points. It is expressed in percentage. The Omission and Commission errors are calculated for each validated class, it can have a value between 0 and 100%. An error of omission results when a validation point is omitted from its correct class. An error of commission

[59] IPCC 2003b Good practice guidance for land use, landuse change and forestry (GPG-LULUCF). In: Penman, J., Gytarsky, M., Krug, T., Kruger, D., Pipatti, R., Buendia, L., Miwa, K., Ngara, T., Tanabe, K. and Wagner F. IPCC-IGES, Kanagawa (eds.)

results when a validation point is committed to an incorrect class. A class with omission/commission error 0 means that no error has been measured for that class.

The method used for the accuracy assessment follows four steps:

1. The image is opened in a GIS software, together with the delineation of the classification and the validation point dataset
2. An image interpreter zooms to each validation point and interprets the correct class for the validation point based on the image and the MMU. The image interpreter considers the level of minimum mapping unit during the interpretation.
3. The visual interpretation of the image interpreter is compared with the classification results in a confusion matrix.
4. Overall accuracy, omission and commission errors are calculated from the confusion matrix.

9.3 Results

Results are provided separately for the study site in Congo, and the one in Gabon. The whole methodology described in 9.2 was only applied for the study site of Gabon where two images (t_0 and t_1) were acquired in a reasonable time window matching with the project schedule.

9.3.1 Congo

In Congo, the whole methodology described above which is based on multi-temporal analysis could not be applied because of the acquisition delay of the Quickbird image. As mentioned before, this image was only acquired on the 12th of July 2012. Nevertheless, a mono-temporal analysis was performed on the Worldview image of Augustus 29, 2011. The Quickbird image was pre-processed to enhance visual comparison with the Worldview image.

9.3.1.1 Mono-temporal analysis

The aim of the mono-temporal classification realized on the worldview image from 2011 was to guide the field missions and evaluate the potential of VHR images to detect small forest degradation features (logging roads, small clearings) and forest types. Figure 9.3 shows the results of this classification. Ten classes were discriminated, namely primary forest, secondary forest, swamp forest/wetland, fallow, bare soil, build-up area, water, cloud, haze and cloud shadow. First, clouds, hazes and cloud shadows were masked and forest was separated from non-forest areas based on the methodology described in 9.2.2. Secondly, non-forested areas were discriminated between fallow, bare soil, water and build-up areas. Finally, bare soil areas smaller than 0.5ha were detected within the forest class and then primary forest, secondary forest and swamp forest were distinguished.

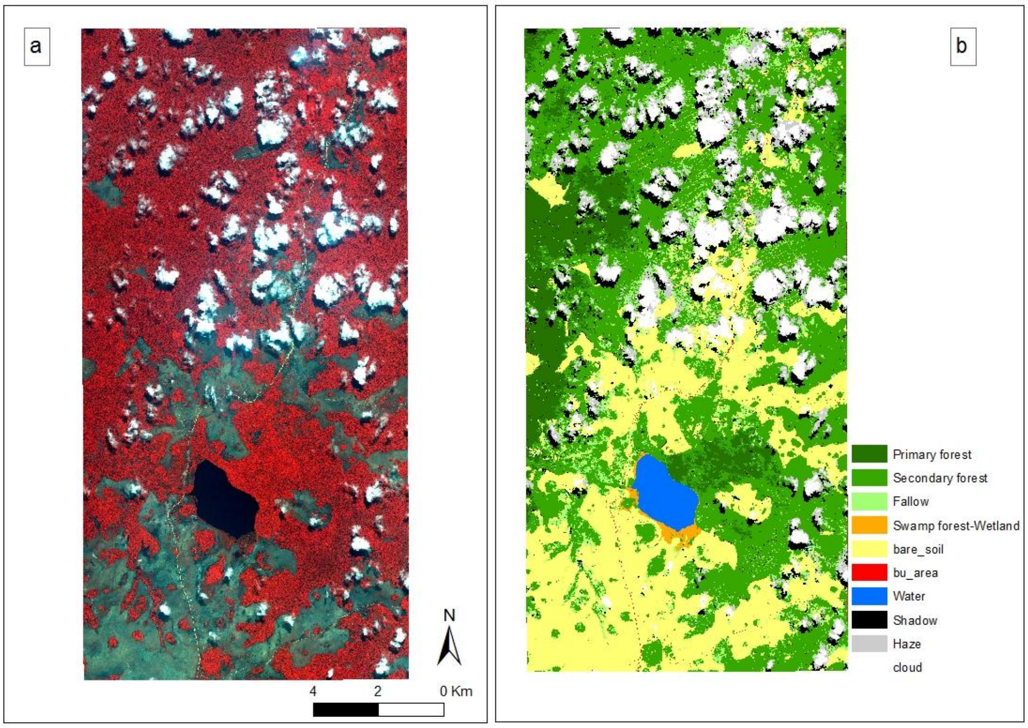

Figure 9.3: Mono-temporal land cover classification (b) based on the Worldview image of Augustus 29, 2011 (a)

The area is dominated by secondary forest with fallow fields in between and includes build-up areas along the main road. Figure 9.4a shows that the main road separates a protected area on the west from a logging concession on the east. The significant presence of small clearing areas and a pattern of narrow (<5m wide) logging roads in the vicinity of villages and the main road indicates high human activities (Figure 9.4b). Moreover, the presence of these logging roads in the western part of the area provides evidence that the phenomenon of forest degradation also took place in the protected area.

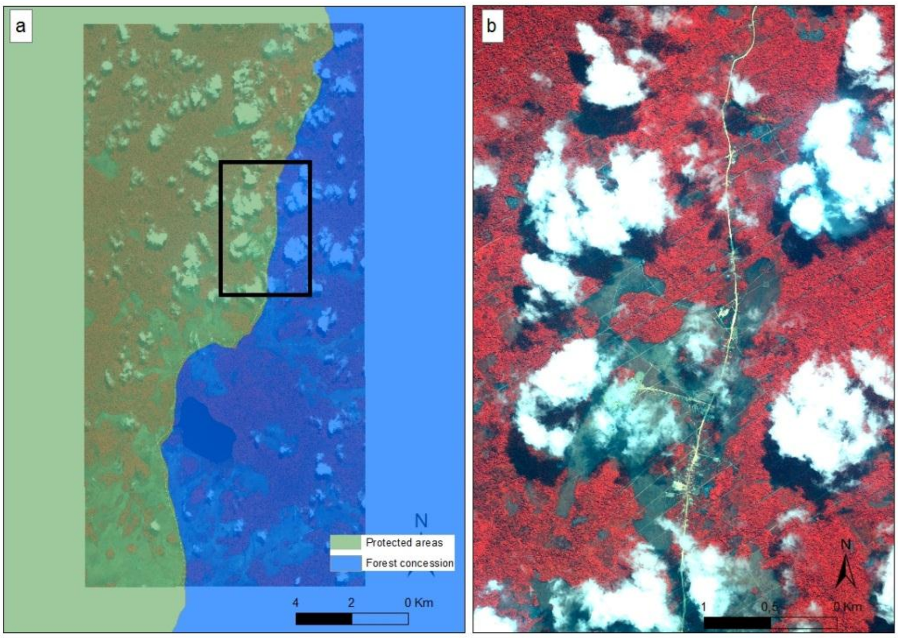

Figure 9.4: Worldview image of 2011 showing the location of the protected area and the forest concession (a) and an image subset of forest degradation.

Although the detection of very small degradation feature is effective with optical very high resolution imagery such as Worldview, the vegetation regenerates very quickly (<one year) and canopy closure prevents the detection of some degraded areas. This phenomenon, which is clearly observable when trying to detect narrow logging roads, causes an underestimation of forest degradation areas (Figure 9.5).

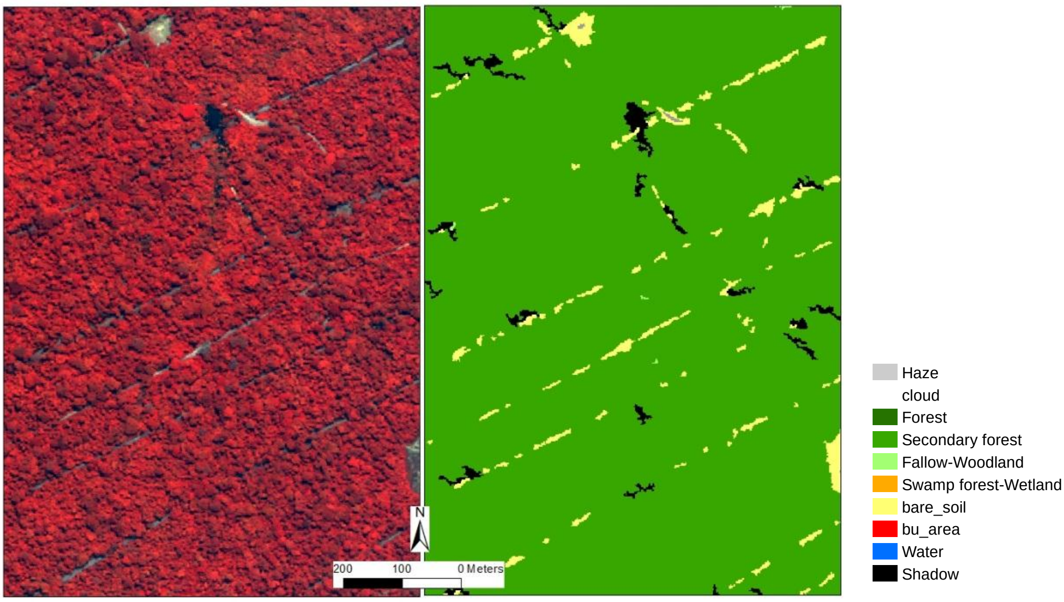

Figure 9.5: Detection of narrow logging roads from the Worldview image

Table 9.1 summarizes the accuracy assessment results of the classification. The overall accuracy was 80%. Most classification errors were found for points located in the neighbourhood of high level of clouds and haze where the image suffers from diffuse haze (not included in the cloud-haze mask). The diffuse haze modifies the spectral values of the objects and lead to omissions and commissions errors. The discrimination between fallow and secondary forest classes was particularly sensitive to this phenomenon. Therefore, areas with diffuse haze need to be specifically delineated and classified separately (manually or semi-automatically) which increases the processing time.

Table 9.1: Accuracy assessment results of the land cover classification map of 2011 - Congo

Congo Forest types 2011		Automatic								
		Bare soil	BU area	Forest	Sec. forest	Fallow	Swamp forest Wetland	River	Total	CE (%)
Visual	Bare soil	19			1	2			22	14%
	BU area	1	14						15	7%
	Cloud		1							
	Forest			15					15	0%
	Sec. forest			5	16	8	2		31	48%
	Fallow				3	10			10	23%
	Swamp forest-Wetland						13		13	0%
	River							5	5	0%
	Total	20	15	20	20	20	15	5	84	
	OE (%)	5%	7%	25%	20%	50%	13%	0%		80%

Atmospheric corrections should be tested on this image to determine whether it can remove diffuse haze and enhance the quality of the image.

9.3.1.1 Multi-temporal analysis

The newly acquired Quickbird image was coregistred with the Worldview image to reduce the spatial shift between them and facilitate visual multi-temporal analysis. Some first semi-automatic classification tests were realized on the Quickbird image to mask clouds and haze and, separate forest from non-forest but preliminary results indicated that the accuracy of the automatic procedure was limited by the quality of the image. The image suffers from clouds, high level of haze, cloud shadows and effects of the atmosphere that modify the reflection values of Earth’s surface. Atmospheric corrections should have been applied to enhance the quality of the image and enable accurate automatic classifications. Unfortunately, the project schedule did not allow for more pre-processing steps such as atmospheric corrections and further tests. Therefore, only visual comparison between the Worldview and Quickbird image was realized to evaluate changes within forest classes. However, this chapter focuses only on the major trends in terms of changes as this analysis is detailed further in 10.3.2 when comparing radar data with optical data.

The visual comparison between the WorldView image of august 2011 and the QuickBird image of July 2012 indicates that forest regeneration has occurred in most of the cleared areas including logging roads. Besides regeneration, forest gaps were created in the vicinity of the main road and villages for opening up of new agricultural fields (shifting cultivation) and for logging activities for timber production. Figure 9.6 shows an image subset of the area which illustrates these changes. Green points indicate areas where regeneration occurred, whereas yellow points illustrate areas of forest canopy loss between 2011 and 2012. The bigger blue point refers to the location of a new forest gap where photos were taken during field missions (see figure 9.6). This forest gap was created for cassava cultivation. Figure 9.6 illustrates also how quickly the vegetation regenerates and covers the logging tracks. In less than a year, almost all forest tracks are no longer detectable from very high resolution data. This emphasizes the importance of acquiring images at short time intervals to measure forest degradation.

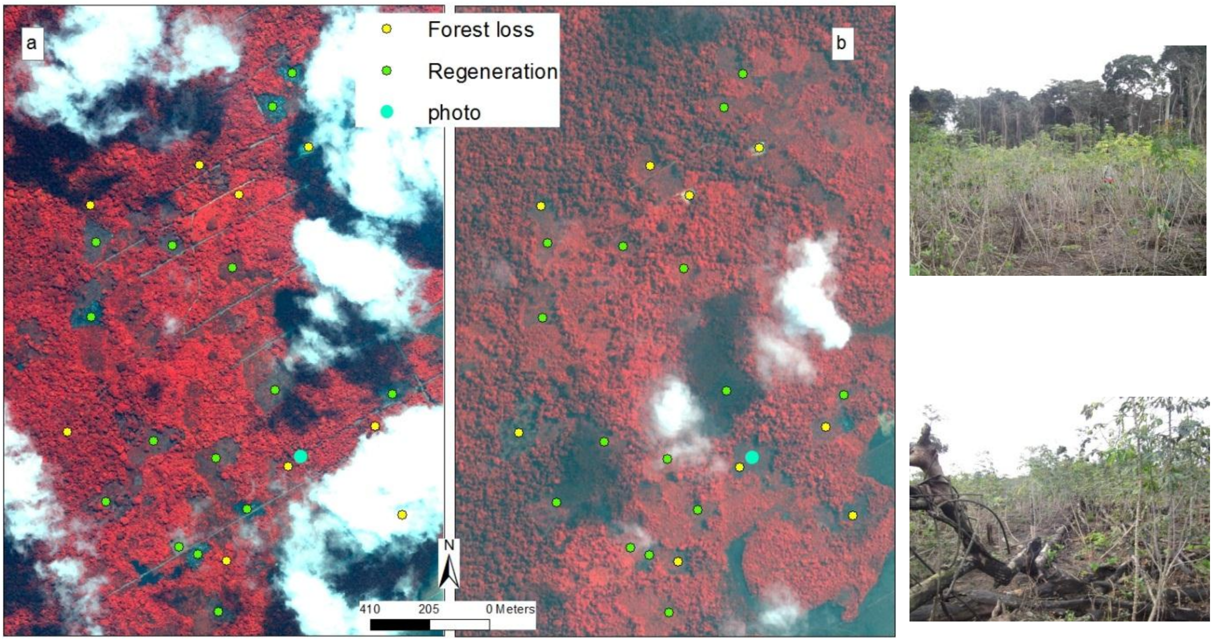

Figure 9.6: Visual multi-temporal analysis between the WorldView image of august 2011 (a) and the QuickBird image of July 2012 (b)

9.3.2 Gabon

In Gabon, the whole methodology described in 9.2 could be applied thanks to the acquisition of the second image within a reasonable time window. The results presented in this chapter follow the methodology steps.

9.3.2.1 Forest, Non-forest classification

The forest/non-forest classification map produced for both Quickbird VHR images (2010 and 2012) is illustrated in Figure 9.7. Shadows and clouds show areas of no data. This first intermediate product of the whole method was the most time consuming one because of the manual editing needed to mask hazy areas. As for Congo, atmospheric corrections should be tested to reduce the extent of these areas where spectral values are modified. The forest/non-forest classification performed on both dates allows us to focus subsequent classifications to the forest class remaining forest. Moreover, it avoids performing the time consuming classification of the many different classes included in the non-forest class. As described in 9.3.2, the combination of these two intermediate results will serve as a basis for the detection of forest loss and regeneration areas bigger than 0.5ha.

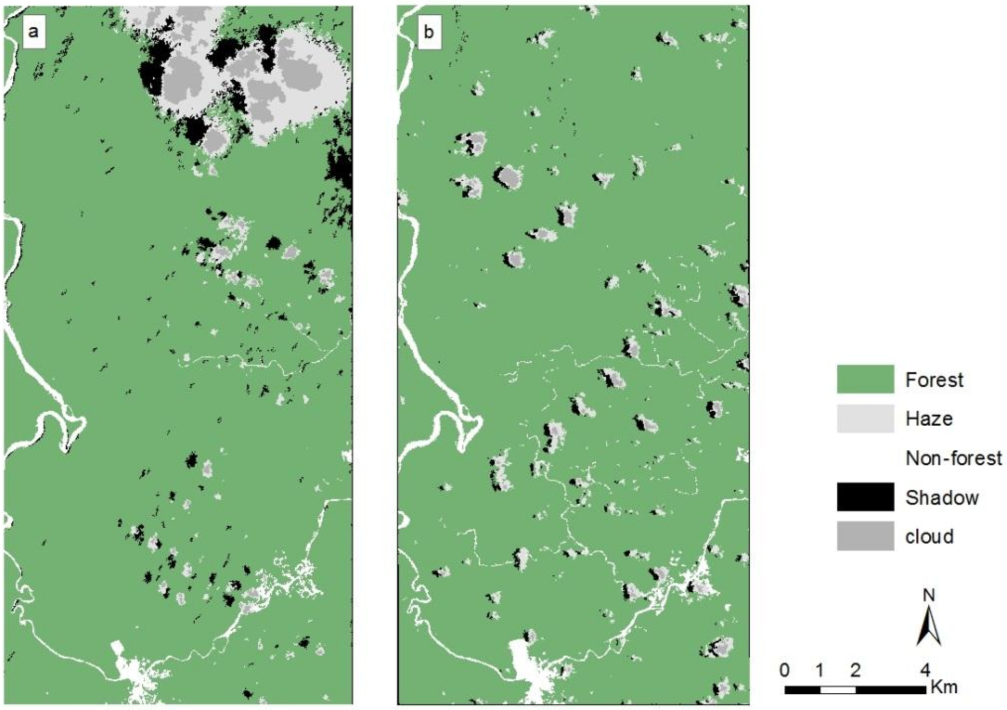

Figure 9.7: Forest/Non-forest classification based on Quickbird imagery at t_0 (a) and t_1 (b)

Table 9.2 and 9.3 summarizes the accuracy assessment results of the forest/non-forest classification respectively for 2010 and 2012. The overall accuracy is 99.3% for 2010 and 93% for 2012.

Table 9.2:Accuracy assessment of the *Forest/Non-forest* map of 2010 - Gabon

Gabon 2010		Automatic			
Visual		Forest	Non-forest	**Total**	**CE** (%)
	Forest	**171**	1	172	**1%**
	Non-forest	0	**28**	28	**0%**
	Total	171	29	**200**	
	OE (%)	**0%**	**3%**		**99,5%**

Tableau 9.3: Accuracy assessment of the *Forest/Non-forest* map of 2012 - Gabon

Gabon 2012		Automatic			
Visual		Forest	Non-forest	**Total**	**CE** (%)
	Forest	**100**	14	114	**12%**
	Non-forest	0	**86**	86	**0%**
	Total	100	100	**186**	
	OE (%)	**0%**	**14%**		**93,0%**

9.3.2.2 Forest loss and regeneration map

The forest loss and regeneration map resulting from the union between the two forest/non-forest classifications is shown in Figure 9.8. The yellow points in the subset classification (figure9.8b) refers to the location of the photos took during the field missions. The methodology used to perform this first change detection analysis and to define the classes is based on the definition of forest from the FAO[60]. Areas of forest loss or regeneration were classified as "forest loss" or "regeneration" if the

[60] Land spanning more than 0.5 hectares with trees higher than 5 metres and a canopy cover of more than10% or trees able to reach these thresholds in situ. (FAO, FRA 2010)

area reached a minimum threshold of 0.5 ha. The term of forest loss was used to avoid the term of deforestation which considers a change of forest to other land use. Indeed, the time-lap was too short to ensure that land use change had occurred. However, field visits confirmed a change in land use for some areas. Figure 9.8 shows an example of forest loss area where land use changed for cassava and banana cultivation. A photo of the regenerated area is also illustrated in figure 9.8.

If the 0.5 ha threshold of the area was not reached, these areas were considered as being part of a forest degradation process and were reintroduced in the forest mask for further analysis. Based on this methodology, the extent of forest loss and regeneration areas was evaluated between December 29, 2010 and March 12, 2012. From a forest extent of 16,223.9 ha on the satellite image of December 2010, about 80.2 ha of forest were lost between December 2010 and March 2012. 5.7 ha of non-forest areas in 2010 were regenerated in 2012. Most of the forest loss (except for logging roads) and regenerated areas are located in the vicinity of the main road and villages. Changes within the forest class remaining forest of this forest loss and regeneration map was analyzed in more detail to detect canopy gaps and smaller clearings by using multi-threshold and multi-date segmentation techniques.

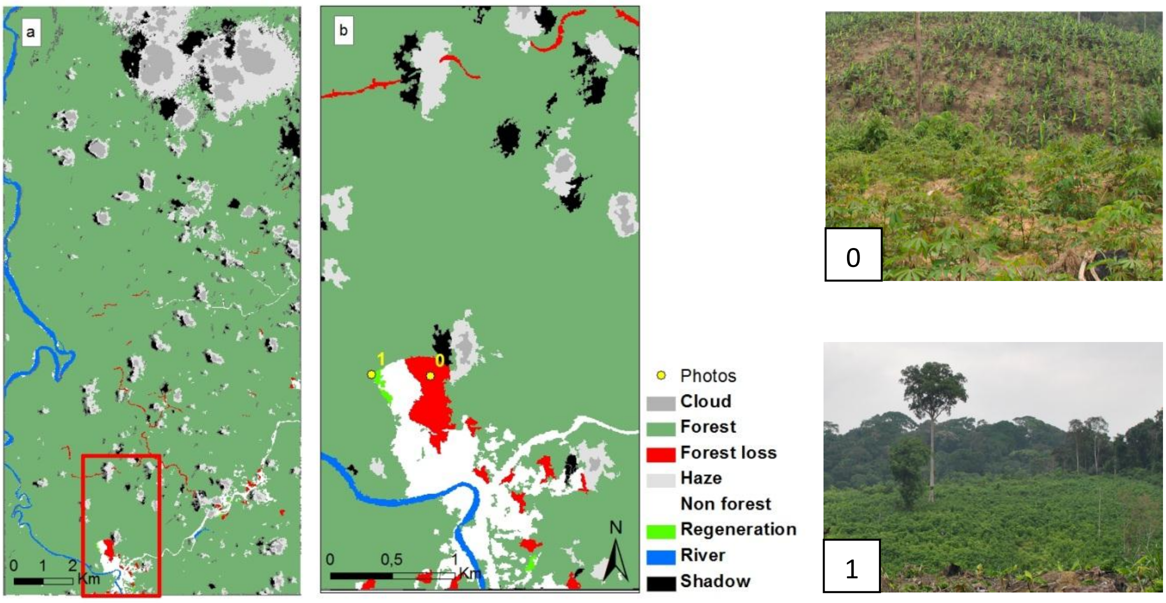

Figure 9.8: Forest loss and regeneration map over the whole study site (a) and a subset of the study site (b)

9.3.2.3 Degradation map

Starting from the "forest remaining forest" class (forest t_0/t_1) defined in the forest loss and regeneration map, the forest degradation map was obtained in two steps (Figure 9.9):

1. Delineation of the two levels of segmentation (large level 1 objects and small objects of canopy gaps and clearings) on each Quickbird imagery (2010 and 2012);
2. Percentage difference of small canopy gaps and clearings objects per level 1 objects between 2010 and 2012.

Canopy gaps and small clearings detected within forest t_{+0}/t_{+1} covered an area of 7.2 ha in December 2010 and 40.5 ha in March 2012. Thus, 33.3 ha of canopy cover were degraded between 2010 and 2012. By adding this degradation level to the areas of forest loss calculated previously (80.2 ha), we were able to estimate the area of forest cover loss between December 2010 and March 2012 at 113.5 ha. In order to highlight differences between image 2010 and 2012, five levels of forest degradation were defined based on the percentage difference of bare soil per level 1 object (see

9.2.4). Areas of forest loss previously delineated (see Figure 9.8) were included in the fifth level of degradation which gathers areas of forest cover loss superior than 70%.

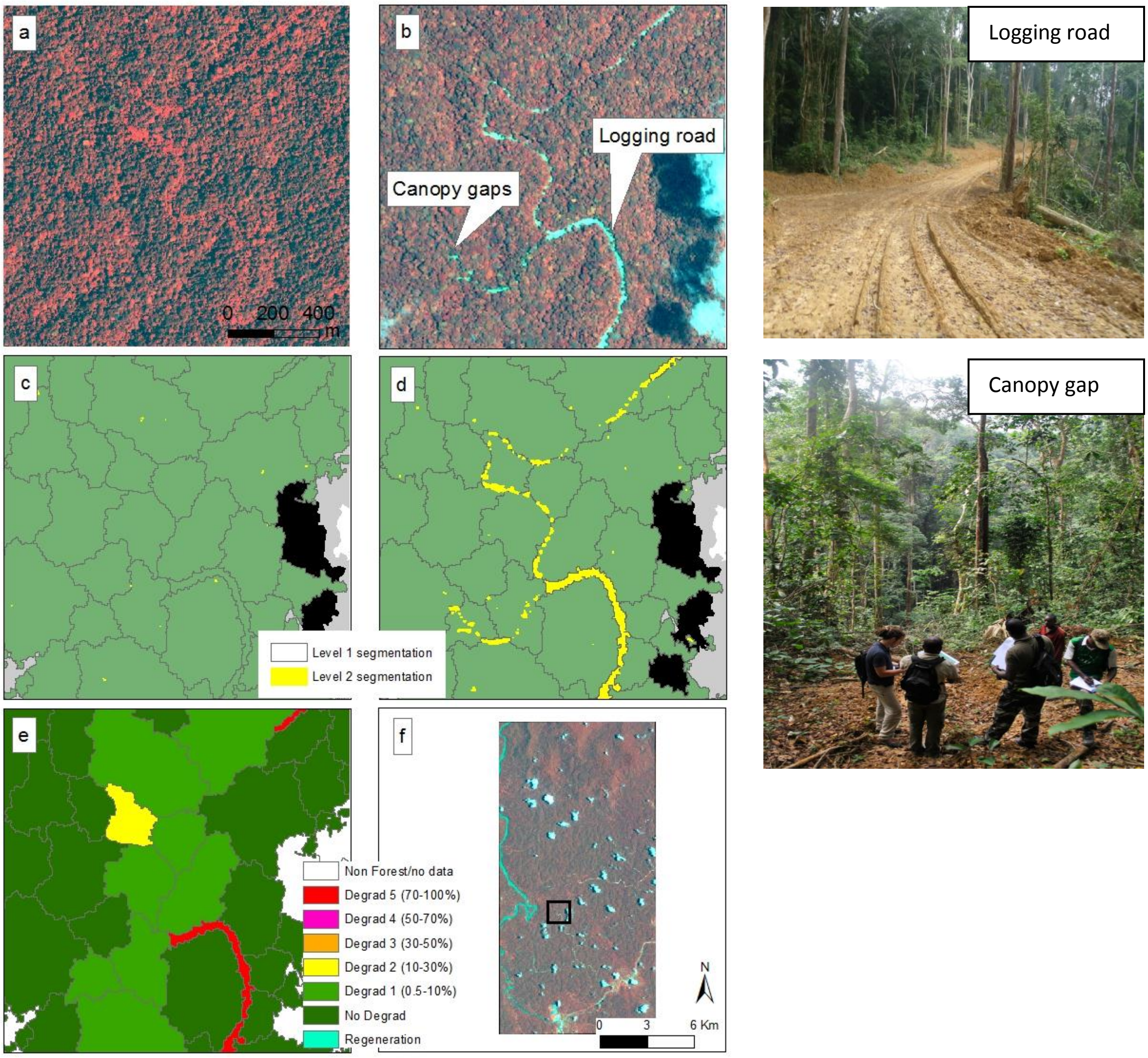

Figure 9.9: Input data used to create the forest degradation map between 2010 and 2012 where: a) is the Quickbird imagery from 2010, b) the Quickbird imagery from 2012, c) shows the two levels of segmentation resulting from Quickbird 2010, d) the two levels of segmentation resulting from Quickbird 2012, e) the degradation map showing the percentage difference of small patches of bare soil per level 1 object between 2010 and 2012, f) shows the image subset extent.

The degradation map over the whole area of 20x10km is shown in Figure 9.10. This map highlights areas of forest degradation and regeneration between 2010 and 2012. If we do not consider logging roads, most areas of very high level (level 5) of forest degradation (sometimes reported as deforested areas by the field visit), are located near human settlements and along the main road. Areas of forest cover loss bigger than 0.5 ha that were visited in the field mission showed land use change for agriculture purposes including slash and burn agriculture (Figure 9.11). Areas with lower rates of forest degradation were mostly situated along or in the vicinity of the logging roads traced in the forest. Forest gaps in these areas are due to logging activities for timber production.

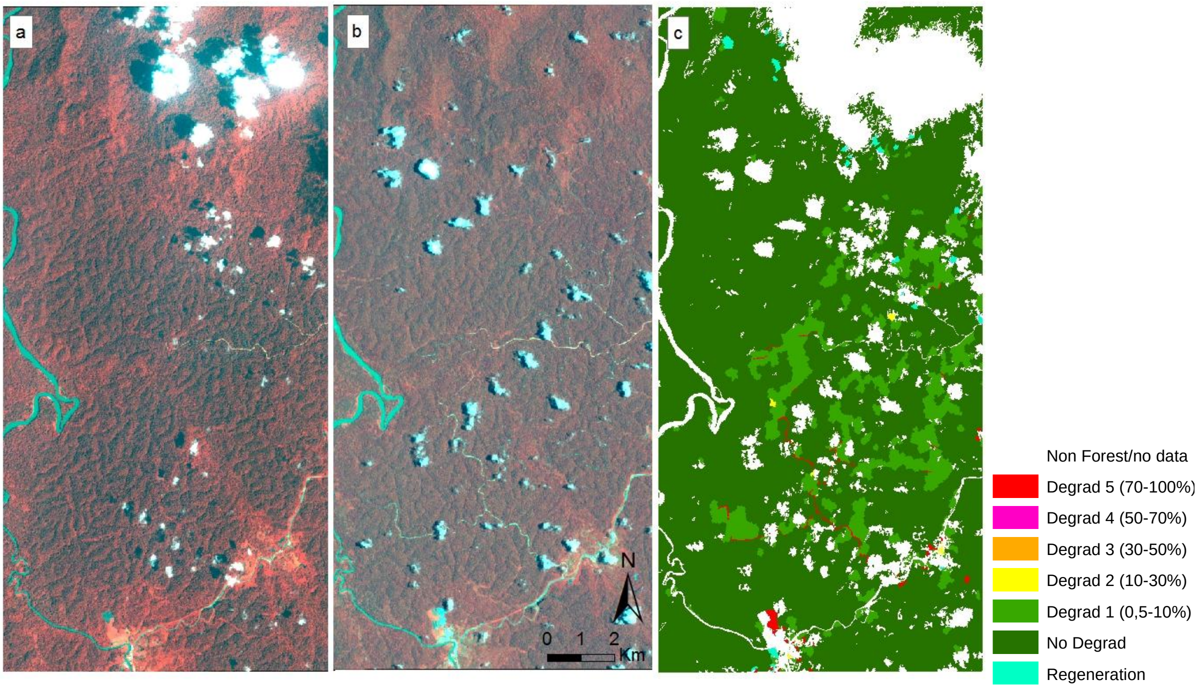

Figure 9.10: Forest degradation map (c) based on Quickbird imagery 2010 (a) and 2012 (b).

Figure 9.11: Slash and burn agriculture in the vicinity of the main road

According to the method described in 9.2.6, we carried out an accuracy assessment of the map produced to calculate the degradation levels. This map include four classes namely, forest, non-forest, bare soil and river. The bare soil class combines forest loss areas (>5ha – see figure 9.8) and the small canopy gaps and clearing detected within forest (<5 ha). A stratified random point dataset was generated and interpreted by an experienced image interpreter, using the two Quickbird images as background. The visual interpretation results were compared with the automatic classification in an error confusion matrix. The map has on overall accuracy of 88%. Detailed results of the accuracy assessment are given in table 9.4.

Tableau 9.4: Accuracy assessment of the *forest loss and Reforestation* map - Gabon

Gabon Changes		**Automatic**					
		Forest	Non forest	Forest loss	River	**Total**	**CE (%)**
Visual	Forest	**22**	4	4		30	27%
	Non forest		**14**		1	15	7%
	Forest loss			**21**		21	0%
	River				**9**	9	0%
	Total	22	18	25	10	**66**	
	OE (%)	0	22%	16%	10%		**88%**

9.3.2.4 Forest types

The methodology described above focuses on measuring activity data by estimating the extent of forest which undergoes degradation. However, emissions associated with this activity data will be influenced by the type of forest in which the changes occurred. Although the calculation of emissions is outside the scope of the project, we wanted to go a little further in the methodology by distinguishing different three types of forest, namely primary forest, secondary forest and woodland (figure 9.12). Based on the map produced, we performed a spatial analysis to identify in what types of forests canopy cover loss had occurred (figure 9.13). On 80.2 ha of forest loss areas (>0.5 ha), 59.1ha (73.7%) were cleared in primary forest and 21.1ha (26.3%) in secondary forest. On 40.5ha of degraded areas (<0.5 ha), 36.7 ha (90.5%) were cleared in primary forest and 3.8ha (9.5%) in secondary forest. If we combine these two classes we can conclude that over a total of 120.7 ha of forest cover loss, 95.8 ha (79.4%) were cleared in primary forest and 24.9 ha (20.6%) were cleared in secondary forest.

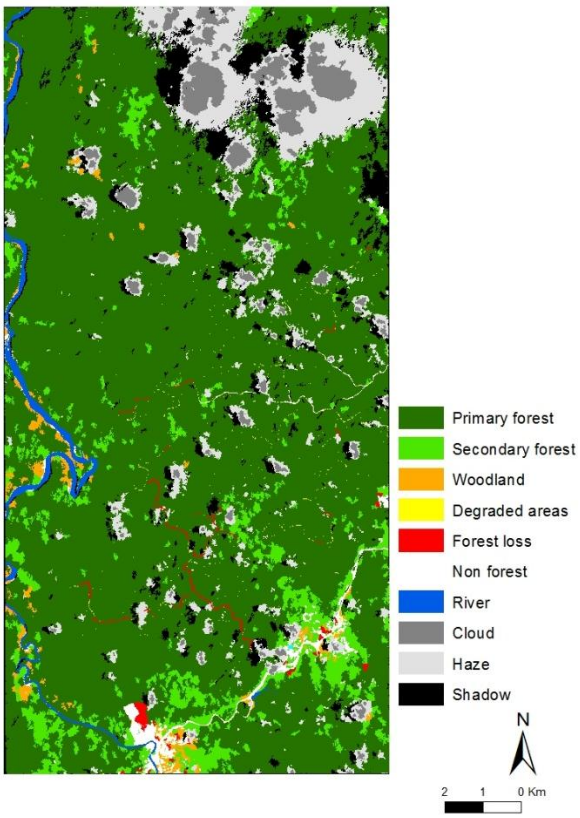

Figure 9.12: Classification of different types of forest

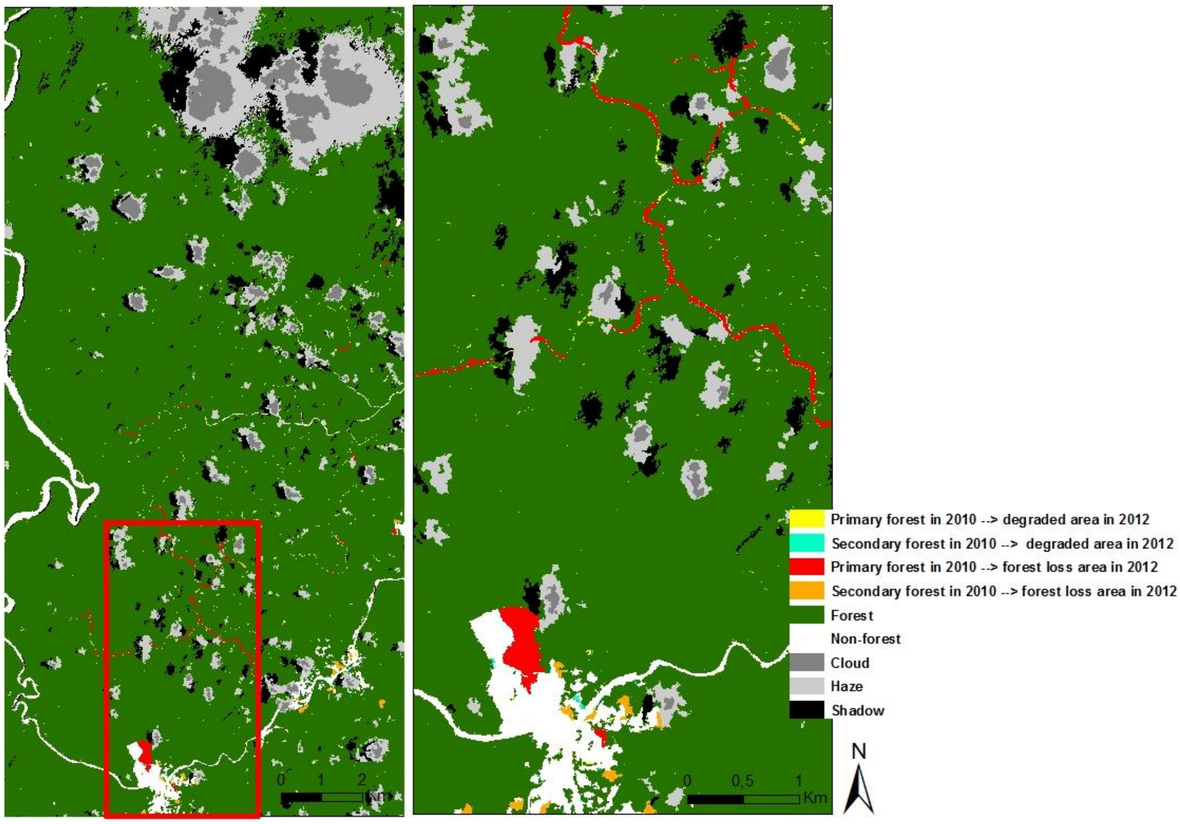

Figure 9.13: Identification of classes from 2010 transformed in bare soil in 2011

9.4 Conclusion

Although it could not be applied in Congo because of the image acquisition delay, this study proposes a method to map forest degradation areas over complex tropical sites. The two levels of image segmentation offers two levels of analysis to evaluate forest degradation. Level 1 objects aggregate small degradation features information over larger area to highlight five level of forest degradation whereas smaller level 2 objects show the extent and the exact location of these small features. Based on this methodology, we were able to evaluate activity data associated with forest degradation by calculating the extent of forest cover loss areas (small clearing, canopy gaps and logging roads). Moreover, the spatial analysis performed on these forest cover loss objects indicated the distribution of this activity data among the three types of forest identified. This information could be linked with emission factors for estimating carbon emissions.

The forest degradation map facilitated the rapid identification of the location of forest cover loss areas and their intensity. It provided useful information for understanding the phenomenon of forest degradation in the study area. In Congo as in Gabon, degraded areas were located in the vicinity of villages and major roads. The main activities related to forest degradation are shifting cultivation and logging activities. The field visit provided evidence of deforestation for such areas where land use change occurred (opening up of new agricultural fields in forested areas).

Through this study, although we have shown the effectiveness of optical very high resolution imagery to detect small degradation features, some limitations remain for monitoring forest degradation with this type of data:

- Vegetation regenerates very quickly (within a year) which reduce the detection of small features related to degradation. Therefore, good-quality cloud-free remote sensing imagery needs to be acquired at frequent intervals (at least once per year). However, this study showed that archives of very high resolution data are very limited in Congo and Gabon and acquisition of new good-quality imagery is often delayed given the persistent cloud cover in the area. Moreover, the presence of a relatively high percentage of cloud cover over the acquired images decreases areas where change detection can be performed. These acquisition limitations underline the difficulty of obtaining optical satellite imagery in the Congo Basin and confirm that other type of data should be acquired in parallel the potential of radar data.
- Atmospheric effects modify object spectral values which limit automatic classification. This phenomenon could be reduced by adding atmospheric corrections in the pre-processing procedure but it often requires advanced processing tools. These processing tools are often implemented in commercial software packages (which can be expensive) and require training of people. This is also true for object-based (semi-) automatic classification that uses image segmentation techniques.
- Costs of very high resolution data could be prohibitive for national coverage. Therefore, these data would have to be used in a sampling scheme or as validation data.

10 Synthetic aperture radar

10.1 Introduction

Given the persistent cloud cover in the Congo Basin, remote sensors with all-weather capabilities have an advantage in enabling frequent image acquisition of the earth surface. Therefore, the scientific steering committee advised in Kinshasa in October 2011 (see Section 2.3) that radar imagery should be included when assessing the usefulness of satellite data for the assessment of forest degradation. Following the advice, also other stakeholders (local partners and the European Commission Research Executive Agency) indicated that inclusion of radar in the analysis is essential. Although none of the partners had extensive experience with radar, the REDDiness project decided to take this challenge and evaluate the potential of radar in the direct detection of forest degradation processes.

Imaging radars onboard satellites are all synthetic aperture radars (SAR). SAR uses repeated energy pulses towards the same target (earth surface) and special signal processing algorithms to synthetically create longer radar antennas, and thus images with finer spatial detail. The SAR field is dominated by technical experts who often work with highly advanced techniques and processing software. Within REDDiness we propose to evaluate what SAR may offer for forest degradation assessment with relatively simple techniques. This includes basic pre-processing and visual analysis. In the framework of a SICA (Specific International Cooperation Actions) project and in view of the REDDiness work package 2 (WP2) outcomes, this makes sense. For both countries WP2 showed that local technical knowledge on remote sensing in general is quite limited. Any outcome of REDDiness that should be transferred to increase the countries' capacities for building MRV systems, should build on the currently available capacity.

Section 6.2 described the archive and newly-ordered SAR imagery that we obtained for both sites. A good set of multiple images was acquired after careful analysis of data archives and evaluating possible new acquisitions within the GMES Data Portfolio. Nonetheless we want to stress two points related to the time line of the project and the obtained imagery:

- Following previous phases of the REDDiness project, a final selection of the study sites was only made in December 2011, thus limiting the time for new image acquisitions. Basically we tried initially to obtain all new acquisitions before May 2012 in order to leave time for initial analysis before the planned field visit dates. Therefore we could not always obtain an image during the same season as an archive image or create ideal multi-temporal data sets.
- When possible we have tried to complement existing archive data (with specific polarization and incidence angle) with new acquisitions that use the same observation characteristics. For a more complete evaluation of SAR capabilities for forest degradation assessment, we should ideally have observations using the same viewing geometry and polarization during the same season (or more seasons) for a good number of years that continue until present. However, for obvious reasons (limited SAR data archives, end of lifetime of satellites, limited time frame and budget of REDDiness for collection of a more complete data series) compromises to this ideal situation had to be made.

This chapter will report on the methods used for pre-processing and visual analysis (section 10.2). We will provide separately the results for the study site in Congo, and the one in Gabon (section 10.3). We then draw our conclusions on SAR's usefulness to detect forest degradation (section 10.4).

10.2 Methods

10.2.1 Pre-processing of SAR imagery

The main software that we used for pre-processing the SAR imagery was the freeware NEST – Next ESA SAR Toolbox – Version 4C-1.1 developed by Array Systems Computing Inc. for the European Space Agency (ESA). We have chosen to base ourselves largely on this software because it can easily be transferred to the two countries given that it has no cost. Licenses for other specialized SAR processing software packages are quite expensive (including SARscape and the GAMMA Software), even if they may offer enhanced capabilities. Besides NEST the more common remote sensing software IDL-ENVI was used. To evaluate the spatial fit with other images we used ArcGIS.

Figure 10.1 shows the general pre-processing steps taken to generate calibrated (dB) geo-referenced SAR images from the original data products. These steps were in principle followed for all SAR images, including ALOS PALSAR, ENVISAT ASAR, RADARSAT-2, and TerraSAR. Multi-temporal refers to images that were acquired by the same sensor (satellite) using precisely the same polarization and image geometry (incidence angle). However, the two (multi-temporal) TerraSAR StripMap acquisitions over Congo are the only exception: they were treated as mono-temporal acquisitions, because their very large size did not permit automatic coregistration and multi-temporal speckle filtering in NEST (also for subsets this did not work). Other slight adaptations to the general flowchart were made in specific cases when problems were encountered. We will discuss the processing steps one by one.

Calibration: SAR calibration is performed to obtain an image that provides values that directly relate to the radar backscatter (expressed as sigma nought, or σ^0). Sigma nought gives the average radar reflectivity of a ground element, normalized to a unit area on the horizontal ground plane. In the strict sense, σ^0 depends on the local surface slope towards the radar. Accurate determination of σ^0 therefore requires good-quality digital elevation models (DEMs) at a similar resolution as compared to the radar imagery. The best quality DEM that was readily available for the study area was the 90-m DEM from the Shuttle Radar Topography Mission (SRTM): the 30-m ASTER global DEM (GDEM) suffers from clouds in the study sites and thus also uses the SRTM. The NEST software achieves local

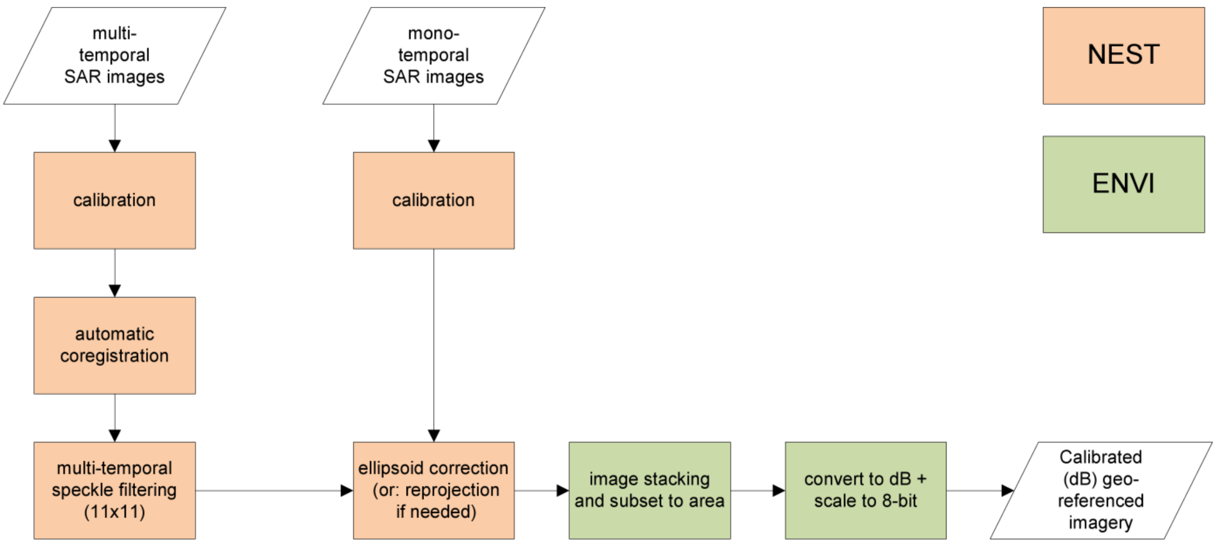

Figure 10.1: General flowchart of SAR pre-processing steps using NEST and ENVI. Based on the image type some small modifications to this general flowchart have been made (discussed in the text).

slope correction of σ^0 through the tool "SAR Simulation Terrain Correction Operator". However, this tool does not support all SAR imagery used. Because of this, and the coarse resolution of the available DEM, we performed the calibration to σ^0 for all image types only with reference to the ellipsoid. Often σ^0 is expressed in decibels (dB) to better represent its range of values and for improved visualization. However, for this step we kept the linear scaling (amplitude) which is needed for subsequent steps (particularly the speckle filtering).

Automatic coregistration: To obtain a precise fit between multi-temporal SAR images (of the same sensor, polarization, and viewing geometry), automatic coregistration is performed. For example we performed automatic coregistration for all ALOS PALSAR Fine Beam Dual images for Congo that were acquired in ascending satellite orbit, but the other PALSAR modes (Fine Beam Single, or Fine Beam Polarimetric) were treated separately. One image is selected as the master image (in our case generally we selected the most recent image) and the others as slaves. During the coregistration process, the cross-correlation between master and slave images is calculated for a number of small areas across the image scene. The slave image is then shifted for the offset that gives a maximum cross-correlation between the slave and the master image. As stated previously, the only multi-temporal set of images that was not subjected to automatic coregistration in NEST were the two TerraSAR StripMap images for Congo. The size of these images (4GB per image) was likely the cause that NEST could not perform this step – even when creating a subset this was not achieved. Nonetheless, manually shifting the image (adapting the ENVI-header file) resulted in a good fit.

Multi-temporal speckle filtering: Speckle is granular noise in SAR images that is caused by random interference between multiple radar return signals from small objects present within a single resolution cell. Speckle gives SAR images a grainy appearance (salt-and-pepper effect) and makes effective image interpretation more difficult. Several techniques exist to reduce this noise: a common technique is to average multiple resolution cells (creating larger pixel sizes) through a process called multi-looking. Multi-looking is already applied on most so-called 'detected' SAR image products (which give the amplitude of the radar return). Multi-looking increases the image quality, but decreases the image resolution. Another technique to reduce speckle is the use of spatial filters, such as the Mean, Median, Lee, or Gamma MAP filters. The main challenge of a spatial speckle filter is to reduce the speckle but simultaneously keep features of interest. For REDDiness we have tested a number of spatial speckle filters, but found that any filter changes the image to an extent that potential features of interest are obscured or lost. For our purpose of largely visually exploring potential information content of the SAR images (for example to detect narrow logging roads or small clear-cuts), we decided not to use spatial speckle filters. A third approach to speckle reduction is through the use of multi-temporal speckle filtering methods. The advantage of such methods is that the original SAR image characteristics (spatial and temporal information) are largely maintained, while speckle is strongly reduced, especially when using a larger number of images. It requires the multi-temporal SAR scenes to be acquired with the same viewing geometry (and polarization). NEST implements the multi-temporal speckle filter by Quegan et al (2000)[61]. The only parameter it requires is window-size, which is the size of the moving window that is used to calculate spatial average backscatter values. After testing, we selected an 11x11 window for all images, which provided best results judging from visual analysis of the output (see also Figure 10.2).

[61] Quegan S, T. L. Toan, J. J. Yu, F. Ribbes and N. Floury, 2000. Multi-temporal ERS SAR analysis applied to forest mapping. *IEEE Transactions on Geoscience and Remote Sensing* 38(2): 741 - 753.

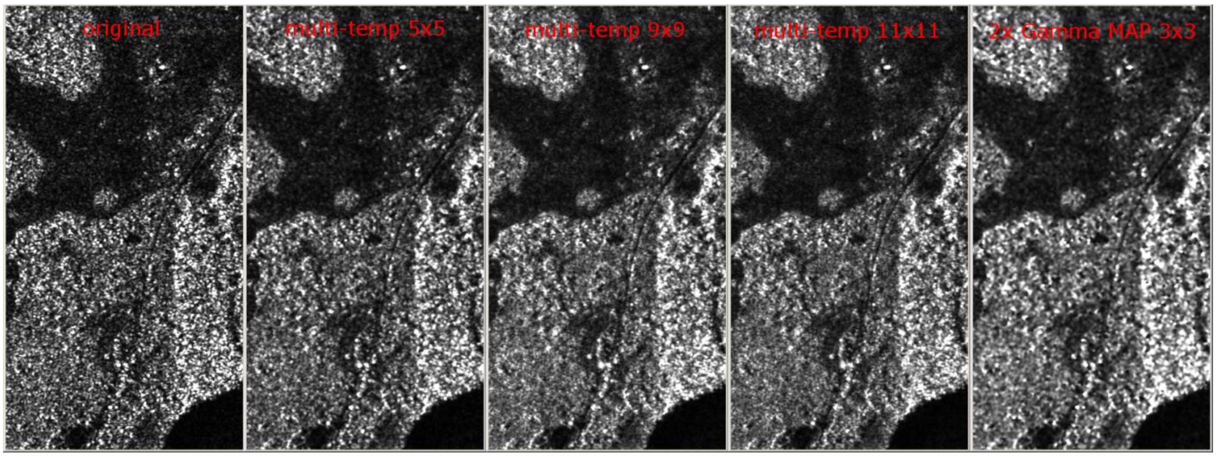

Figure 10.2: Comparison of the original calibrated Radarsat-2 Multi-Look Fine image of 4 March 2012 (left) with three multi-temporal filters of different window sizes (5x5, 9x9, and 11x11) and a spatial speckle filter (Gamma MAP with two iterations). The multi-temporal speckle filter with a window size of 11x11 gave highest speckle reduction while preserving spatial detail.

Ellipsoid correction (or reprojection): Most acquired images were oriented in the direction of the radar satellite flight line, i.e. not yet reprojected to a ground projection. For effective comparative analysis inside a geographic information system (GIS) these images need to be projected to the earth surface using a map projection. This is most accurately done when also correcting for the earth curvature, which is achieved through ellipsoid correction. The ellipsoid correction could be applied to ENVISAT ASAR and RADARSAT2 data. For ALOS PALSAR ellipsoid correction was not supported in NEST and we used simple reprojection. For TerraSAR High Resolution SpotLight data the ordered data were already projected (EEC and GEC products). For TerraSAR StripMap we experienced major difficulties in NEST (due to large file size) but managed to reproject in ENVI. We converted each image to the geographic latitude-longitude projection with WGS-84 as the datum. In all cases bilinear interpolation was used for data resampling. A number of difficulties were encountered however in this step:

- ENVISAT ASAR scenes: prior to ellipsoid correction we needed to flip the data (invert east and west) in order to obtain a properly georeferenced image. For some reason NEST did not account for this properly when using the IMP and APP products that were acquired during descending orbits. We achieved the flipping of the scene by writing a simple code in the programming language IDL (interactive data language).
- TerraSAR StripMap scenes gave a poor fit with other images (for example QuickBird), which could not be resolved by simply shifting the data. We largely solved this by manually selecting a large number of ground control points and applying a first-degree polynomial to warp the image. Perhaps this problem could have been prevented if we had known in time that EEC products (Enhanced Ellipsoid Corrected) could be obtained through the GMES Data Access Portfolio. We now had ordered GEC products (Geocoded Ellipsoid Corrected) which have poorer geolocation accuracy. To us this also stresses that selection of the correct SAR products (especially for a range of different satellites) is not an easy task for relatively non-experts. In our case however, we had wrongly interpreted GMES data access guidelines. This was clarified later through direct contact with ESA and the GMES Services Coordinated Interface. However, we could only update to EEC for a limited number of scenes, for which we selected the 5 TerraSAR High Resolution SpotLight of Gabon. The GEC-versions of these scenes were hard to mosaic and gave a poor fit with other data.

- For none of the images we obtained directly a perfect fit with the other imagery, particularly the very high resolution optical images (QuickBird and WorldView). However, in most cases the fit became very reasonable after a simple shift (north-south, and east-west) of the data. This was simply achieved by adapting the ENVI-headers and evaluating the overlay in ArcGIS.

Image stacking and subset to area: To facilitate access to and joint analysis of multi-temporal imagery, all images of the same sensor, polarization, and viewing geometry were stacked into a single file. Among others this allows easy creation of colour composites. To reduce image size we created a subset of the data to fit the study areas.

Conversion to decibel and scaling to 8-bit: Linearly-scaled radar reflection (σ^0) values generally span a wide range with a skewed distribution for a specific image. To facilitate image interpretation, σ^0 is commonly converted to a logarithmic decibel (dB) scale. We scaled all images to dB in ENVI using a simple band math function. The SAR image pre-processing resulted in large data files, especially for the higher resolution SAR images. To improve image opening and rendering in GIS-software (in our case ArcGIS) we scaled the images to 8-bit, i.e. we rescaled the σ^0 (dB) values to a range between 0 and 254. The value 255 was kept as a no-data value for areas outside the SAR image. For each image type and polarization we selected the appropriate scaling based on the image histograms. We made sure that approximately 1-2% of the values were below the lower cut-off value (so set to 0) and 1-2% of the values in the image above the higher cut-off value (and set to 254). In between these values σ^0 (dB) was linearly scaled between 0 and 254. We wrote a simple ENVI band match function to achieve this.

10.2.2 Visual interpretation of SAR imagery

We visually examined all SAR images and compared these with optical data. We took the very high resolution optical data (QuickBird and WorldView-2) as the main reference, and where possible complemented with ground evidence obtained during the field visits. In this chapter we will provide a visual comparison and discussion of a number of subsets from the imagery, which illustrate our main findings. We try as much as possible to compare similar image dates with each other. However, for some images (like ALOS PALSAR) no recent data exist because the satellite has ended its operation in 2011 or no images could be or have been acquired (from archives or new acquisitions). Our analyses are structured in the following way:

1. Mono-temporal detection of degradation signs: focusing on logging roads, and canopy gaps.
2. Multi-temporal change detection: for images where we have multi-temporal acquisitions we compare between different dates of the same image type to evaluate if changes can be detected.
3. Large-scale differences in forest types: we evaluate major patterns that emerge which could be indicative of forest types, including a distinction between more or less degraded forests.

10.3 Results

10.3.1 Congo: mono-temporal analysis

Figure 16 shows an area along the main road (10 m wide) that crosses the study area. The area is dominated by secondary forest and includes bare areas (with some houses) along the road and fallow fields in between the forest (Figure 10.3a). A pattern of narrow (<5m wide) logging roads can be observed east from the road. Comparison with the July 2011 WorldView image (not shown) indicates that these logging roads are already at least one year old, and some regeneration of vegetation took place during the year. Comparison with the SAR data shows that only TerraSAR (both at 1 and 3m resolution: Figure 10.3b and 10.3c) is able to detect these narrow logging roads. RADARSAT (e) and ALOS PALSAR Fine Beam Single (h) merely detect the main road, while the road does not show up clearly from the coarser-resolution ALOS PALSAR Fine Beam Polarimetric (i) and ENVISAT ASAR (f). When degrading the resolution of QuickBird to 9.6 m (similar to Sentinel-2) we also observe that only parts of the logging roads are apparent from the image. This example shows that a high spatial resolution is needed, particularly for SAR, to detect narrow logging roads.

Not all logging roads can easily be observed from the high-resolution TerraSAR imagery. Figure 10.4 shows an area which is located in a denser, more continuous forest as compared to Figure 10.3. A narrow logging road is present with an apparent width of about 5m in the QuickBird image. Although the road vaguely shows up on the 1m TerraSAR SpotLight imagery as a line of high backscatter, it cannot be well discerned from its surroundings. The logging road is not visible on the 3m TerraSAR StripMap image. A likely explanation is that the trees surrounding the road are relatively high and tree crowns frequently cover the road. Because the radar observes under an angle (approximately 38° in this case) from its perspective the canopy is relatively closed: no major radar shadows are casted, nor does strong backscattering from tree trunks (double bounce) or layover (when ground elements and tree canopy both create backscattering in the same resolution cell) give significantly higher returns. This could also partly be because of the orientation of the logging road which is approximately perpendicular to the satellite flight line.

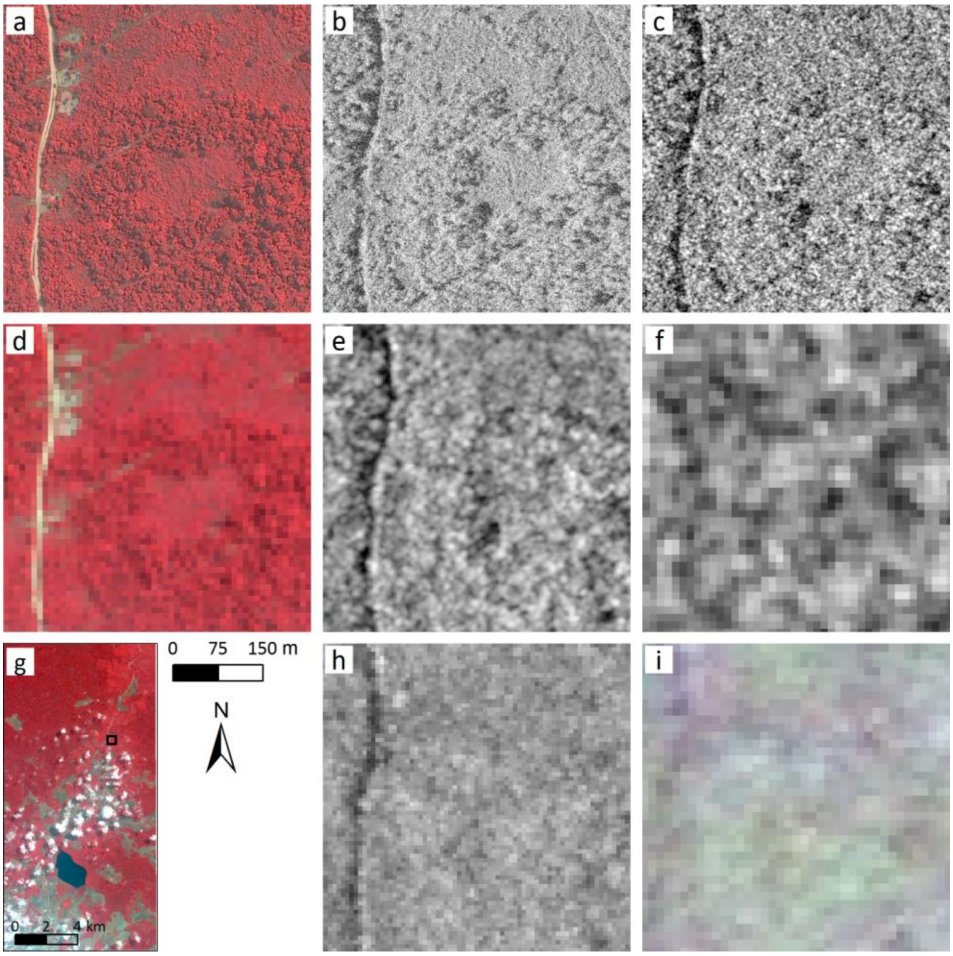

Figure 10.3: Mono-temporal imagery for a small part of the Congo study site. At the left of the image a main road is present with approximate width of 10m (oriented north-south), while a rectangular pattern of logging roads (<5m wide) is visible on the right of the road. The images show: a) a QuickBird false-colour composite of July 2012, b) a TerraSAR High Resolution SpotLight image of March 2012, c) a TerraSAR StripMap image of May 2012, d) a degraded QuickBird false-colour composite at 9.6m resolution, e) a RADARSAT Multi-Look Fine image of March 2012, f) an ENVISAT ASAR image of March 2012, g) an overview of the 20x10 km study site with the black box showing the location of the other images (QuickBird), h) an ALOS PALSAR Fine Beam Single image of March 2011, and i) an ALOS PALSAR Fine Beam Polarimetric image of March 2011 (R=HH, G=HV, B=VV).

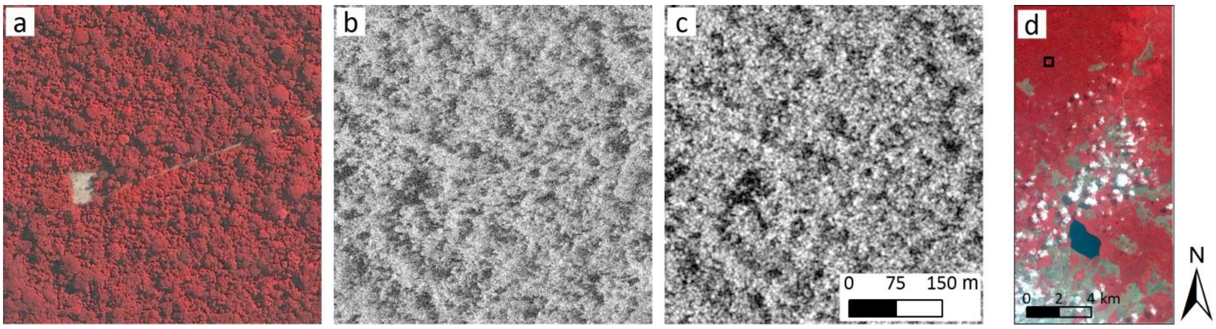

Figure 10.4: Narrow (about 5m) logging road with small clear-cut as observed from a) QuickBird - July 2012, b) TerraSAR High Resolution SpotLight - March 2012, c) TerraSAR StripMap - May 2012. The precise location of the subset in the 20x10 km study site in indicated with the black box in d).

Figure 10.5 schematically illustrates some of the main scattering mechanisms that were discussed here. Whatever the precise reasons, it is apparent that the logging road is not well observable from these SAR images (nor from the other image types shown in Figure 16). The forest gap on the left of the image in Figure 10.4 (approximately 40 by 50m) was detected by the SAR imagery. It is darker than its surroundings due to less volume scattering from the bare ground surface and because of high trees on the edges that cast a radar shadow.

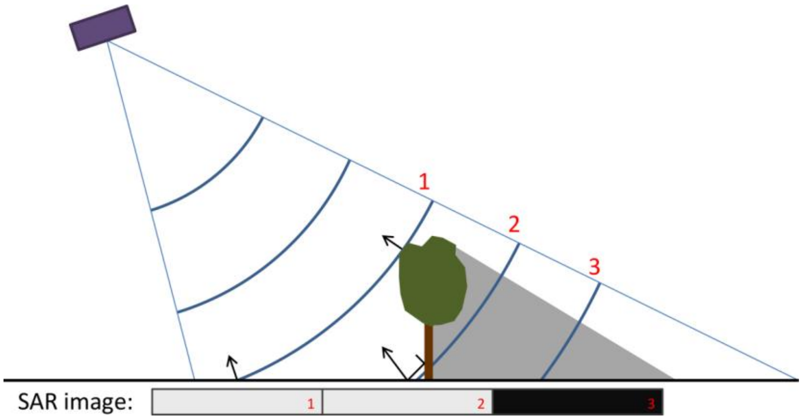

Figure 10.5: A simplified representation of some scattering mechanisms that can explain backscatter variation on the boundary between forest and non-forest. A satellite sends out pulses of energy. Pulse 1 is reflected simultaneously by the tree crown and the ground surface: these combined signals create a high backscatter (white in SAR image). Pulse 2 interacts with the tree trunk which creates a double bounce, thus high backscatter. Pulse 3 is in the radar shadow and not interacting with any elements, i.e. no backscatter causing a dark appearance on the SAR image. Note that the tree crown (pulse 1) is imaged before the tree trunk (pulse 2), causing the layover effect.

The separation of forest versus non-forest is normally well achieved with a single SAR image (Figure 10.6). Optical imagery suffers from clouds and Landsat-7 also from the Scan Line Corrector failure causing striping (Figure 10.6a and d). Irrespective of weather conditions, mono-temporal SAR images provide a clear delineation between surfaces with substantial tree cover and areas with less vegetation (bare or grassland). This does not necessarily require very high resolution imagery (TerraSAR), but also the RADARSAT, ENVISAT, and PALSAR imagery shown in Figure 10.6 clearly delineate forest and non-forest patches. ENVISAT ASAR performs poorest, and does not image well the forest patches smaller than approximately 150m, likely due to the low resolution and the steep incidence angle used in standard mode (23°). The longer-wavelength L-band (approximately 23 cm) of PALSAR provides deeper penetration of the signal into the forest. Its backscatter is therefore more related to larger structural elements like tree trunks and large branches, thus giving a strong difference between forest and non-forest. The X-band (3cm) of TerraSAR and the C-band (6cm) of RADARSAT and ENVISAT ASAR generate more scattering from the tree crowns.

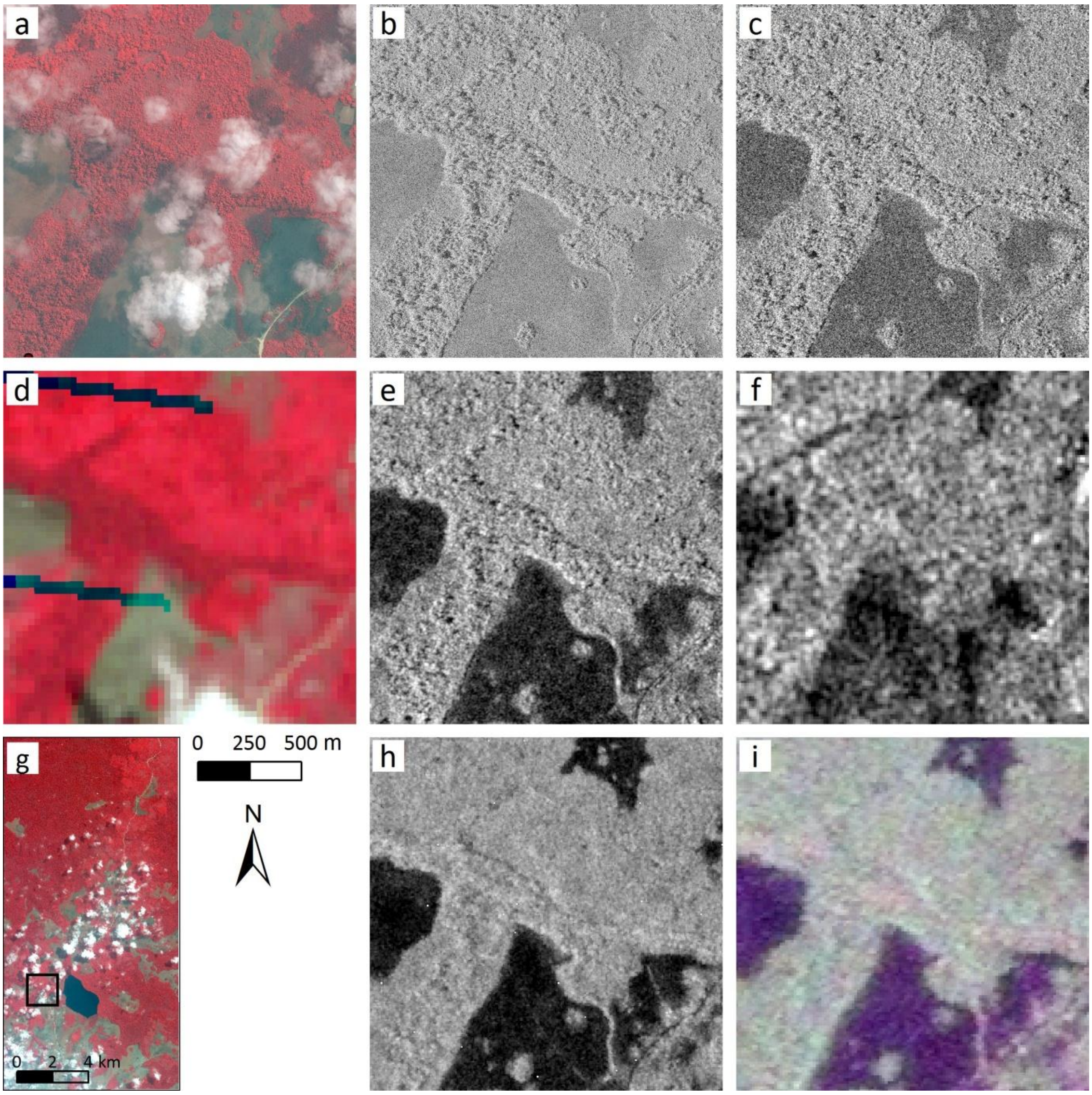

Figure 10.6: Distinction forested and non-forested land at coarse-scale from a variety of satellites: a) QuickBird - July 2012, b) TerraSAR StripMap - June 2010, c) TerraSAR StripMap - May 2012, d) Landsat-7 false colour composite – April 2011, e) a RADARSAT Multi-Look Fine image of March 2012, f) an ENVISAT ASAR image of March 2012, g) a QuickBird overview of the 20x10 km study site with the black box indicating the subset, h) an ALOS PALSAR Fine Beam Single image of March 2011, and i) an ALOS PALSAR Fine Beam Polarimetric image of March 2011 (R=HH, G=HV, B=VV).

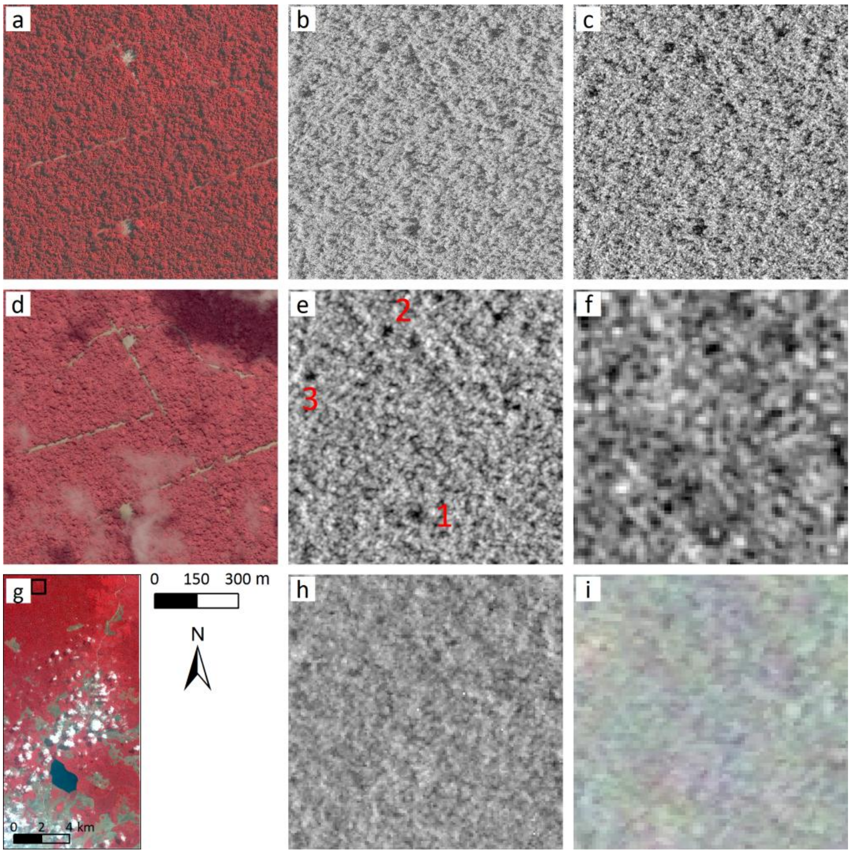

Figure 10.7: Small forest gaps (about 50x50m) observed by: a) QuickBird - July 2012, b) TerraSAR StripMap - June 2010, c) TerraSAR StripMap - May 2012, d) WorldView-2 false colour composite – August 2011, e) a RADARSAT Multi-Look Fine image of March 2012 (numbers are discussed in text), f) an ENVISAT ASAR VV-polarized image of March 2012, g) a QuickBird overview of the 20x10 km study site with the black box indicating the subset, h) an ALOS PALSAR Fine Beam Single image of March 2011, and i) an ALOS PALSAR Fine Beam Polarimetric image of March 2011 (R=HH, G=HV, B=VV).

Most forest gaps that were found in the part of the study area with denser forest had a small spatial size (about 50x50m, or 0.25 ha), and were located adjacent to current or older logging roads (see also Figure 10.4). Figure 10.7 shows small forest gaps in the north of the study area. On the QuickBird image (20a) two clear gaps can be discerned. These result from older logging activities, as these gaps and logging roads were clearly present in August 2011 (10.7d). In fact it seems that vegetation has regenerated to a certain extent between both image dates. The RADARSAT image (10.7e) shows three numbers that refer to dark patches (radar shadows), which will be discussed in more detail now. The forest gap at location 1 is apparent on both TerraSAR and RADARSAT images and corresponds to a forest gap in the QuickBird image. At location 2, two dark patches are present in TerraSAR and RADARSAT imagery, while QuickBird only shows one gap. Likely the leftmost dark patch corresponds to the broad junction of logging roads, visible in the WorldView image. The dark patch of location 3 is apparent in TerraSAR and RADARSAT imagery. This patch does not correspond to anything that can be observed from the very high resolution optical images. Possibly there is a relatively large tree that casts a radar shadow on lower trees surrounding it. This observation indicates that confusion may occur when interpreting small areas with deviating characteristics in SAR imagery, even when using very high resolution data. From the coarser resolution ENVISAT ASAR (10.7f) and ALOS PALSAR (10.7h and i) the forest gaps are not visible. In case of PALSAR there is a chance that the clear cuts were made between the time of their image acquisition (March 2011) and the WorldView image data (August 2011). We could not verify this based on acquired field data or information from logging concessions.

To evaluate ALOS PALSAR more in detail, we used the aerial photograph of October 2007 that was obtained through Winrock. This aerial photograph is acquired closer in time from the PALSAR images as compared to the QuickBird and WorldView images. Figure 10.8 shows a forested area with inclusions of a large patch of grassland, and some smaller gaps. Two gaps towards the left of the image (approximate width 60-80 m) are clearly visible on both 2007 PALSAR images (b and c). However the aerial photograph shows some recent logging activities (h) which are not apparent on those PALSAR images. One explanation could be that the logging activity took place between 7 October (PALSAR acquisition) and end of October (aerial photograph). We therefore checked the presence of the new clear-cut as well on 2008 imagery. While Landsat (d) is observing it, to our surprise 2008 PALSAR imagery does not show it (e and f). The PALSAR FBD only shows slightly bluer colours, possibly due to less volume scattering caused by fewer trees. We do not have a satisfactory explication for this. Therefore, although PALSAR well delineates stable gaps in the forest canopy of about 60-80 m in width, the effective observation of recent clear-cuts seems problematic.

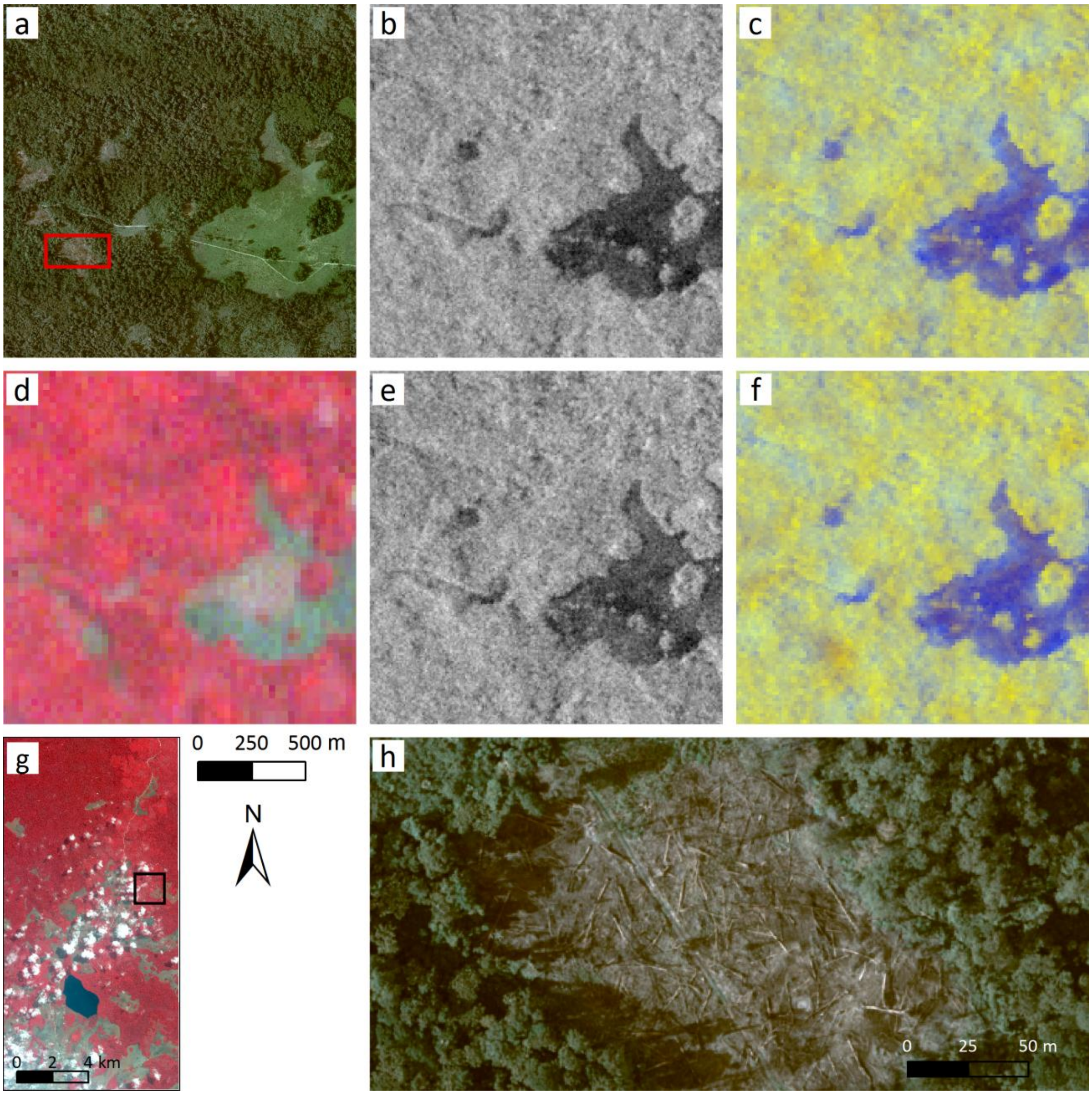

Figure 10.8: Forested areas with large and small gaps: a) aerial photo obtained between 28-31 October 2007 through Winrock, b) ALOS PALSAR Fine Beam Single (FBS) image - 7 October 2007, c) ALOS PALSAR Fine Beam Dual image – August 2007 (R=HH, G=HV, B=HH/HV), d) Landsat – July 2008, e) ALOS PALSAR FBS – April 2008, f) ALOS PALSAR FBD – August 2008, g) a QuickBird overview of the 20x10 km study site with the black box indicating the subset, h) part of the aerial photo (red box of a) that clearly shows recently logged trees.

10.3.2 Congo: multi-temporal analysis

Given our findings from the previous section, and the multi-temporal image availability, we focussed the multi-temporal analysis for Congo on TerraSAR StripMap and RADARSAT Multi-Look Fine imagery of 2010 and 2012. We also analyzed multi-temporal ASAR and PALSAR imagery, including those with 4 to 6 years between acquisitions, but found few changes in forested areas. This could be because 1) little logging activity took place prior to 2011 (latest PALSAR image is from start 2011), 2) logging activities took place on too small scales to be observed, or 3) of other unidentified reasons (see also Figure 21). ASAR and PALSAR multi-temporal analysis did identify some changes, but mostly in non-forested (agriculture or build-up) areas. These images may be useful for large scale monitoring of deforestation, but in our study area did not allow the detection and monitoring of small-scale clearings and logging roads.

Figure 10.9 shows a large area of secondary forest east of the main road. Clouds are present in the optical QuickBird and WorldView images, but nonetheless a rectangular pattern of approximately 10m wide logging roads is clearly visible. It seems that between August 2011 and July 2012 the number of logging roads has not increased, but rather vegetation regenerated. From the 3m resolution TerraSAR StripMap image of May 2012 the rectangular pattern of logging roads is very clear, but absent from the June 2010 image. This means that the logging roads were created between June 2010 and August 2011. If a TerraSAR StripMap acquisition would have been available for 2011, the logging roads may have been more pronouncedly visible on the image. The 8m resolution RADARSAT imagery of March 2012 does not show the appearance of these logging roads. Both RADARSAT and TerraSAR were acquired with HH polarization with a difference in incidence angle of merely 3°. However, RADARSAT observes in C-band (about 6 cm wavelength) and TerraSAR in X-band (3 cm), and RADARSAT has a lower spatial resolution (8 vs. 3 m). X-band could be more appropriate for logging road detection because the backscatter relates more directly to changes in the small elements of the canopy. However, very likely the resolution also plays a decisive role.

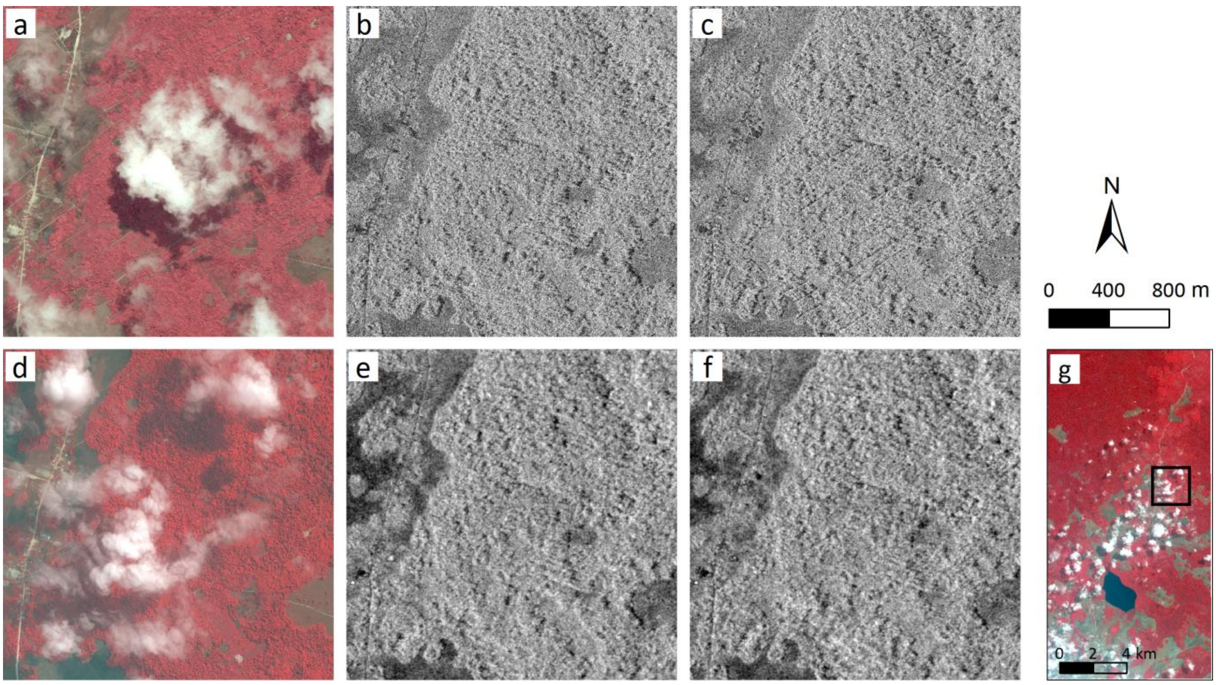

Figure 10.9: Logging road appearance in secondary forest: a) WorldView – August 2011, b) TerraSAR StripMap - June 2010, c) TerraSAR StripMap - May 2012, d) QuickBird - July 2012, e) RADARSAT-2 (34.8° incidence angle) - March 2010, f) RADARSAT-2 (34.8° incidence angle) - March 2012, g) overview image with black box indicating location of subsets.

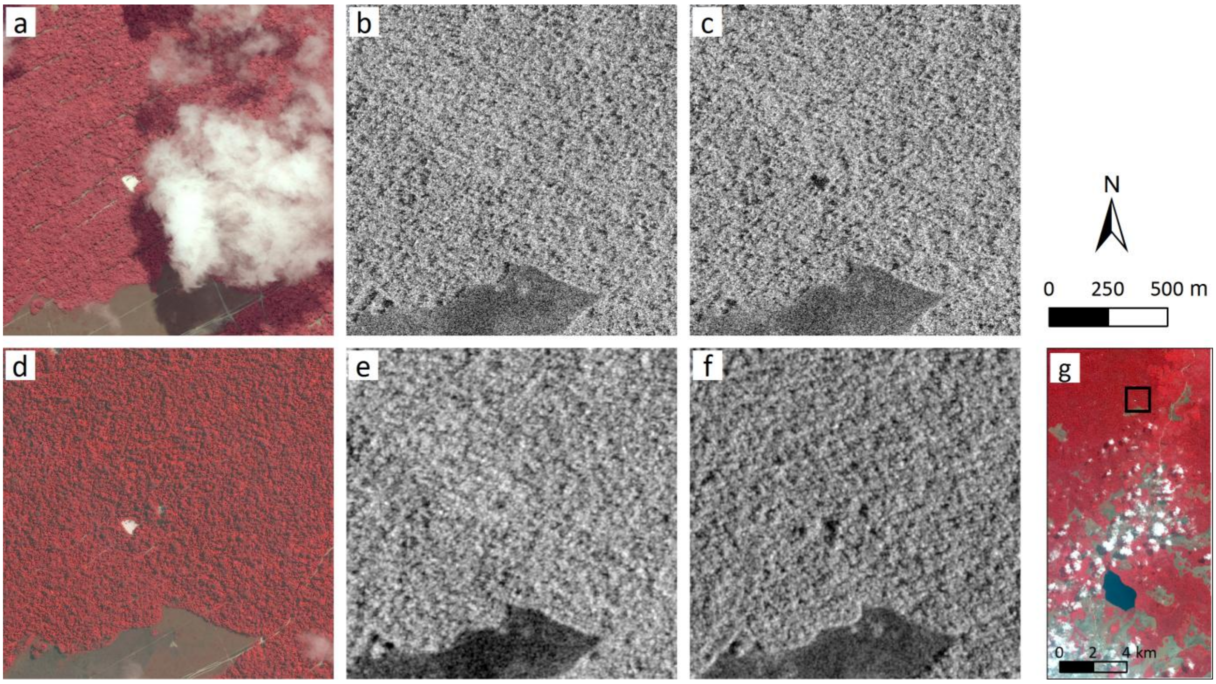

Figure 10.10: Logging roads in dense forest with strong regeneration: a) WorldView – August 2011, b) TerraSAR StripMap - June 2010, c) TerraSAR StripMap - May 2012, d) QuickBird - July 2012, e) RADARSAT-2 (34.8° incidence angle) - March 2010, f) RADARSAT-2 (34.8° incidence angle) - March 2012, g) overview image - black box indicates location of subsets.

TerraSAR StripMap imagery is not always equally successful in detecting logging roads. Figure 10.10 shows another example of a forest with higher tree density and tree height. Like for the previous example logging roads are clearly visible on the WorldView image, and less visible on the QuickBird image, indicating forest regeneration between August 2011 and July 2012. The forest gap (white colour on the optical images, approximately 50x50m) is related to the creation of the logging roads. It shows up clearly in the 2012 TerraSAR and RADARSAT images, whereas it is absent from the 2010 SAR images. This means that change analysis using either TerraSAR or RADARSAT allows successfully detecting the formation of this new gap. However, unlike in Figure 10.9, the logging road network is not clearly visible on the 2012 TerraSAR image. Only a limited number of logging roads can be observed very faintly after careful inspection of the image. Two factors could be responsible for this: 1) the narrow logging roads do not create a significantly different backscatter when surrounding by high and dense trees; 2) between August 2011 (WorldView) and May 2012 (TerraSAR) already significant regeneration had occurred. Given this quick regeneration of vegetation on logging roads (apparent from comparison WorldView and QuickBird), it seems mandatory for detection of logging roads in these environments that an image is obtained at least every year, and possibly more frequent. These could be very high resolution optical data (although costly and acquisition problems due to cloud cover), while TerraSAR StripMap is also a good candidate meriting further analysis with more frequent data (as apparent from the example in Figure 10.9).

The creation of small forest gaps in the study area can relate fully to logging activities for timber production (Figure 10.10). In addition, forest gaps are created due to opening up of agricultural fields (shifting cultivation), mostly in secondary forests in the vicinity of a main road and village. Figure 10.11 shows a forest gap where cassava is cultivated. The location was visited by the field team, and they estimated the age of the cassava plants at approximately one year old. The forest gap clearly appears on the 2012 TerraSAR and RADARSAT image, which were acquired during ascending orbits with 37.8° and 34.8° incidence angle respectively. A strong radar shadow appears on the western side of the gap (see Figure 10.5 for an explanation of the scattering mechanisms responsible). On the eastern side of the forest gap, increased backscatter can be observed, particularly in the RADARSAT scene. For TerraSAR, the texture and overall backscatter levels on the cassava field are different from its forested surroundings. These features were not visible on the 2010 image, which indicates that the forest gap was created between 2010 and 2012. This corresponds to field observations in 2012. Figure 10.11h and 10.11i show RADARSAT images from similar dates, but in this case acquired during descending orbits at a larger incidence angle of 48.1°. This causes a very different interaction of the radar pulses with the ground elements as compared to the 34.8° ascending acquisitions. For the descending acquisitions 2012 shows somewhat higher backscatter levels than 2010 within the forest gap area. However, in contrary to the ascending acquisitions, the changes between both years do not allow for a straightforward interpretation that a forest gap was created. This implies that besides sensor and resolution characteristics, also the viewing geometry of the satellite acquisition is an important factor determining the potential to observe features and changes of interest in the field.

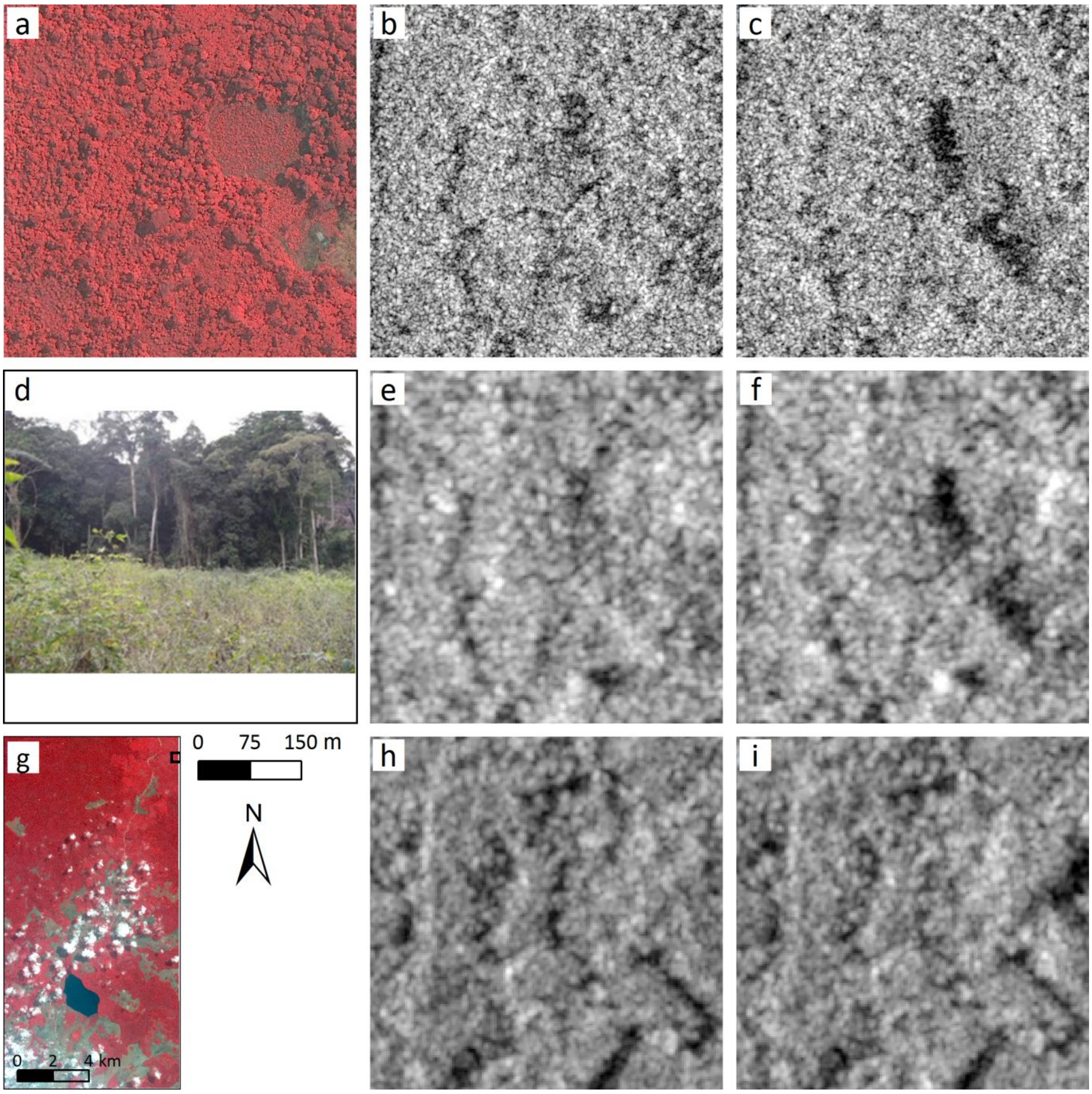

Figure 10.11: Cassava fields of approximately one year old within a secondary forest as seen by: a) QuickBird - July 2012, b) TerraSAR StripMap - June 2010, c) TerraSAR StripMap - May 2012, d) photo taken during fieldwork of fields with secondary forest on the background - August 2012, e) RADARSAT-2 scene at 34.8° incidence angle looking towards the right - March 2010, f) same geometry RADARSAT-2 image - March 2012, g) overview image with black box indicating location of subsets, h) RADARSAT-2 scene at 48.1° incidence angle looking towards the left - March 2010, and i) same geometry RADARSAT-2 image - April 2012.

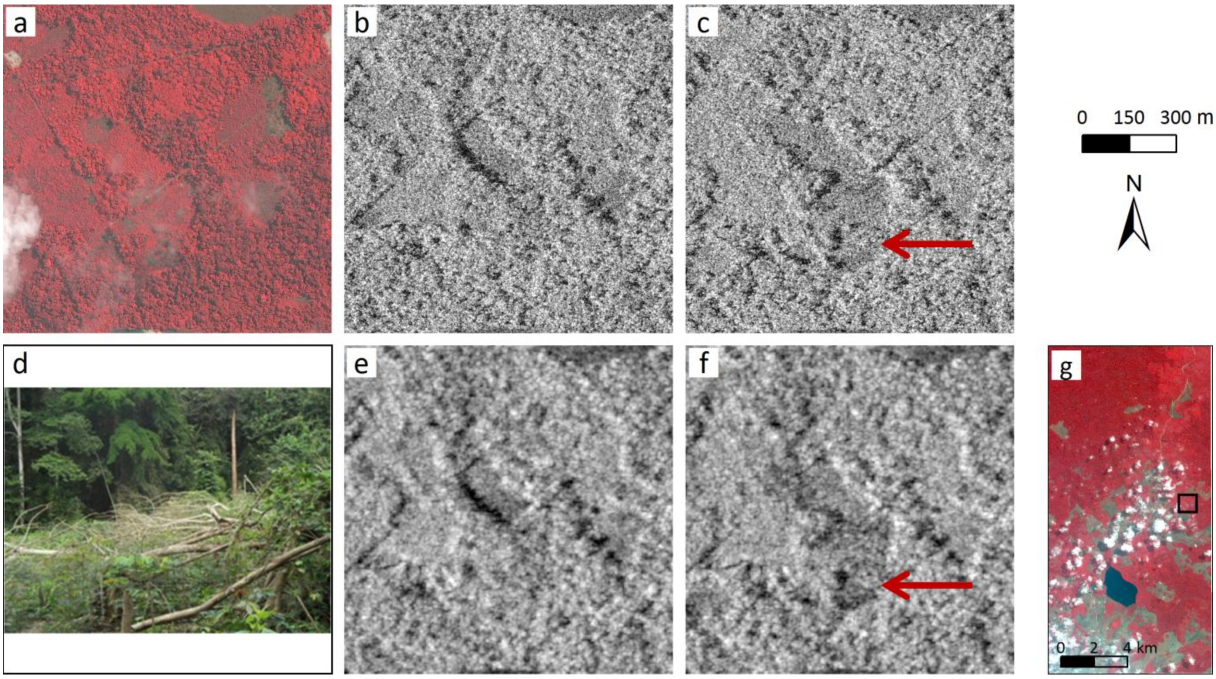

Figure 10.12: Expansion of cassava fields in a secondary forest through shifting cultivation practices. a) QuickBird - July 2012, b) TerraSAR StripMap - June 2010, c) TerraSAR StripMap - May 2012, d) photo taken during fieldwork showing recent clearings - August 2012, e) RADARSAT-2 scene at 34.8° incidence angle - March 2010, f) same geometry RADARSAT-2 image - March 2012, g) overview image with black box indicating location of subsets. The red arrow in the 2012 SAR images indicates new fields that were still forest in 2010. Note: this is a smaller part of the image shown in Figure 10.9

Figure 10.12 provides an example of cassava fields that expanded in southern direction between 2010 and 2012. At the location of the red arrow (10.12c and f) recent forest clearings are visible that correspond to the location pictured during fieldwork (10.12d). On both 2012 images the new clear-cut shows up as an area of overall decreased backscatter with a smoother texture. Simultaneously fields north of that clearance also changed between 2010 and 2012. Radar shadows found in 2010 (both TerraSAR and RADARSAT) have largely disappeared. This could imply that 1) large trees near the forest-agricultural boundary have been cut as well, or 2) regeneration near the forest boundary took place (trees become high enough to not fall in the radar shadow anymore). Given that east of the shadowed area also high backscatter areas (as caused by high trees, see Figure 10.5) largely disappeared, and backscatter levels of a larger area have become similar to those of the cassava field, the first explanation is more likely. Hence from our perspective based on the 2010 and 2012 SAR imagery, this image represents a zone with secondary forest that has further degraded.

10.3.3 Congo: large-scale spatial patterns and forest types

In this section we evaluate large scale patterns that emerge within the entire 20x10 km study area based on the different SAR data used in this study. Such patterns could potentially provide information of forest types, for example to separate more degraded from intact forests. Figure 10.13 displays mono-temporal images of all SAR image types used in this study. The figure shows that separation between forest and non-forest can be made in a reasonable way for most SAR images. In the QuickBird image this non-forest (mostly bare areas and savannah grasslands) shows up with green colours, while SAR shows lower levels of backscatter and mostly a smoother texture. Probably the least clear separation is achieved with ENVISAT ASAR image mode: this may be attributed to the low incidence angle and coarser spatial resolution. The low incidence angle also causes more lay-over effects, including in areas with relatively gentle slopes. In the north-east of the study site QuickBird shows a distinct red colour from the darker red in the north-west part. This area is in the vicinity of the main road. Detailed analysis and fieldwork indicates a less continuous, more disturbed forest with a high degree of anthropogenic activities such as shifting cultivation agriculture. On TerraSAR and RADARSAT-2 imagery this area shows up with a different texture; however ALOS PALSAR and ENVISAT ASAR do not clearly distinguish this area from denser forests. Most SAR images (except for ENVISAT) identify a zone of increased backscatter immediately south of the lake: the field visit indicated that this is a humid zone. East of that zone an inverted U-shaped feature is found that shows up white on the PALSAR polarimetric image (10.13j): also on other ALOS images this zone is clearly different from its surroundings and has higher backscatter values. Fieldwork confirmed that this is also a humid zone dominated by Raffia palms. Other images show this area less clearly. As L-band penetrates more through the canopy it is more sensitive to water presence on the soil surface. Water creates a specular reflection surface which causes backscatter towards the sensor to increase through double-bounce mechanisms with tree trunks.

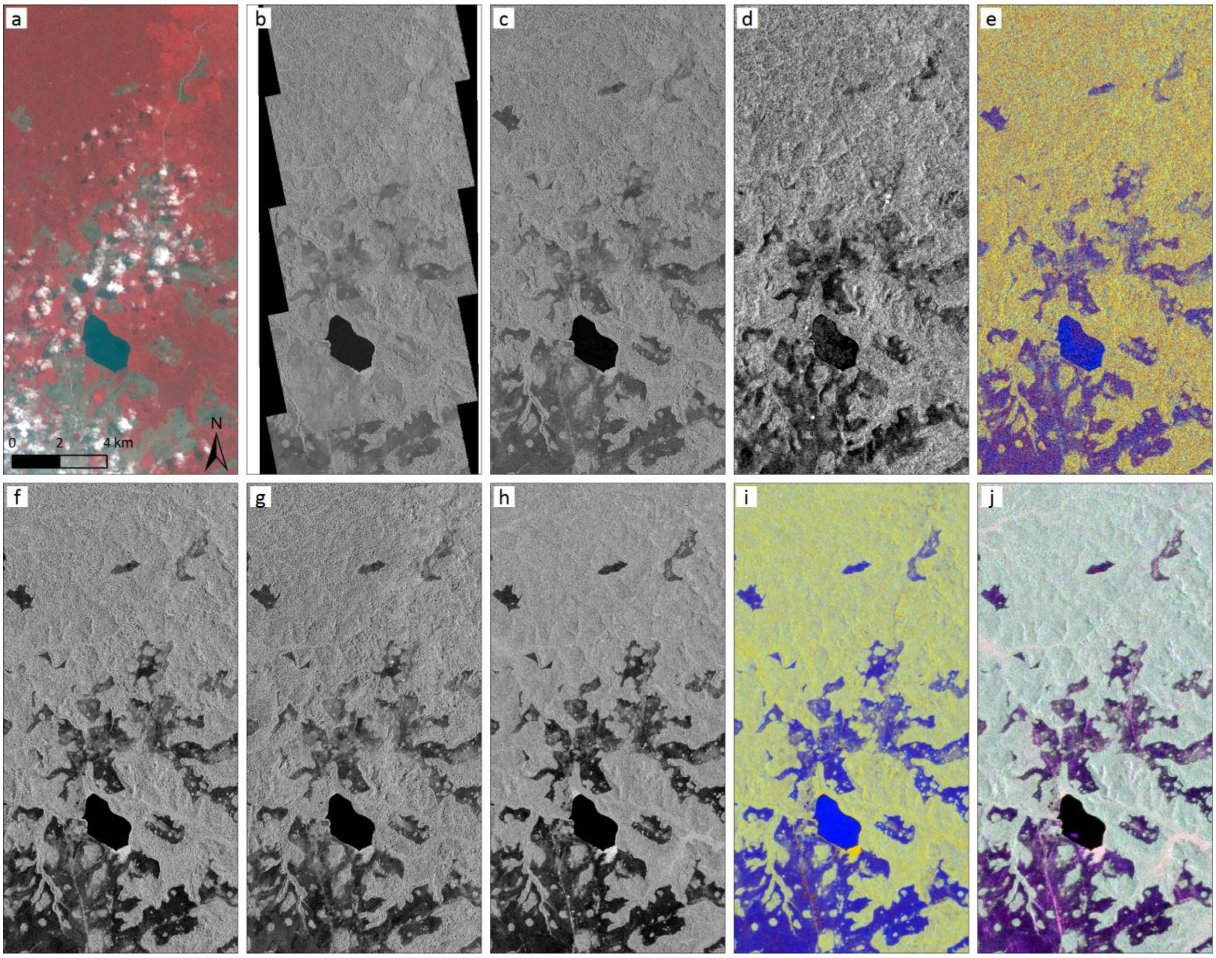

Figure 10.13: Overview of the 20x10 km study area of Congo from different mono-temporal images: a) QuickBird false colour composite - July 2012, b) TerraSAR High Resolution SpotLight – February-April 2012, c) TerraSAR StripMap - May 2012, d) ENVISAT ASAR VV Image mode – March 2012, e) ENVISAT ASAR VV/VH Alternating Polarization – April 2010 (R=VV, G=VH, B=VV/VH), f) RADARSAT-2 multi-look fine with 34.8° incidence angle March 2012, g) RADARSAT-2 multi-look fine with 48.1° incidence angle looking April 2012, h) ALOS PALSAR Fine Beam Single - March 2011, i) ALOS PALSAR Fine Beam Dual – May 2010 (R=HH, G=HV, B=HH/HV), j) ALOS PALSAR Fine BEAM Polarimetric - March 2011 (R=HH, G=HV, B=VV).

Depending on the SAR system used, to a certain extent the imagery allows for interpreting differences in forest types. Here we have not attempted to classify SAR imagery, but effective automatic classification should take into account both backscatter levels, as well as textural information, particularly for the very high resolution data. In Figure 10.13 we showed only a few colour images that could be created because the image was acquired at multiple (at least two) polarizations. As for multispectral acquisitions in optical data, the various polarizations give more information as compared to a single (grey-scale) image.

We can also enhance information content through combination of images acquired at different dates. Figure 10.14 displays multi-temporal composites for a number of SAR images. Non-forest areas show large differences with the mono-temporal displays of Figure 10.13, particularly for RADARSAT and ENVISAT. The likely reason is that soil moisture content was different at the times of image acquisitions and also varied within the area. Particularly in the ENVISAT composite this is apparent judging from the dark blue, cyan, and green colour at non-forest locations. Such effects can be more pronounced with imagery from different seasons, but also a single rain storm shortly before acquisition can cause strong variability particularly for short wavelengths as X- or C-band. Forested areas remain relatively stable (note that we focus now mainly on large patterns and not on small-scale changes treated in the previous section). As for the mono-temporal display the more disturbed forest in the north-west of the image still shows up best on TerraSAR and RADARSAT, while PALSAR best distinguishes the humid areas. For PALSAR, this is particularly clear from the multi-temporal display of the HH/HV ratio which shows the humid areas as dark green colours: the green band displays an August image. August is during the dry season when humid areas differ even more from their dry surroundings. This leads us to two concluding remarks regarding multi-temporal data display:

- if the purpose is to detect forest degradation signs, multi-temporal data should be acquired during similar seasons to avoid confusion with seasonal influences;
- however, if we want to enhance information content for improved mapping of vegetation types, we should select imagery from different seasons, because the seasonal influences may work out different on different forest/vegetation types.

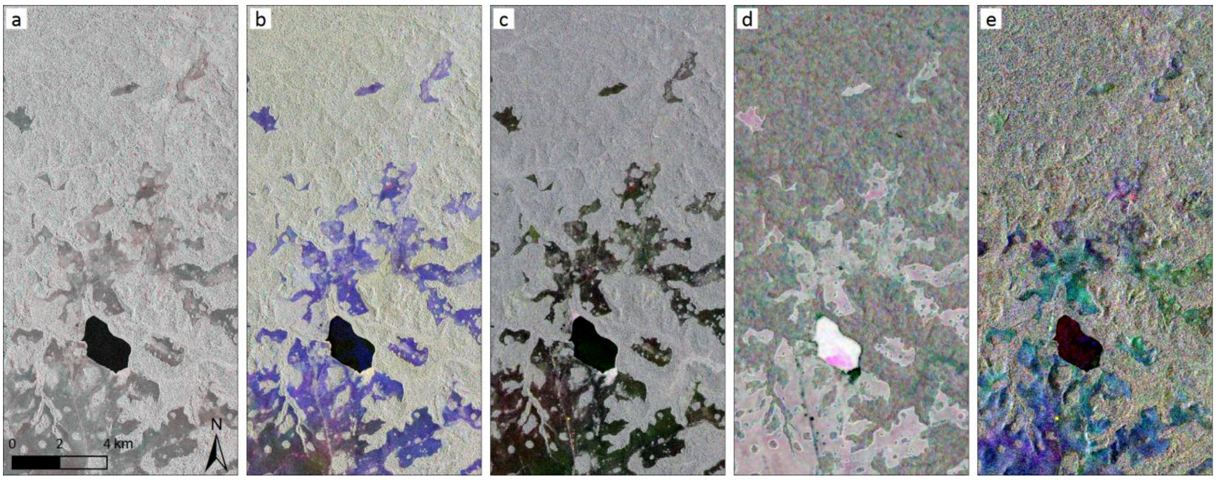

Figure 10.14: Overview of the 20x10 km study area of Congo from different multi-temporal composites: a) TerraSAR StripMap (R=May 2012, G&B=June 2010), b) RADARSAT-2 multi-look fine with 34.8° incidence angle (R=March 2012, G=March 2010, B=December 2009), c) ALOS PALSAR Fine Beam Single (R=March 2011, G=April 2010, B=February 2009), d) ALOS PALSAR Fine Beam Dual displaying HH/HV for three dates (R=November 2010, G=August 2010, B=May 2010), e) ENVISAT ASAR VV Image mode (R=March 2012, G=March 2011, B=April 2006).

10.3.4 Gabon: mono-temporal analysis

The study site of Gabon does not have a clear pattern of logging roads as found in the study site of Congo. New logging roads that appear on the imagery have a lower density and are wider. In our analysis of logging roads for Gabon we focus first on a pattern of several roads (Figure 10.15) and then on a specific narrow road (Figure 10.16). Figure 10.15 shows an area with multiple roads surrounded by a dense forest; three of them have been created between December 2010 and March 2012. The main road (width between 10 and 25 meters) appears white-blue on both QuickBird images (10.15a - 2012 and d - 2010). From that road five secondary logging roads are diverted, which show in cyan colours on the QuickBird image (10.15a - 2012). The three logging roads (black ovals in Figure 10.15a) are all approximately between 10 and 14 m wide. The other two logging roads (yellow ovals) are wider (20 m). The main road, existing before 2010, is visible on all images displayed in Figure 10.15, except for PALSAR FBP (10.15f) (only slight visibility at places where visibility is not linked to the size of the road) and ENVISAT ASAR (10.15i). From the two roads diverging of the main road (image of 2010 – 10.15d), only the one in the North-East is visible from ALOS PALSAR FBS (10.15e). FBD and FBP (10.15f) modes have a rougher spatial resolution and do not allow the clear distinction of the road in the North-East. In 2012, TerraSAR High Resolution SpotLight allows for the detection of all five logging roads. From TerraSAR StripMap the bottom left road is not visible. Besides the lower resolution, this may be because this road is more covered by tree crowns.

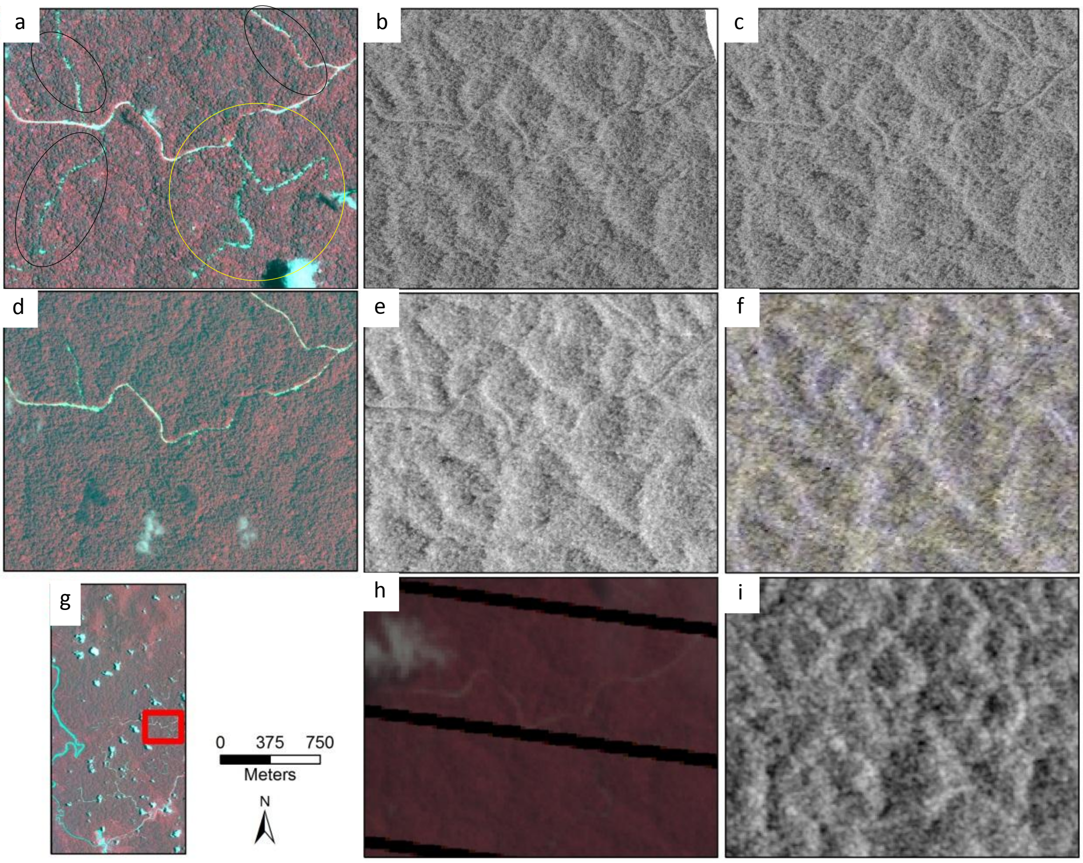

Figure 10.15: Visual comparison of mono-temporal imagery for a small part of the Gabon study site – localized on logging roads created between 2010 and 2011. On the middle of the image a main road is present, while several logging roads are visible to the north and south of the main road. The images show: a) a QuickBird of March 2012, b) a TerraSAR High Resolution SpotLight image of February 2012, c) a TerraSAR StripMap image of April 2012, d) a QuickBird of December 2010, e) an ALOS PALSAR Fine Beam Single image of February 2011 (polarization : HH), f) an ALOS PALSAR Fine Beam Polarimetric image of November 2011 (R=HV, G=VH, B=VV), g) an overview of the 20x10 km study site with the red box showing the location of the other images (QuickBird), h) a Landsat image of April 2012, and i) an ENVISAT ASAR image of March 2012 (polarization : VV).

Then, we selected one of the narrowest roads (~10m wide) of the study site (Figure 10.16a) to test the ability of the different sensors and modes to detect it. We can see that only part of the road (yellow oval) (10.16b) is visible only on the higher resolution SAR imagery, including TerraSAR-X, PALSAR FBS and FBD (the last image is not included in Figure 10.16). The part of the road north of the yellow oval does not appear: partly this is because forest canopy is covering the road more, but also the viewing geometry of the SAR system could play a role as this part is oriented parallel to the satellite flight line. That orientation can imply that less radar shadows are casted by the trees surrounding the road (whereas for the detectable part the logging road is clearly in the radar shadow). Landsat image (10.16h) allows the detection of the road while ENVISAT ASAR does not.

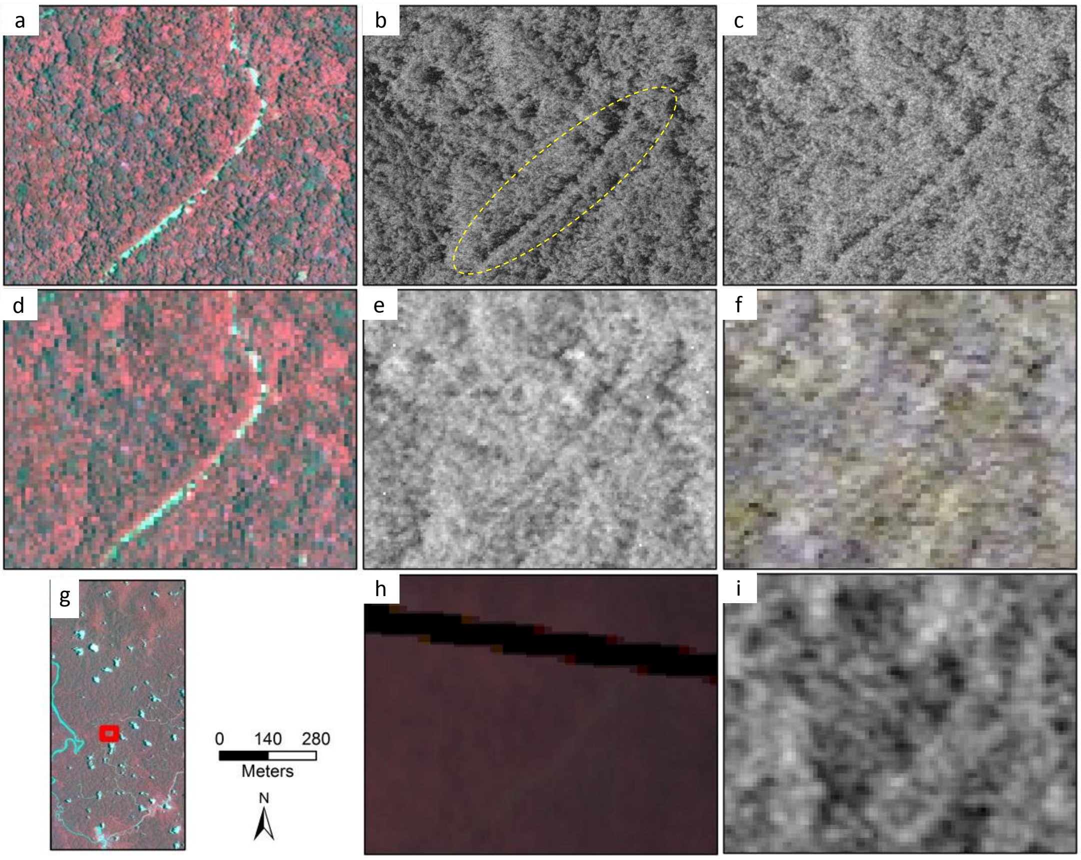

Figure 10.16: Visual comparison of mono-temporal imagery localized on a small logging road reopened between 2010 and 2011 – average width 10 meters. The images show: a) a QuickBird of March 2012, b) a TerraSAR High Resolution SpotLight image of February 2012, c) a TerraSAR StripMap image of April 2012, d) a degraded QuickBird false-colour composite at 12m resolution, e) an ALOS PALSAR Fine Beam Single image of February 2011 (polarization : HH), f) an ALOS PALSAR Fine Beam Polarimetric image of November 2011 (R=HV, G=VH, B=VV), g) an overview of the 20x10 km study with the red box showing the location of the other images (QuickBird), h) a Landsat image of April 2012, and i) an ENVISAT ASAR image of March 2012 (polarization : VV).

Table 10.1 summarises, in a quantitative way, the conclusions of the analysis done on the figures 10.15 and 10.16. TerraSAR-X images enable the detection of most narrow logging roads (~10m width) that were visible from the QuickBird image. PALSAR FBS and FBD modes can only detect a few of these roads, and the visual detection of such roads can lead to a misinterpretation (Figure 10.17). The PALSAR FBP and ASAR images have a lower level of spatial detail; the roads have to be wider to be detected by these sensors. A road of 15 meters wide can be detected but it is not always clear if it is well a road or if it is a feature due to some particularities of the terrain (see Figure 10.17). A road of 30 meters wide is required to be detected without misinterpretation (for the Gabon test site). We can also note that the old roads, large and without crown cover (appearing highly blue on QuickBird – see Figure 10.24, the South-East road) are the easier ones to detect. However, these old roads do not represent a direct sign of degradation. They are often a driver to open new logging roads and their surroundings have to be monitored with more appropriate images such as TerraSAR-X.

Table 10.1: Minimum width of the roads visible on the Gabon test site 20*10 km with the different images types and the number of roads from Figure 1a which are visible.

Satellite	Mode	Roads	
		Width (m)	Number of visible roads (/6)
TerraSAR-X	*SpotLight*	10	6
	Strip Map	10	5
ASAR		15	0
			Number of visible roads (/3)
PALSAR	*FBS*	10	2
	FBD	10	1
	FBP	15	0,3

Figure 10.17 shows an example of misinterpretation: a linear feature is observed from the TerraSAR data within the forest. Nonetheless the two QuickBird images do not indicate road presence at that location. According to the WRI Atlas (hydrographical lines of 2008), the line feature could be a stream. Therefore despite the high level of spatial detail of TerraSAR images (Spotlight and StripMap) logging roads are not easily detected, because there are a lot of discontinuities in the forest landscape (visible on both TerraSAR and PALSAR images) which can be confounded with roads. Moreover, in more undulating terrain, lay-over and shadowing effects may show up as linear features but are principally a result of SAR image acquisition.

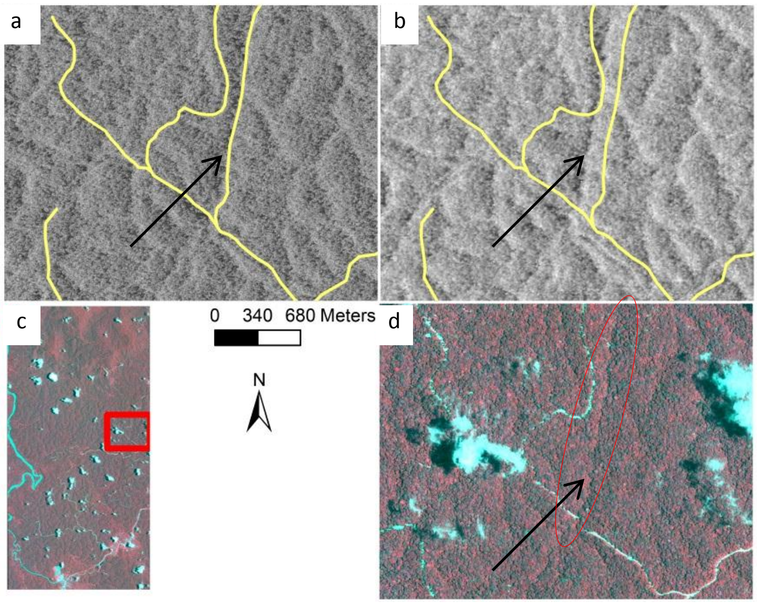

Figure 10.17: Illustration of the manual delineation of the roads (yellow lines) based on the visual interpretation of (a) a TerraSAR StripMap image of April 2012 without the additional use of optical images. The black arrow indicates a line misinterpreted as a road. These road-lines have been projected on (b) a PALSAR FBS image of February 2011 (polarization: HH) where the black arrow indicates the feature confounded with a road (note the shift due to the difference of view angle between TerraSAR and PALSAR). On the QuickBird image of March 2012 (d), the line confounded with a road is pointed with the black arrow. There is discontinuity in the forest, probably due to a stream, but no road. The image (c) gives an overview of the 20x10 km study with the red box showing the location of the other images (QuickBird).

Figure 10.18 illustrates the ability of the different SAR images acquired on the Gabon test site, to detect clear-cuts made in the forest. A large clear-cut of this area (grossly delineated in black on image a), which has a width of approximately 200 meters, can be seen on all images except on ENVISAT-ASAR. This gap is poorly visible on the Landsat image. The ALOS PALSAR FBS mode (10.18e) is more adapted to detect the clear-cuts than the FBP mode (10.18f). As seen on Figure 10.16, the mode FBP has a poorer visual quality, with lower spatial detail than the FBS. This is due to (1) the pre-processing treatment which does not include the multi-temporal speckle filtering (11x11) step, (2) the lower spatial resolution of FBP and (3) the smaller incidence angle (24° vs 38.8°). A higher incidence angle allows a better distinction between forest and non-forest[62].

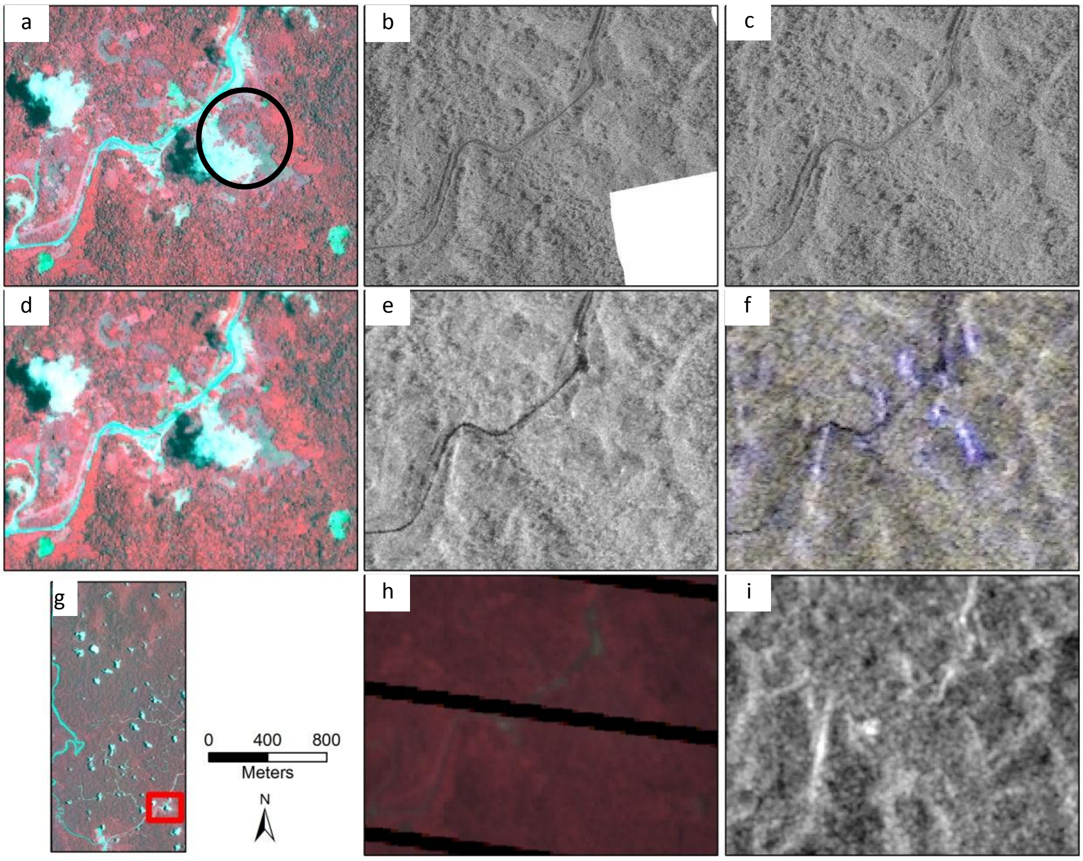

Figure 10.18: Visual comparison of mono-temporal imagery for a small part of the Gabon study site – localized on a zone of intense clear cuts. On the middle of the image a main road is present, while several clear cuts are visible either side of the road. The images show: a) a QuickBird of March 2012, b) a TerraSAR High Resolution SpotLight image of February 2012, c) a TerraSAR StripMap image of April 2012, d) a degraded QuickBird false-colour composite at 12m resolution, e) an ALOS PALSAR Fine Beam Single image of February 2011 (polarization : HH), f) an ALOS PALSAR Fine Beam Polarimetric image of November 2011 (R=HV, G=VH, B=VV), g) an overview of the 20x10 km study with the red box showing the location of the other images (QuickBird), h) a Landsat image of April 2012, and i) an ENVISAT ASAR image of March 2012 (polarization : VV).

A quantitative analysis is realized to determine the minimum width of the clear-cuts which can be seen by image type. The results of the analysis are presented in the Table 10.2 and Figure 10.19.

[62] Centre Canadien de Télédétection (CCT), Ressources naturelles Canada et Globe SAR. Applications liées à la foresterie.

Table 10.2: Minimum width of visible clear cuts on the Gabon site by available imagery type.

	Satellites					
	TerraSAR-X		PALSAR			ASAR
	SpotLight	*Strip Map*	*FBS (HH)*	*FBD (HH)*	*FBP*	
Min. width (m)	17	22	50	300	300	300
Comments				Not adapted in monotemporal analysis		

The smallest clear-cut visible is 17 m wide (~570 m² or 0,057ha) on the TerraSAR High Resolution SpotLight image (Figure 10.19b1). The same clearance can be guessed on the TerraSAR StripMap image (10.19c1) but can't be clearly distinguished. From the coarser resolution (10.19c1 to 10.19g1), this feature is not visible. Twenty-two meters corresponds to the width of the smallest clear-cut (~1650m² or 0,165 ha) visible on the TerraSAR StripMap image (10.19b2). This clearance is still distinguishable on the PALSAR FBS image (10.19c2) but not with a high degree of certainty while observing the image without comparison. On the Gabon test site, the only feature distinguishable with all images is a clear-cut of 300 meters wide (537 222m² or 53 ha).TerraSar High Resolution SpotLight is the only image adapted to detect the degradation. Note however, that the logging of a tree causes a gap of +/- 300 square meters[63]; the logging of minimum two trees is so required to be visible from a TerraSAR HR image.

[63] Dixit Jean Louis Doucet, at the conference "REDD+ day" held in Gembloux the 24th of October 2012.

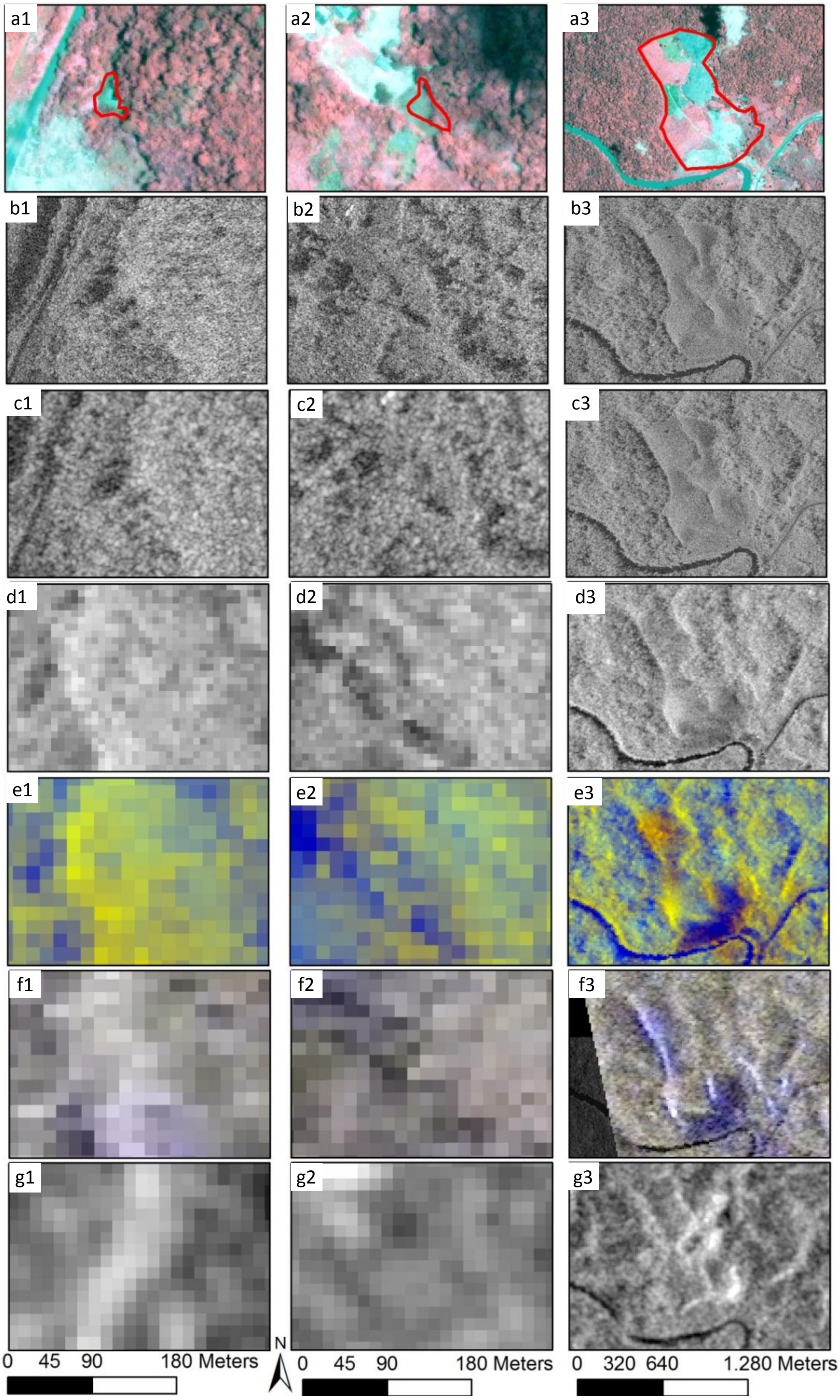

Figure 10.19: Visual comparison of mono-temporal imagery for three clear cuts of different size (1-2-3, respectively 17-22 and 300m) illustrating the results of the table 1. The red polygon on the three first images (a1-2-3 – QuickBird March 2012) represent the clear cuts areas manually delineated based on the TerraSAR High Resolution SpotLight image of February 2012 images (b1-2-3). On the examples below, exactly the same location is presented by image type (b to g) and by number (1 to 3). The images show: c) TerraSAR StripMap image of April 2012, d) ALOS PALSAR Fine Beam Single image of February 2011 (polarization: HH), e) ALOS PALSAR Fine Beam Dual image of October 2010 (R=HH, G=HV, B=HH/HV), f) ALOS PALSAR Fine Beam Polarimetric image of November 2011 (R=HV, G=VH, B=VV), g) ENVISAT ASAR image of March 2012 (polarization: VV). Remarque: the clear cuts chosen existed yet in 2010.

TerraSAR very high resolution is the most appropriate sensor to detect the degradation. So, we test its ability to capture the variability of the soil occupation after the logging of trees. The data from the terrain (pictures from June 2012) are used. On the following figures (10.20 to 10.23) the yellow polygons, representing the clear-cuts, have been manually delineated on the basis of the TerraSAR Strip Map only. TerraSAR images (1.5 or 3 m) do not allow the detection of forest regeneration occurring on a time scale of 1-2 years (Figure 10.20). The regeneration appears in green on the QuickBird image (10.20a point c – 10.20c) while the white patterns reflect another soil occupation (10.20a point d – 10.20d). On TerraSAR (10.20b) only the slope induces a visual difference between these patterns, there is no textural difference. The big trees remaining uncut after the deforestation are visible (on this example the tree has a crown width of 20 meters, black dot in the north of the image).

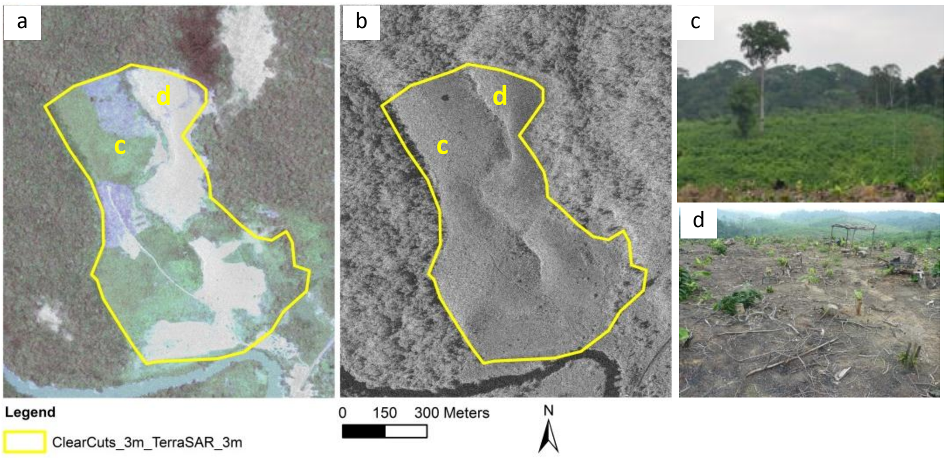

Figure 10.20: Illustration of the ability of a QuickBird image of March 2012(a) to differentiate (c) the forest regeneration on a time scale of 1-2 years associated with crops (picture from the field) from (d) a young banana plantation, which isn't visible on (b) the TerraSAR HR SpotLight image.

From TerraSAR, the distinction between a road of bare soil and one recolonized by vegetation (Figure 10.21 and 10.22) is visible thanks to the texture of the image, which is rougher for the recolonized one (21e and 22c). Two other types of soil occupation are also well detected: the secondary forest regrowth, sign of a previous degradation (21d) and a marsh (21c).

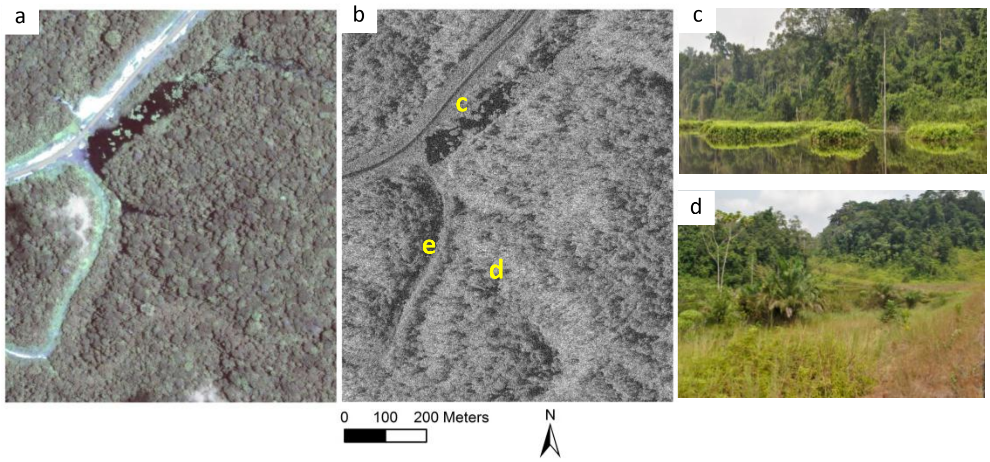

Figure 10.21: Illustration of the ability of (b) a TerraSAR HR SpotLight image of February 2012 to detect the difference of land cover seen on the terrain and on (a) a QuickBird image of March 2012. The three different land cover visually detected on TerraSAR-X: (c) marsh, (d) secondary forest regrowth and (e) colonization of road by vegetation are visible on TerraSAR.

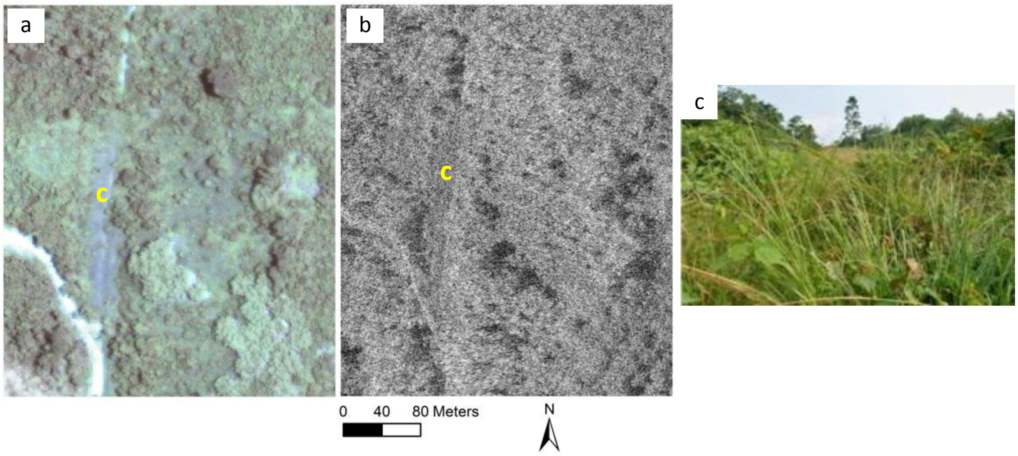

Figure 10.22: Illustration of the ability of (b) a TerraSAR HR SpotLight image of February 2012 to detect the difference of land cover seen on the terrain (c) - an old road colonized by herbaceous vegetation- and on (a) a QuickBird image of March 2012.

Figure 10.23 illustrates the aptitude of TerraSAR to (i) detect relatively large clear-cuts (10.23b) and to (ii) differentiate the fallows (10.23c) from a new plantation on slash and burn agriculture (10.23d). The texture of the fallow is rougher, while the slash and burn agriculture present a smooth texture easily separated from the surrounding trees.

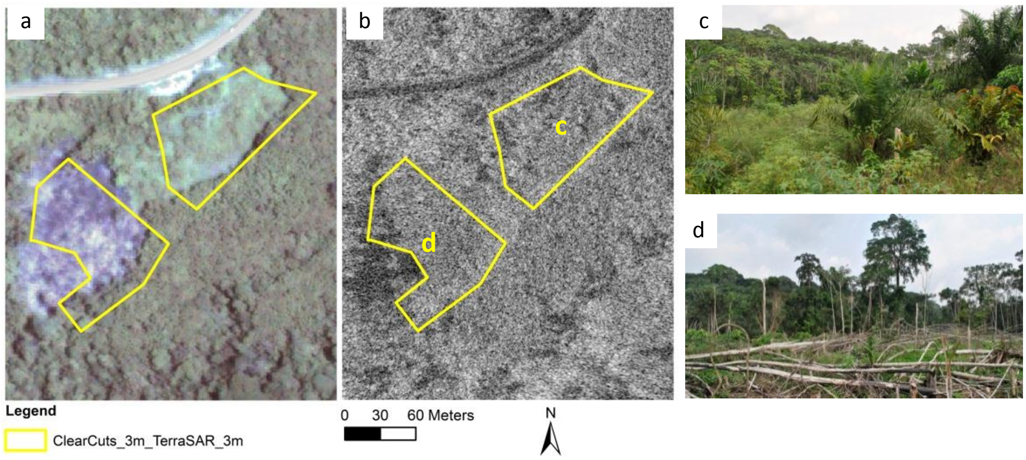

Figure 10.23: Illustration of the ability of (b) a TerraSAR HR SpotLight image of February 2012 to detect the difference of land cover seen on the terrain and on (a) a QuickBird image of March 2012. The detection of (c) fallow (width 58 m) and (d) a new plantation on a slash and burn agriculture field (width 72m) is possible with TerraSAR.

10.3.5 Gabon: multi-temporal analysis

The data acquired for the Gabon tests site, give us limited possibility to test the advantages of the multi-temporality of the images. We have multi-temporal data only for the sensors PALSAR and ENVISAT ASAR. No analysis can be done on the detection of new roads between 2010 and 2012 because (i) there's no correspondence between the dates acquired with PALSAR and QuickBird and (ii) the precedent tests have shown that ENVISAT ASAR is not appropriate to detect "small" roads.

The multi-temporality of data is useful to detect changes occurring between years. The Figure 10.24 illustrates the highlighting of changes by the combination of multi-date data. The changes appear in darker color on the images (10.24b, c, d, f, g). As we can see, the Gabon study site doesn't present a lot of changes (10.24 e). The changes consist principally into new roads and some clear-cuts near the main road localized in the south-east of the image 10.24 e. The high resolution radar images (PALSAR and ASAR) don't allow the detection of small scale changes. For example, new roads do not appear highlighted; well visible changes (10.24 f and g) have a large size (hundred meters). The capability of this type of images seems to be limited to the detection of changes appearing (10.24 f and g) near urban zone, in area already occupied by agriculture, which grows bigger but not for the forest cover in dense forest.

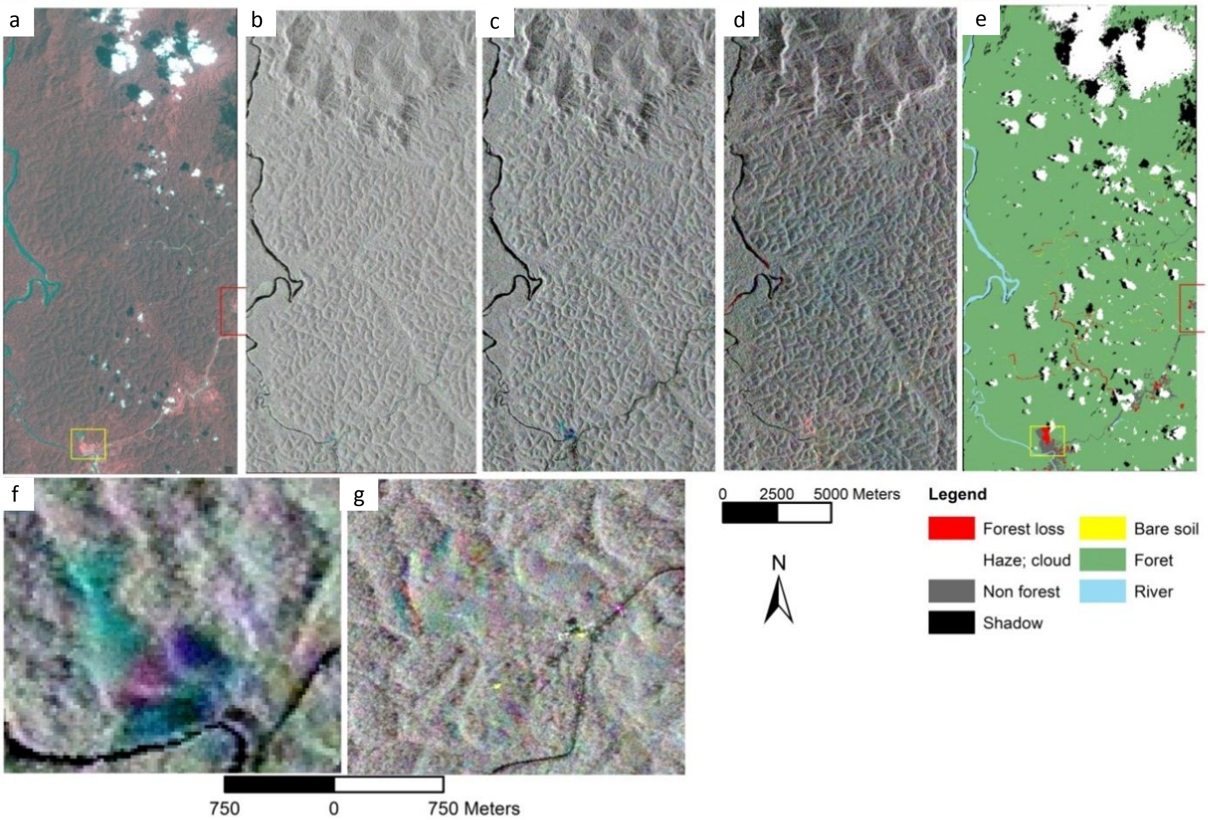

Figure 10.24: Multi-temporal changes visualized with SAR data. The images show: (a) a Quick Bird image of March 2012 with two boxes showing the extension of the images (f) and (g); (b) a PALSAR FBS image in polarization HH (R: Feb 2011; G: Feb 2009; B: Feb 2007); (c) a PALSAR FBD image in polarization HV (R: Aug 2010; G: Jul 2009; B: Aug 2007); (d) an ENVISAT ASAR image in polarization VV (R: Mar 2012; G: Dec 2006; B: Aug 2005); (e) a change classification of 2010-2012 based on two QuickBird images; (f) a zoom of the PALSAR FBS image following the yellow box (~300m) (c); (g) a zoom of the PALSAR FBS image following the red box (~600m) (d).

10.3.6 Gabon: large-scale spatial patterns and forest types

A different type of forest seems appear in a lighter red on the QuickBird image in the center-south east (Figure 10.25 a, yellow circle) and all along the river and the main road in the south. On all SAR images, the large pattern of forest in the center-east of the image appears highly visible. This difference could be explained by the altitude rather than a different forest type because this feature appears like a continuous line. We haven't any field data on this zone to confirm this hypothesis.

Along the road, no significant difference is detected. However, along the river the difference of texture – smoother – seems to be due to a difference of forest type. This difference is present on all images type and may be due, in part, to the presence of gallery forest.

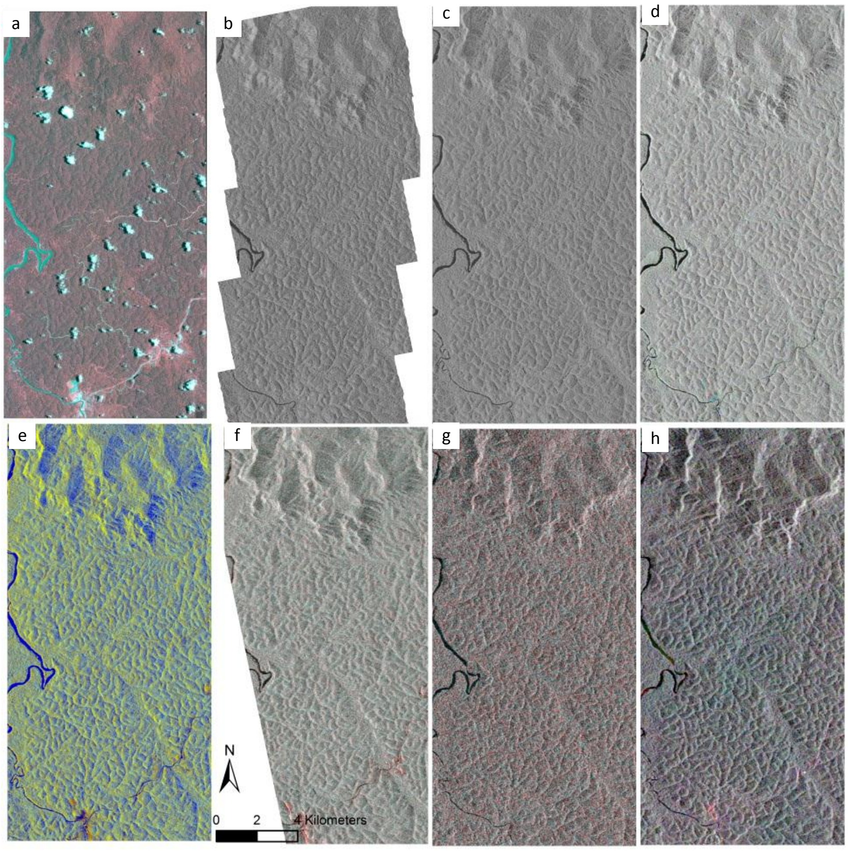

Figure 10.25: Overview of the 20x10 km study area of Gabon from different mono-temporal images: a) QuickBird false colour composite - March 2012, b) TerraSAR High Resolution SpotLight – February-April 2012, c) TerraSAR StripMap - April 2012, d) PALSAR FBS in polarization HH (R: Feb 2011; G: Feb 2009, e) PALSAR FBD – Oct 2010 (R: HH; G: HV; B: HH/HV), f) ALOS PALSAR FBP - Nov 2010 and 2011 (R=HH, G=HV, B=VV), g) ENVISAT ASAR with 33° incidence angle – Apr 2010 (R: VV; G: VH; B:VH), h) ENVISAT ASAR with 23° incidence angle - VV polarization (R: Mar 2012; G: Mar 2011; B: Dec 2006), i) ALOS PALSAR Fine Beam Dual – May 2010 (R=HH, G=HV, B=HH/HV), j) ALOS PALSAR Fine BEAM Polarimetric - March 2011 (R=HH, G=HV, B=VV).

10.4 Conclusions

The main question of this chapter was: "does SAR satellite data allow for an effective assessment of forest degradation in the two study areas?" We have shown and interpreted a large number of processed SAR image subsets from a variety of satellites with different resolutions, polarizations, and viewing geometries, of which some were acquired at multiple dates. This followed an extensive selection on SAR data availability in the archives, and where possible new acquisitions were made, in part to obtain a multi-temporal set of data. Based on our discussions and reflections, we list below a number of conclusions from our analysis.

- SAR imagery does provide useful spatial information, especially in regions where optical image acquisition is difficult due to persistent cloud cover. SAR can provide a good separation of forest from non-forest, at least at large spatial scales. Detection of small-scale features or changes (logging roads or clear-cuts) is possible, but this depends on the size and orientation of the feature, and the specific SAR sensor that is imaging that feature. For the SAR sensor, from our analysis we can underline the importance of spatial resolution and viewing geometry. Based on data availability we cannot make strong conclusions regarding optimal polarizations or radar wavelength to be used, because 1) these changed together with resolution, and 2) L-band imagery was not acquired after March 2011.

- Detection of logging roads of 10-15m wide requires high-resolution data: with TerraSAR StripMap imagery (3m resolution) a large number of narrow logging roads could be detected, while for Congo these were not clearly picked up from 8m resolution RADARSAT multi-look fine imagery. Nonetheless, comparison with optical very high resolution data showed that TerraSAR StripMap was not successful in detecting logging roads in dense forest. This could be partly explained by quick regeneration of vegetation, which calls for frequent acquisitions - at least every year - of TerraSAR StripMap imagery with the same polarization and viewing geometry.
- Forest gap detection with SAR strongly depends on the size of the gap, and spatial resolution and viewing geometry of the SAR sensor. Clear-cuts of approximately 0.25 ha could only be detected from TerraSAR and RADARSAT imagery with 3 and 8m resolution respectively. Although 1m resolution TerraSAR imagery provides more detail, 3m resolution provides sufficient information for effective detection of the clear-cuts. For larger gaps also coarser resolutions could be sufficient, even though for Congo PALSAR seemingly had problems with identifying recent clear cuts.
- Given the importance of image resolution vis-à-vis feature size, the selection of appropriate SAR imagery requires good a-priori knowledge on the spatial size of these features, such as logging roads and clear-cuts. This spatial size could depend on very local practices regarding logging for timber or shifting cultivation, but also on national rules and regulations.
- As stated previously, the viewing geometry of SAR acquisitions is very important for detecting features on the ground or changes in these. In many cases radar shadows or strong returns due to double bouncing or lay-over constitute an important key to understand ongoing processes. It becomes hard or even impossible to detect changes based on different incident angles, or look directions.
- The previous point also stresses the fact that interpretation of SAR imagery for the detection of limited-size features (as for forest degradation assessment) is not 'easy' as with optical data. Optical data are usually acquired at angles close to nadir, and their measured reflection at two time periods provides direct information on a surface that is changing. Interpretation of SAR imagery requires a good understanding and appreciation of the scattering mechanisms and thus more about how the scene was observed (under what angle were radar pulses sent to target, etc). Only then a good interpretation of shadows and areas of increased backscatter in the image can be made.
- Terrain slope makes interpretation of SAR imagery for forest degradation assessment even more complex: it causes additional lay-over and shadowing effects. Some correction for this is possible with advanced methods, but requires high resolution digital elevation models. SAR data acquired at low incidence angles suffer more from lay-over, while very high incidence angles create large radar shadows in areas with much relief.
- We acknowledge that much more analysis could be performed to evaluate best SAR characteristics for detecting forest degradation signs at both study sites, and in the Congo Basin in general. Such analysis could benefit from similar acquisitions with a higher temporal frequency, and dissimilar multi-temporal acquisitions from the same SAR sensor with a range of incidence angles and polarizations from ascending and descending orbits. Nonetheless, we found that limited SAR data exists in current archives – especially for <10m resolution - , not only for our study sites, but also for many places across the Congo Basin. This is partly due to the fact that SAR is an active system and acquisitions need to be programmed: someone should pay for programming the satellite before an image is recorded. Our project was fortunate because

through GMES arrangements we could freely obtain archive and new acquisitions, which normally imply a high purchasing cost. In our view not many projects or research articles exist that have evaluated such a high number of different SAR images simultaneously: even though we have not entered into advanced processing for potential automatic detection, this intercomparison of different types of SAR imagery is an important contribution of REDDiness.

- Frequent repetitive acquisition with the same SAR observation characteristics (viewing geometry, polarization) is important to detect small degradation signs such as logging roads and clear-cuts. This is because vegetation regenerates quickly in these environments. Although not extensively tested, incidence angles between 33° and 40° seem to be reasonable. We recommend a frequency of minimally once per year during the same season. This is not achieved in our study due to limited archives, and a limited timeline for new acquisitions.
- For future operational services that can be applied to the whole Congo Basin and beyond, systematic observation strategies for SAR acquisition are needed. This means that any location should be imaged with the same sensor using the same characteristics (polarization and incidence angle) at least once per year. ALOS PALSAR was the first satellite sensor that had such a strategy for forested regions of the globe. PALSAR2 (to be launched late-2013) will have a similar coordinated observation strategy. The same is true for the European Sentinel-1 SAR satellite (launch in 2013). Alternatively systematic observations could be requested and paid for - for example by GMES - to a third party, such as commercial operators like Astrium (TerraSAR) or ASI (Cosmo-SkyMed). Especially for very high resolution acquisitions (like TerraSAR StripMap) a sampling scheme[64] could be constructed that incorporates a minimum-orderable area (set by third parties).
- SAR data could be combined with optical acquisitions through data fusion. For REDDiness we did not test this option. Within the logic of operational monitoring systems there may also be a drawback to data fusion:
    1. Ideally we would want to have an optical and SAR image for a similar date or at least year repetitively: however, persistent cloud clover makes this difficult for optical data. One possibility could be to focus with the optical analysis on highly-frequent data (as from MODIS or MERIS) that can be mosaicked first and then fused with higher spatial resolution SAR data.
    2. Data fusion between very high resolution optical and SAR data would create a double acquisition cost, and also the processing and interpretation time will increase. A possible future operational service from the Sentinel-series could be to deliver fused data sets as products.
- From our perspective countries or projects that want to incorporate SAR data in forest monitoring activities but have limited experience will face a number of challenges:
    1. The ordering of SAR data is not easy: a range of satellites exists, and many times from the same satellite a number of characteristics need to be selected (like incidence angle, polarization) which have a profound impact on what can be observed. Especially for new acquisitions, this requires careful consideration. In addition each satellite sensor comes with its own products, and relatively new users need to understand well the benefits and limitations of each data product.

[64] For example as the scheme used by the Joint Research Centre, reported in: Duveiller G., Defourny P., Desclée B., Mayaux P., 2008. Deforestation in Central Africa: Estimates at regional, national and landscape levels by advanced processing of systematically-distributed Landsat extracts. Remote Sensing of Environment, 112 (5), pp. 1969-1981.

2. SAR data archives may contain only a limited amount of information, especially for resolutions below 10m. This can strongly limit the potential to evaluate past changes in forest cover, or forest degradation features.
3. Pre-processing of SAR imagery is not easy and takes time: for REDDiness we spent more time in obtaining a reasonable pre-processing chain than in effective visual analysis. This is because we tested options for speckle filtering and possible slope correction, tried different SAR-processing software, while many of the steps took a long time due to image size (not for all steps and software could we test pre-processing for a subset only). Care should be taken during pre-processing not to create too much smoothing of the images (for example by spatial speckle filters) which would not allow effective detection of small-scale features
4. Interpretation of SAR imagery can be challenging (as discussed above) and requires knowledge about SAR imaging characteristics and about viewing geometry, especially when focussing on small-scale feature detection.
5. Working with SAR imagery becomes even more challenging in non-flat terrain (undulating or mountainous). Here small incidence angles may create already large lay-over effects, while steep terrain can cast long radar shadows where no observation is possible, especially for larger incidence angles. Advanced slope correction methods, high resolution digital elevation models, and knowledge on how to use software that can implement these, are needed to gain better results in such areas.

11 Comparison of satellite systems and outlook

This chapter aims at bringing together some of the findings in chapters 8, 9, and 10. Based on the image types used in REDDiness we provide an overview of their perceived utility for monitoring forest degradation. We also report data sizes and the current commercial prices for the satellite data that we used to compare costs. Subsequently for the data types that we consider most promising, we analyze which alternative satellites could provide such data. Finally we shortly discuss future systems that could improve image availability, reduce costs, or provide alternative options for the assessment of forest degradation. Throughout the chapter we focus largely on optical and radar data. Here we do not consider additional systems like LiDAR, or advanced techniques like SAR interferometry, because these were not tested in REDDiness.

11.1 Satellite data used in REDDiness in relation to forest degradation

The REDDiness project was a short focussed project, and as such cannot be expected to provide the definite answer as to how systems for monitoring forest degradation should be set up. Despite of its limitations, chapters 8, 9, and 10 reported on a number of activities that contribute to defining the potential of various satellite sensors for a direct detection of forest degradation activities, including logging roads, small forest gaps due to logging or shifting cultivation. In addition we evaluated how different satellite sensors reveal coarse spatial patterns, which could give information on forest types. Based on multiple analyses at the two 20x10 study sites, we summarize here our perspective on the characteristics of satellite images that are required for direct assessment of forest degradation. We fully acknowledge that a higher potential could emerge from some of the sources mentioned when evaluating for example a larger dataset with more (cloud free) imagery, multiple incidence angles for SAR acquisitions, interferometric processing of multi-temporal SAR imagery, etc. In addition, some of the analyses carried out in the project could be deepened. Nonetheless, REDDiness worked in a real local setting, i.e. one of relatively low data availability of optical satellite data (partly due to cloud cover) and SAR data. For SAR, especially at higher spatial resolutions, few acquisitions have been made in both countries. Also we stress that most of the analyses and satellite-based forest mapping that are carried out currently by national institutes in African countries are based on conceptually simple visual analysis (even though the activity itself is time-consuming and requires skills from the interpreter). REDDiness has not aimed to reach much beyond that reality by avoiding the use of highly-advanced image processing options.

Table 11.1 provides a summary of our perspective on the potential of different satellite sensors for detecting forest degradation activities. The table concentrates only on our experience in this project. We discuss shortly the three categories under potential:

- The detection of logging roads (<10 m wide) requires image data at very high spatial resolution. For SAR, RADARSAT-2 data of 8m resolution did not allow for detecting most logging roads. TerraSAR StripMap seems the most cost-efficient option, although it may not pick up each and every logging road. For optical data possibly systems with a slightly lower spatial resolution could still detect most logging roads because the logging roads are multiple pixels wide. For NDFI (Landsat) small logging roads were not picked up, probably because spatial resolution was too low or the image availability was not ideal. It would be of interest to further test the approach in other areas of the Congo Basin with more frequent images[65] or test it on multispectral data of higher spatial resolution. Based on very high resolution optical and SAR analysis, effective logging road detection seems to require frequent observations (at least once per year, cloud-free) due to quick regeneration of vegetation.

- Forest gaps due to logging are somewhat wider than logging roads. For Congo for example we found various small clear-cuts of about 0.25 ha, but still at least 40m wide. We need high spatial resolutions for detecting these small features. However, in addition to the sources useful for detecting logging roads, also RADARSAT-2 at 8m resolution proved very useful to identify these clear-cuts.

Table 11.1: Summary of the potential of different satellite images used in REDDiness for the detection of forest degradation. ++=very high potential, +=high potential, o=potential only in some cases, -=low potential, --=impossible to detect. Question marks indicate that the evaluation within REDDiness did not permit a full evaluation of the potential due to limited images. The potential is rates for 1) narrow logging roads of up to 10m wide, 2) small forest gaps, 3) forest types that could possibly be related to degradation levels. Costs indicate commercial costs of archive products (between brackets for non-time-critical new acquisitions)[66]. Note that most satellite products require a minimum area to be ordered (e.g. for RADARSAT-2 a full scene of approximately 2500km^2). Data size is for the original unprocessed product.

Source	Res.	Potential for degradation detection			Cost	Data size	Remarks (incl. method used in REDDiness)
	(m)	roads	gaps	types	(€/100km^2)	(kB/km^2)	
QuickBird	2.4 (0.6)	++	++	+	1300 (1800)	6554	- problem with cloud cover - semi-automatic classification
WorldView	2.0 (0.5)	++	++	+	2500 (2900)	11758	- problem with cloud cover - semi-automatic classification
Landsat	30 (15)	- (?)	o (?)	+	0	13	- problem with cloud cover - spectral unmixing and evaluate changes
TerraSAR-X SpotLight	1	+	+	+	6750 (13500)	7812	- visual analysis - SAR knowledge required from interpreter
TerraSAR-X StripMap	3	+	+	+	125 (250)	1250	- visual analysis - SAR knowledge required from interpreter
RADARSAT-2	8	o	+	+	110 (113)	191	- visual analysis - possibly useful for wider logging roads
ALOS PALSAR FBS	10	-	o	+	12	50	- visual analysis - recent small clear-cuts not detected
ALOS PALSAR FBD	20	--	o	+	12	25	- visual analysis - recent small clear-cuts not detected
ALOS PALSAR FBP	30	--	-	+	29	50	- visual analysis - low spatial resolution - less coverage per image than FBS and FBD
ENVISAT ASAR IMP	30	--	-	o	4	13	- visual analysis - low resolution for small-scale features
ENVISAT ASAR APP	30	--	-	o	4	26	- visual analysis - low resolution for small-scale features

[65] Some positive results on NDFI were reported for Cameroon in: Rodriguez Montellano, A., and E. Armijo, 2011. Detecting forest degradation patterns in SouthEast Cameroon. Anais XV Simpósio Brasileiro de Sensoriamento Remoto - SBSR, Curitiba, PR, Brasil, pp 1601-1613.

[66] Costs were derived mostly from the E-GEOS price list and converted to Euros where needed using exchange rates of October 2012. Prices for TerraSAR were obtained through the Astrium website.

- Although not evaluated in great detail, all image types quite clearly distinguish forested areas from non-forested areas. Except for ENVISAT ASAR, all other image types also provided at least some differentiation within the forest, as apparent from 1) different levels of spectral reflectance or radar backscatter, or 2) differences in texture.

Based on our experience we thus recommend the use of data at rather high spatial resolution (<10m) that is frequently acquired (at least once per year a good acquisition) for effective analysis of forest degradation. For optical acquisitions, cloud cover is clearly the main limiting factor. For SAR data, we place a few additional remarks:

- Repetitive acquisition means acquisitions with the same viewing geometry.
- Mountainous terrain can prohibit effective SAR analysis due to strong lay-over effects and radar shadows: some correction is possible though with advanced processing software.
- Pre-processing of SAR data requires some additional expertise.
- Interpreters that use visual observation of SAR data should understand the basic principles of how SAR images are formed in order to interpret things like radar shadows casted by high trees on adjacent recently logged locations.

Image data of high spatial resolution (still) comes with a price. This price can be prohibitive for many countries: a wall-to-wall coverage at very high resolution may cost too much. TerraSAR SpotLight is the most expensive per square kilometre, but fully covering a single time the entire Gabon with QuickBird for example would currently cost about 5 million Euro (although certainly discounts would apply, but no guarantee for a complete cloud-free coverage). In this case it would be better to apply a sampling approach, possibly stratified by analyses at coarser resolution to focus on areas where degradation is more likely to occur. Per square kilometre, the price of TerraSAR StripMap seems reasonable, and could possibly allow for an annual wall-to-wall coverage in many countries.

Besides image cost, there is also the issue of image storage and processing (and possibly data transfer). Data at higher spatial resolution require more disk space, especially when considering also (pre-)processing outputs. For example a single full coverage of Congo by TerraSAR StripMap would total 400 GB of basic image data. This number increases strongly when considering the processing steps that need to be performed on these data. If countries are to perform such processing locally, they need to set up systems to store, process, and back-up these large data files. This may also imply investing in specialized software packages and capacity of persons that can operate these, e.g. for atmospheric correction of optical data, or advanced SAR terrain correction tools.

We should stress once more that a number of systems in Table 11.1 are not anymore operational, i.e. ALOS PALSAR and ENVISAT ASAR. Follow-up missions are expected in 2013-2014 (see section 11.3).

11.2 Alternative satellite systems

Besides the image data that was obtained within REDDiness, a number of alternative satellite sensors or products exist. Following the discussion in Section 11.1 that identified the need for high spatial resolution data, we list here a number of data sources with resolutions below 10m that could form an alternative to those used in REDDiness. Note that several SAR satellites provide imagery at different resolutions, but we do not identify those with resolutions of 10m and above here. Table 11.2 provides an overview of some current alternatives that are actively operating.

Table 11.2: Overview of common active satellite systems and products that could be used as alternatives to the data used in REDDiness. The list is not complete: for example more IRS satellites exist that obtain data at 5m resolution. Optical systems are on the left side of the table, SAR systems on the right.

Source	Res.	Cost	Source	Res.	Cost
	(m)	(€/100km²)		(m)	(€/100km²)
IKONOS	3.2 (0.8)	772 (1544)	**COSMO-SkyMed SpotLight**	1	4725 (9450)
Geo-Eye	2.0 (0.5)	965 (1930)	**COSMO-SkyMed StripMap**	3-5	113 (225)
IRS-P5 (CARTOSAT-1)	2.5 PAN	480	**RADARSAT-1 Fine**	8	111 (115)
SPOT-5 2.5m colour	2.5	225 (247)	**RADARSAT-2 SpotLight**	1	4500 (4593)
SPOT-5 5m colour	5	150 (172)	**RADARSAT-2 UltraFine**	3	1042 (1135)
RapidEye	5	95 (95)			

11.3 Future satellite systems

A good number of satellites are planned for launch in the near future, which would either 1) allow for continuity of observations made by current or past satellite sensors, or 2) provide new capabilities for the monitoring of forest degradation. Several satellite missions have been planned in the past that could greatly advance forest monitoring activities. One of them is the BIOMASS mission, which has finalized the feasibility study and is competing with two other missions to be selected as the next Earth Explorer mission of the European Space Agency. It would carry a P-band SAR that has a larger wavelength than L-band thus more penetration into the canopy and higher sensitivity to forest biomass. Another highly interesting mission that was planned for launch in 2017 is DESDynI: while its core mission was to monitor ice sheet, its imaging LiDAR system would provide important information on forest biomass. Regrettably its development was cancelled in 2011 due to budget constraints at NASA. We discuss here some interesting missions that should start providing data in the coming two years and which have the capacity to greatly enhance current monitoring capabilities through the provision of frequent data at limited or no cost.

Sentinel-1 will provide C-band SAR imagery with a typical spatial resolution of 10m as part of the European Global Monitoring for Environment and Security (GMES) Space programme[67]. Although its resolution is somewhat low for detection of narrow logging roads and small forest gaps, its systematic observation strategy and short revisit times could strongly benefit the monitoring of forest cover and larger (>1ha) forest gaps. In addition the data should become freely available which will provide an important incentive for its use and the development of applications. Sentinel-1 is planned to be launched in 2013 followed the next year by an identical satellite.

The optical equivalent of Sentinel-1 is the European Sentinel-2 mission. As for Sentinel-1 it aims at providing systematic global acquisitions of high-resolution multi-spectral imagery with a high revisit frequency (five days at equator), and should provide continuity with current optical satellite sensors[68]. It will acquire multi-spectral data in 13 spectral bands, of which four at 10m resolution.

[67] Torres, R., et al., 2012. GMES Sentinel-1 mission. Remote Sensing of Environment 120, 9-24.

[68] Drusch, M., et al., 2012. Sentinel-2: ESA's Optical High-Resolution Mission for GMES Operational Services. Remote Sensing of Environment 120, 25-36.

Even though the spatial resolution is not as high as for current very high resolution sensors (like QuickBird) it can image much larger areas within shorter time intervals, thus providing good potential for improved detection of forest degradation features. The high revisit frequency (when two satellites are in orbit) should allow for better potential to obtain cloud-free imagery. Moreover, Sentinel-2 should also have an open data policy, which would greatly enhance its use and the development of applications. The first satellite of Sentinel-2 is planned for launch in 2014.

ALOS-2 is a follow-up from ALOS that stopped operating in April 2011, and is developed by the Japan Aerospace Exploration Agency (JAXA). It will carry an L-band SAR which is particularly suited for forest applications as it penetrates deeper into the canopy. In that respect it is similar to ALOS PALSAR, but this time the SAR will have a spotlight mode (1 to 3m) and a high resolution mode (3 to 10m) and right-left looking capabilities. ALOS-2 will also have a systematic observation strategy which ascertains observations with the same viewing characteristics. The satellite is scheduled for launch in December 2013. Its high resolution in combination with L-band observation will likely offer great advances in detecting small-scale forest degradation features.

12 Final conclusions

Work package 3 of REDDiness identified that remote sensing data has potential to detect forest degradation activities. We specifically evaluated the possible detection and change analysis of narrow (<10m wide) logging roads and small forest gaps (<1ha). In addition we looked at larger spatial patterns that could provide information on forest types with possibly different stages of forest degradation. The REDDiness project was a short focussed project with limited resources, and as such cannot be expected to provide a definite answer as to how systems for monitoring forest degradation should be set up. Nonetheless based on our analyses we can draw a number of general conclusions on the direct detection of forest degradation with remote sensing:

- Monitoring of forest degradation activities requires good-quality cloud-free remote sensing imagery at frequent intervals (at least once per year). We could not achieve this within our project for all image types that we evaluated due to limited archive data and the short duration of the project. Nonetheless we found that vegetation regenerates quickly (within a year) which affects both radar backscatter and spectral reflectance, thus rapidly obscuring features related to degradation.
- Monitoring of forest degradation requires data at high spatial resolutions. Very high resolution (<1m) optical data is very effective in detecting logging roads and forest gaps. SAR data with resolutions above 3m did not allow for effective detection of narrow logging roads. High-quality (multi-looked) SAR data at 8m resolution did allow for the detection of small forest gaps. We cannot yet make strong conclusions regarding the potential of optical data at 30m resolution, partly due to limited data availability. However, most small degradation-related features were not identified on Landsat imagery. We recommend further testing methods as for example spectral unmixing in the Congo Basin, including a detailed assessment of the minimum spatial resolution required for detection of some of the small features. Possibly this could be done using the WorldView data, which has 8 spectral bands, and for which the spatial resolution could be degraded. In this way it would be possible to further evaluate the potential of optical imagery at resolutions between 2.5 and 30m (from current and future systems) for forest degradation monitoring.
- While the main problem for optical imagery is persistent cloud cover (especially in the Congo Basin), SAR has its own intrinsic difficulties. These include 1) the relative complexity of image products and pre-processing requirements for non-experts, 2) the strong dependence of the radar backscatter on viewing geometry meaning that some changes in these can drastically affect what is observed in the scene, 3) the difficulty of interpretation requiring a good understanding of radar scattering mechanisms by the interpreter, 4) strong terrain-related radar shadow and lay-over effects in mountainous or undulating terrain.
- Costs increase when the spatial resolution of satellite data increases. Higher resolution means higher data acquisition costs, but also higher costs for data transfer, storage, processing, and interpretation. Proper pre-processing of image data often requires advanced processing tools for atmospheric correction to create images with comparable spectral characteristics (optical data) or for calibration, speckle filtering, and terrain correction (SAR data). These processing tools are often implemented in commercial software packages (which can be expensive) and require training of people. This is also true for (semi-) automated interpretation that uses for example image segmentation techniques. Data providers can (and in many cases do) play a role in delivering higher level products that are further processed. Still best results are often

obtained with non-standard tailored approaches, for example multi-temporal SAR filtering improves image interpretability, but does not provide good results on single images that already underwent advanced pre-processing.

- Archives of very high resolution optical and SAR data have a limited coverage over Gabon and the Republic of Congo. This makes that at present it is difficult to set proper baselines (reference levels) on forest degradation, which need historical time series. A main focus should be now on increasing the coverage of very high resolution data at present, so that in future more accurate assessments of trends in forest degradation can be made. Programs like GMES could play an important role in increasing this availability. In this respect also emerging techniques like LiDAR are interesting, and several developing countries are ordering national coverage. Costs could still be prohibitive because such data can currently only be derived from aerial missions: however, in the long run the benefits (assessment of standing biomass) may outweigh the costs of investment by a country.
- Systematic observation strategies for SAR data acquisition are needed for effectively setting up future operational services that can be applied to the whole Congo Basin. These strategies need to ascertain a frequent coverage of the territory using the same observation parameters such as incidence angle and look direction. For optical data, especially at very high resolution, such strategies could be useful. However, in this case the acquisition of good-quality images is less certain given possible cloud cover.
- Finally we could ask ourselves whether MRV-systems for REDD+ should focus on small features like logging roads and clear-cuts, or look at a more aggregate level to what is changing in terms of forest cover. Given the difficulty in observing and interpreting such small features, even for limited-size test sites, monitoring for REDD+ may want to give priority to approaches that map non-intact degraded forests versus natural intact forests[69], or to approaches that directly map carbon levels of forests[70]. This question would be most pertinent for cases where some forest degradation occurs, but is followed by quick regeneration: for REDD+, based on current definitions of forest degradation, these short-term changes are not considered to be degradation. We showed that coarse analysis of optical and SAR data for forest cover type mapping provides interesting patterns, but these do not change much over time, even though very high resolution data showed substantial changes. Therefore based on our analyses we think that if forest degradation should be seriously included in monitoring for REDD+, we do need to include frequent observation schemes at high spatial resolutions (minimally once per year and <5m resolution). This does not have to be wall-to-wall imaging, but should follow a systematic sampling scheme. For this, SAR can provide an important input, especially in the cloudy Congo Basin.

[69] Bucki, M., et al., 2012. Assessing REDD+ performance of countries with low monitoring capacities: the matrix approach. Environmental Research Letters 7, 014031.
[70] Goetz, S., Dubayah, R., 2011. Advances in remote sensing technology and implications for measuring and monitoring forest carbon stocks and change. Carbon Management 2, 231-244.

13 Annexes

13.1 Field forms used for the terrain activities (3 pages)

FICHE D'OBSERVATION DE TERRAIN

1. Transect

Transect n°	
Système de projection	

2. Coordonnées du point d'observation

	Point d'observation	Système de projection
Longitude		
Latitude		

3. Topographie

Cocher la case correspondante

Sommet	Plateau	Pente			Plaine	Vallée
		Haut de pente	Milieu de pente	Bas de pente		

%	
Orientation	

4. Présence d'eau

Oui / Non	
Type (rivière, lac, marécage, etc.)	
Observations	

5. Occupation du sol

Localiser le point au centre d'une zone d'occupation du sol homogène, et identifier selon les axes pré-définis selon la direction du transect l'occupation du sol en bordure de la zone. Prendre une photo sur les axes pré-définis et noter le numéro de la photo.

La classe d'occupation du sol se réfère aux classes pré-défines (codes et directions en annexe)

Point	Direction Par rapport au transect (0-360)	Distance approximative (m)	Classe (Code)	Photo (ID)
P0 Observation				
P1				
P2				
P3				
P4				
P5				
P6				
P7				
P8				

FICHE D'OBSERVATION DE TERRAIN

6. Description de l'occupation du sol

6.1 Couvert dominant

Cocher la case correspondante

Arboré	Arbustif	Agricole	Herbacé

6.2 Couverture du sol

	Pourcentage couvert (%)	Hauteur moyenne (m)
Couvert arboré		
Couvert arbustif		
Couvert herbacé		

6.3 Activités humaines

Cocher la (les) case(s) correspondante(s)

Agriculture (petite échelle)			
	Culture annuelle		
	Agroforêt (cacao, café)		
	Plantations		
	Jachère		
	Autre	Préciser :	
Agriculture (grande échelle)			
	Préciser :		
Présence de feux			
	Origine		
Exploitation forestière (bois)			
	Industrielle		
	Artisanale		
Observations			

FICHE D'OBSERVATION DE TERRAIN

Code de classification d'occupation du sol (conformité typologie GIEC)

Forêt	
FO	Forêt intacte
FD	Forêt dégradée (exploitation)
FS	Forêt secondaire (succession jachère)
FI	Forêt dégradée (origine indéterminée)
Prairie	
SA	Savane arbustive
SH	Savane herbacée
SN	Sol nu
Agriculture	
CA	Culture annuelle (monoculture)
CM	Culture annuelle (mixte)
JA	Jachère
CC	Culture commerciale (plantation)
AF	Agroforêt (cacao/café)
Zone humide	
ZH	Marécage
Infrastructure	
VO	Voie d'accès (route, piste)
BA	Zone bâtie
Autre	
AU	Autre

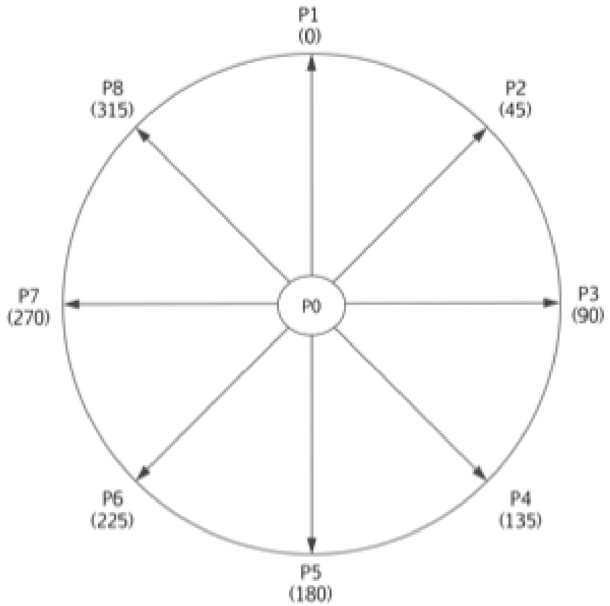

14 Bibliography

Angelsen, A. Ed. (2008). Moving ahead with REDD: issues, options and implications. CIFOR, Indonesia

Asner, G. (2009). Tropical forest carbon assessment: integrating satellite and airborne mapping approaches. Environmental Research Letters, 4, 3.

Baatz, M. & Schäpe, A. (1999). Object-oriented and multi-scale image analysis in semantic networks. Proc. of the 2nd International Symposium on Operationalization of Remote Sensing, August 16th-20th 1999. Enschede. ITC

Bigot (1996). Stabilité de la variation pluviométrique de l'Afrique tropicale entre 1951 et 1988, Dynamique à long terme des écosystèmes intertropicaux, CNRSI Orstom : 13-16.

Bucki, M., et al. (2012). Assessing REDD+ performance of countries with low monitoring capacities: the matrix approach. Environmental Research Letters 7, 014031.

Centre Canadien de Télédétection (CCT), Ressources naturelles Canada et Globe SAR. Applications liées à la foresterie.

Coordination National REDD (2011). Proposition pour la Préparation à la REDD+ (RPP) République du Congo.

Coppin, P. R., Bauer, M. E. (1996). Digital change detection in forest ecosystems with remote sensing imagery. Remote Sensing Reviews, 13, pp. 207-234. In Desclée, B., de Wasseige, C., Bogaert, P., Defourny, P. 2006. Tropical forest monitoring by object-based change detection: towards an automated method in an operational perspective. Proceedings of the 1st International on Object Based Image Analysis,(OBIA2006) Salzburg University, July 4-5, 2006.

De Wasseige, C., de Marcken, P., Bayol, N., Hiol Hiol, F., Mayaux, P., Desclée, B., Nasi, R., Billand, A., Defourny, P. Eds (2012). Les forêts du bassin du Congo – Etat des forets 2010. Office des publications de l'Union Européenne, 276p.

DeFries R, Achard F, Brown S, Herold M, Murdiyarso D, Schlamadinger B, Souza C (2007). Earth Observations for Estimating Greenhouse Gas Emissions from Deforestation in Developing Countries. Environmental Science and Policy 10: 385 394.

Desclée, B., de Wasseige, C., Bogaert, P., Defourny, P. (2006). Tropical forest monitoring by object-based change detection: towards an automated method in an operational perspective. Proceedings of the 1st International on Object Based Image Analysis, (OBIA2006) Salzburg University, July 4-5, 2006.

Drusch, M., et al. (2012). Sentinel-2: ESA's Optical High-Resolution Mission for GMES Operational Services. Remote Sensing of Environment 120, 25-36.

Duveiller G., Defourny P., Desclée B., Mayaux P. (2008). Deforestation in Central Africa: Estimates at regional, national and landscape levels by advanced processing of systematically-distributed Landsat extracts. Remote Sensing of Environment, 112 (5), pp. 1969-1981.

Fabing A. (2001). Bilan spatial et structurel de l'antagonisme « Préssion Anthropique/Dynamique forestière naturelle» en zone de forte croissance urbaine. Le cas de Pointe Noire et de sa Région R. du Congo. Thèse d'université, Biogéographie. Faculté de Géographie, 46 Université de Strasbourg I. France, 321 p.

Goetz, S., Dubayah, R. (2011). Advances in remote sensing technology and implications for measuring and monitoring forest carbon stocks and change. Carbon Management 2, 231-244.

GOFC-GOLD (2011). A sourcebook of methods and procedures for monitoring and reporting anthropogenic greenhouse gas emissions and removals caused by deforestation, gains and losses of carbon stocks in forests remaining forests, and forestation: GOFC-GOLD Report version COP17-1. GOFC-GOLD Project Office, Natural Resources Canada, Alberta, Canada.

Herold, M. (2009). An assessment of national forest monitoring capabilities in tropical non-Annex I countries, Recommendations for capacity building, GOFC-GOLD Land Cover Project Office, Friedrich Schiller University Jena.

Herold, M., et al. (2011). Options for monitoring and estimating historical carbon emissions from forest degradation in the context of REDD+. Carbon Balance and Management 6, 13.

IPCC (2003). Definitions and methodological options to inventory emissions from direct human-induced degradation of forests and devegetation of other vegetation types. Intergovernmental Panel on Climate Change.

IPCC (2003). Good practice guidance for land use, landuse change and forestry (GPG-LULUCF). In: Penman, J., Gytarsky, M., Krug, T., Kruger, D., Pipatti, R., Buendia, L., Miwa, K., Ngara, T., Tanabe, K. and Wagner F. IPCC-IGES, Kanagawa (eds.)

Jacob C. Brenner (2009). Structure, Agency, and the Transformation of the Sonoran Desert by Buffelgrass (Pennisetum Ciliare): An Application of Land Change Science

Lambin, E., Geist, H., Lepers, E. (2003). Dynamics of land use and land cover change in tropical regions. Annual Review of Environement and Resources, 28:205-241.

Liu, Lining, Wang, Yunhong, Wang, Yiding (2011). Adaptive steepest descent method for pan-sharpening of multispectral images. Optical Engineering, ISSN : 0091-3286, Volume : 50, Numéro : 9.

Mayaux P., Bartholomé E., Massart M., Van Cutsem C., Cabral, A., Nonguierma A., Diallo O., Pretorius C., Thompson M., Cherlet M. et al. (2003). A Land Cover Map of Africa, Joint Research Centre, EUR 20665 EN (European Commission, Luxembourg).

Mbeme, F. (2012). Télédétection et SIG : Applications à l'étude de l'évoulution des modes d'occupation du sol et des changements du couvert forestier du Sud Est Gabon, région de Koulamoutou – Lastrouville entre 2000 et 2011. Stage de Master 2 GEEFT, AgroParisTech.

Missamba-Lola, A.-P. (2004). Typologie et méthodes de réhabilitation des forêts secondaires et dégradées de Youbi (Région du Kouilou-Congo). Mémoire de maîtrise. Université Marien Ngouabi. Laboratoire de géographie physique. Biogéographie et restauration forestière. 68p.

Murdiyarso, D., Skutsch, M., Guariguata, M., Kanninen, M., Luttrel, C., Vermeij, P., Martins, O.S. (2008). How do we measure and monitor forest degradation? In: Angelsen, A. Ed. Moving ahead with REDD: issues, options and implications. CIFOR, Indonesia.

Penman, J., et al. (2003). Definitions and methodological options to inventory emissions from direct human-induced degradation of forests and devegetation of other vegetation types IPCC.

Potapov, P., et al. (2008). Mapping the World's Intact Forest Landscapes by Remote Sensing. Ecology and Society 13.

Quegan S, T. L. Toan, J. J. Yu, F. Ribbes and N. Floury (2000). Multi-temporal ERS SAR analysis applied to forest mapping. IEEE Transactions on Geoscience and Remote Sensing 38(2): 741 - 753.

Rodriguez Montellano, A., and E. Armijo, (2011). Detecting forest degradation patterns in SouthEast Cameroon. Anais XV Simpósio Brasileiro de Sensoriamento Remoto - SBSR, Curitiba, PR, Brasil, pp 1601-1613.

Romijn, E., Herold, M., Kooistra, L., Murdiyarso, D., Verchot, L. (2012). Assessing capacities of non-Annex I countries for national forest monitoring in the context of REDD+. Environmental Science and Policy, 19-20, 33-48.

Sannier, C., Massard, E., Fichet, L.-V., Mertens, B., Huynh, F. (2011). Monitoring of forest cover change in the Republic of Gabon between 1990, 2000 and 2010 following IPCC guidelines, International Symposium on Remote Sensing of the Environment.

SBL (2004). Plan d'aménagement de la CFAD SBL/TRB.

Simula, M. and Mansur, E. (2011). A global challenge needing local response. Unasylva, 62, 238, 3-8.

Souza, C.M., Roberts, D.A., Cochrane, M.A. (2005). Combining spectral and spatial information to map canopy damage from selective logging and forest fires. Remote Sensing of Environment 98, 329-343.

de Wasseige C., Devers D., de Marcken P., Eba'a Atyi R., Nasi R. and Mayaux Ph. (2009). The Forests of the Congo Basin - State of the Forest 2008, Editors : Luxembourg: Publications Office of the European Union.

Torres, R., et al. (2012). GMES Sentinel-1 mission. Remote Sensing of Environment 120, 9-24.

Van de Voorde, T., De Genst W., Canters F., Stephenne N., Wolff E., Binard M., (2004). Extraction of Land Use / Land Cover - Related Information from Very High Resolution Data in Urban and Suburban Areas, 23rd EARSeL Annual Symposium 2003, Gent, Belgium; 2-5 June 2003.

van der Werf, G.R., et al. (2009). CO_2 emissions from forest loss. Nature Geoscience 2, 737-738.

Yembé-Yembé, R. (2007). Étude de l'organisation de la filière bois-énergie en zones forestières au Congo : étude du cas des villages de la périphérie du parc national Conkouati Douli. Université Marien Ngouabi. IDR. 52p. in http://www.fao.org/docrep/013/i1973f/i1973f00.pdf